Homochiral Metal−Organic Frameworks for Asymmetric Heterogeneous Catalysis

Minyoung Yoon, Renganathan Srirambalaji, and Kimoon Kim*

Center for Smart Supramolecules, Department of Chemistry, and Division of Advanced Materials Science (WCU project), Pohang University of Science and Technology, San 31 Hyojadong, Pohang 790-784, Republic of Korea

CONTENTS

1. INTRODUCTION

Chirality (handedness; left or right) is an intrinsic feature of various levels of matter.[1−4] Molecular chirality usually refers to a pair of molecules that cannot be superimposed onto each other.

The molecular chirality plays a crucial role in interactions between host and guest molecules. Many biological receptors, for example, preferentially recognize a single enantiomeric form. In some cases, the two enantiomeric forms can have drastically different physiological results. For instance, the drug thalidomide, prescribed to many pregnant women in the 1950s, was subsequently found to have an R-enantiomer with desirable sedative properties, whereas its S-enantiomer was shown to be teratogenic and induces fetal malformations.[5] To avoid such problems, drug developers commonly seek to obtain enantiomerically pure (enantiopure) compounds. For the preparation of enantiopure compounds, two general methods, separation of one enantiomer from racemic mixtures and synthesis of single enantiomer using chiral asymmetric catalysts (asymmetric catalysis), have been used.[6,7] Although chiral separation of racemic mixtures can provide nearly quantitative yields of each enantiomer, the production of undesired enantiomer is perceived as expensive and inefficient. Unlike chiral separation, asymmetric synthesis allows one to directly synthesize one enantiomer dominantly.

Inspired by enzymes that catalyze reactions with high enantioselectivity in living systems, chemists have developed a variety of small-molecule asymmetric catalysts. In particular, homogeneous organometallic asymmetric catalysts composed of transition metal ions coordinated to chiral ligands have been extensively studied since the late 1960s, and the pioneers involved in the development of this area were awarded the Nobel Prize in 2001.[8−11] Among chiral ligands employed in asymmetric catalysts, so-called "privileged" chiral ligands such as BINOL, BINAP, salen, bisoxazoline, and TADDOLate have been proven to be useful, as their metal complexes are highly efficient asymmetric catalysts (privileged catalysts) applicable to a wide range of different reactions.[12] For example, metal complexes of BINAP ligands exhibited high catalytic activity for asymmetric hydrogenation, Diels−Alder, and Heck reactions.[13−15] Chiral salen-based catalysts also catalyze in various asymmetric reactions with high enantioselectivity, including epoxidation, Diels−Alder reaction, and conjugated additions.[16−18]

A remarkable development in homogeneous asymmetric catalysis in the past decade is a renaissance of organocatalysis, the use of small organic molecules to catalyze chemical reactions, especially in an enantioselective manner.[19−25] For example, the most famous organocatalyst, L-proline, and its analogues catalyze various asymmetric transformations including aldol,[26,27] Michael,[28,29] and Mannich reactions.[30,31] A number of other

privileged organocatalysts are known.[12] Organocatalysts offer several advantages over organometallic catalysts including no contamination of metal trace in products, high tolerance to water and air, and high availability and low cost.

Although a number of homogeneous asymmetric organometallic catalysts have been successfully adopted in industrial processes,[32] they often suffer from several shortcomings including tedious separation and recycling of expensive catalysts.[33] The employment of corresponding heterogeneous catalysts can thus improve the processes by offering a number of advantages over homogeneous catalysts, including easy separation, efficient recycling, minimization of metal traces in the product, and improved handling and process control.[33] Moreover, heterogeneous catalysts are more selective than their homogeneous counterparts in some cases.[34,35] Several different approaches for the development of heterogeneous asymmetric catalysts have been taken including immobilization of homogeneous catalysts on solid supports and introduction of chiral modifiers on catalytically active surfaces.[36−40] One of the latest developments in this field involved asymmetric catalysis based on metal−organic frameworks (MOFs), whose application potential in a wide range of areas including gas storage,[41−48] separation,[49−57] sensing,[58−62] magnetism,[63−69] and catalysis[70−77] has been well recognized. Many advantages of metal−organic framework systems such as the high density of active catalytic centers, high level of porosity, crystalline nature enabling elucidation of structural details, and relatively easy immobilization as compared to other heterogeneous systems make these materials invaluable for heterogeneous asymmetric catalysis.[78,79] However, the field is still in its infancy. Since the first example of asymmetric catalysis using MOF was reported in 2000,[80] only two dozen papers concerning MOF-based heterogeneous asymmetric catalysis have thus far been published. Several review articles on asymmetric catalysis using chiral MOFs appeared recently.[81−90]

The goal of this Review is to give an overview of MOF-based asymmetric heterogeneous catalysis by presenting the state of the art in this field and discussing its potential and limitations. In this Review, MOF-based asymmetric catalysts are classified according to their working principles and synthetic strategies. Design, synthesis, and structural characteristics of chiral metal−organic frameworks, as well as their catalytic activities in various asymmetric transformations, are described.

2. METAL−ORGANIC FRAMEWORKS AS ASYMMETRIC CATALYSTS

2.1. Metal−Organic Frameworks (MOFs)

Metal−organic frameworks (MOFs), also known as porous coordination polymers (PCPs), metal−organic porous materials (MOPMs), porous coordination networks (PCNs), or metal organic materials (MOMs), are a class of crystalline materials having infinite network structures built with multitopic organic ligands and metal ions. As many excellent reviews on MOFs are available including this special issue of *Chemical Reviews*,[91−110] here we will only briefly touch on several key aspects of MOFs. Since Robson for the first time introduced a design concept for the construction of 3D metal−organic frameworks using appropriate molecular building blocks and metal ions,[111−116] several groups including Zaworotko,[96,97] Yaghi, and O'Keeffe[41,102,108,110] contributed significantly to the developments of this field, establishing the basic design principles. In particular, the node (or joint-simple metal ions or metal clusters) and spacer (or strut or linker-bridging organic ligands) approach has been remarkably successful in producing

well-ordered crystalline solids with predictable network architectures. Many variations of nodes and linkers are available resulting in structural and functional diversity of MOFs, which endows this class of materials with great potential for various applications including catalysis. In particular, the concepts of secondary building units (SBUs)[102,108] and isoreticular frameworks[102] have been applied with great success to design a series of highly porous and stable metal−organic frameworks with varying pore sizes. For example, the clusters of metal−carboxylates such as $[Zn_4(\mu_4\text{-}O)(O_2CR)_6]$[41] and $[M_2(sol)_2(O_2CR)_4$ (M = Cu(II), Zn(II)] (dinuclear metal paddle wheel)[43,117] have been frequently used as rigid SBUs that act as nodes of frameworks. Isoreticular frameworks, a series of topologically identical frameworks constructed with the same SBUs but different ligands having various sizes and functionalities, provide a useful platform for systematic studies of framework properties and functions.[102,117] Interpenetration of frameworks is a phenomenon frequently encountered in MOFs, especially when the pore size increases. Although interpenetration may enhance the framework stability, and other beneficial properties,[118−120] it substantially decreases the framework capacity to accommodate large molecules for separation and catalysis. Besides control of temperature, concentration, and pH of medium, the use of bulky ligands or bulky solvent molecules as a template often reduces the chance of interpenetration.[121,122] Finally, postsynthetic modification[123,124] offers a versatile way to introduce additional functional groups to the preassembled frameworks resulting in structurally identical but functionally diverse frameworks.

2.2. Brief History of MOF-Based Asymmetric Catalysis

In 1994, Fujita et al. for the first time demonstrated the utility of a crystalline porous coordination polymer as a heterogeneous Lewis acid catalyst, which promoted cyanosilylation of aldehydes with shape selectivity.[70] A few years later, Aoyama and co-workers reported the remarkable catalytic activity of an amorphous microporous solid built with a Ti complex and achiral organic building block in stereoselective Diels−Alder reaction.[125] In both cases, however, achiral metal−organic assemblies were used. Although it was recognized that incorporation of proper catalytic units into homochiral MOFs with accessible pores could produce potentially useful solid materials for asymmetric catalysis, there was no report on asymmetric catalysis promoted by structurally well-characterized metal−organic systems until 2000, when Kim and co-workers reported the first homochiral MOF, POST-1, exhibiting catalytic activity for an asymmetric chemical reaction.[80] This seminal work triggered interests in rational design of chiral ligands and homochiral metal−organic systems for heterogeneous asymmetric catalysis. The first asymmetric catalysis promoted by metal ions at the nodes of framework was reported in 2001 by Lin and co-workers.[126] In 2005, they also adopted a systematic approach to design homochiral MOFs for asymmetric heterogeneous catalysis using privileged chiral ligand to achieve high ee BINOL as a building block.[127] In situ incorporation of catalytically active metal ions into the BINOL units endowed the homochiral MOFs with the catalytic activity in asymmetric transformations. In 2006, Hupp and Nguyen et al. synthesized a homochiral MOF using another privileged chiral catalyst, Mn(salen), as a strut to demonstrate its catalytic activity in asymmetric epoxidation.[128] A new synthetic strategy for catalytically active homochiral MOFs, introduction of privileged organocatalyst units into achiral frameworks by postsynthetic modification, was demonstrated by Kim and co-workers in 2009.[129] A series of isoreticular homochiral MOFs with tunable pore sizes using different sized ligands was synthesized by Lin et al. to demonstrate the
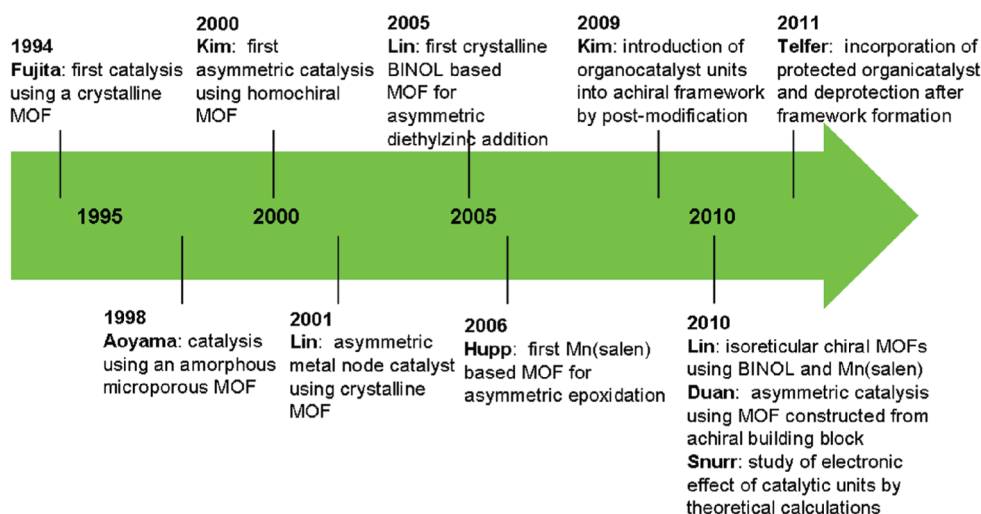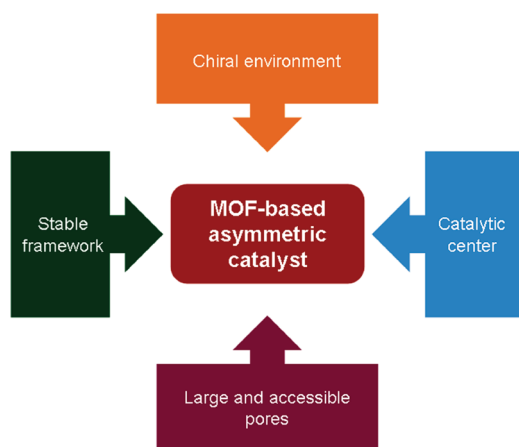
1197

dx.doi.org/10.1021/cr2003147 | Chem. Rev. 2012, 112, 1196–1231

Figure 1. Milestones in MOF-based asymmetric catalysis.

Scheme 1. General Requirements for MOF-Based Asymmetric Catalysts

relationship between the conversion rate and pore size of the frameworks in 2010.[130] Duan and co-workers for the first time demonstrated the catalytic activity of a chiral MOF constructed with achiral building blocks in asymmetric reactions.[131] Snurr and Broadbelt reported theoretical studies on the catalytic activity of Mn(salen)-based homochiral MOFs.[132] In 2011, Telfer and co-workers reported another strategy for MOF-based organocatalysts: construction of a chiral framework using bridging ligand with protected privileged organocatalyst units followed by removal of the protecting group to convert the framework into an active catalyst (Figure 1).[133]

2.3. General Requirements for MOF-Based Asymmetric Catalysis

The great potential of MOFs in heterogeneous asymmetric catalysis demonstrated by Kim and Lin at the beginning of the new millennium promoted the design, synthesis, and catalytic properties of homochiral MOFs during the past decade. However, homochiral MOFs showing high catalytic activity in asymmetric transformations are still scarce in the literature because of stringent requirements for successful applications in asymmetric heterogeneous catalysis (Scheme 1). As was already known in

homogeneous asymmetric catalysis, the catalytic centers and chiral induction sites should be in close proximity with proper relative orientation to achieve strong asymmetric induction, resulting in high enantioselectivity in products. The frameworks should also have large, accessible pores/channels allowing facile diffusion of substrates and products for high catalytic activity. As a recent study demonstrated, not only the catalytic conversion but also the enantioselectivity of MOF-based catalysts highly depend on the shape and size of the cavities (pores) of the MOFs.[130] In addition, the frameworks should maintain the structural integrity during the catalytic process. With these important prerequisites in mind, people have developed several strategies to construct homochiral MOFs for asymmetric catalysts, which will be discussed in detail in the following sections.

2.4. Classification of MOF-Based Asymmetric Catalysts

In this Review, we classify asymmetric MOF catalysts according to their working principles and synthetic strategies (Scheme 2). We first divide MOF asymmetric catalysts into two classes, metal catalysts and organic catalysts. The metal catalysts are further divided into two groups depending on whether the catalysis is performed by metal ions (with open coordination sites) at the nodes of a framework (metal node catalysts) or by privileged metal complexes incorporated at the linkers of a framework (MOF-based privileged metal catalysts). Metal node catalysts are further divided into three subgroups according to the type of linkers (chiral, achiral, or chiral and achiral mixed linkers) used for the framework construction. MOF-based privileged metal catalysts are further divided into two subgroups depending on how the catalytic units are introduced to a framework (direct incorporation and postsynthetic modification).

Similarly, organic catalysts are divided into two groups depending on the types of catalytic moiety (MOF-based simple organic molecules and MOF-based privileged organocatalysts). MOF-based privileged organocatalysts are further divided into two subgroups depending on how the catalytic units are incorporated into a framework (direct incorporation or postsynthetic modification).

Each subgroup is represented by a three letter symbol. For example, MNC stands for metal catalysis—metal node—chiral linker, indicating that the catalysis occurs at the metal ions at the nodes of a framework, which is constructed with chiral linkers.

Scheme 2. Classification of MOF-Based Asymmetric Catalysts
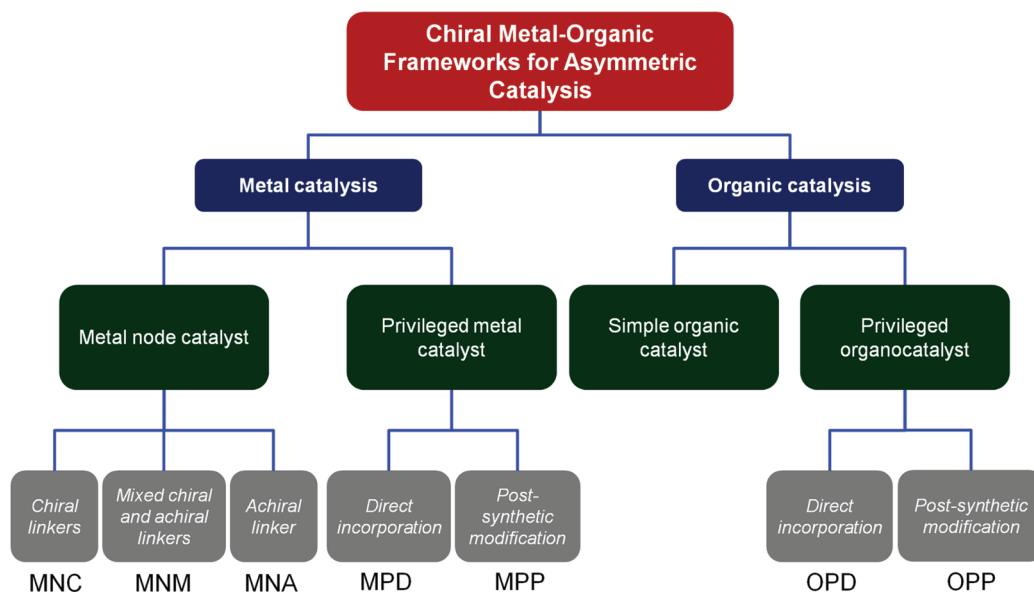
OPP stands for organic catalysis—privileged organocatalyst—postsynthetic modification where the catalysis is performed by a privileged organocatalyst unit incorporated into the framework by postsynthetic modification.

In the following sections, we will describe the design, synthesis, and structure of chiral frameworks and their applications in heterogeneous asymmetric catalysis in detail. In describing the design principles or synthetic strategies for each subclass of MOF-based asymmetric catalysts, we will use graphic symbols and schemes. Graphic symbols are adopted to represent building blocks of MOFs including chiral/achiral linkers, linkers containing privileged metal catalyst or organocatalyst units, (catalytic) metal ions/nodes, and protection groups, which are collected in the toolbox (Table 1). For example, Scheme 3a illustrates a synthetic strategy for MPP (metal—priviledged—postsynthetic modification) type MOF-based asymmetric catalysts (see also Table 2). Here, a chiral, dual-functional ligand, which contains primary framework-forming functional groups and a secondary functional group for a catalytically active metal ion, reacts with a framework-forming metal ion to produce a chiral framework, to which various catalytically active metal ions are introduced by postsynthetic modification. On the other hand, Scheme 3b represents a synthetic strategy for OPP type MOF-based asymmetric catalysts, which involves construction of an achiral framework with open metal coordination sites, using a metal ion and an achiral primary functional ligand (for framework formation), followed by the introduction of a secondary ligand containing a catalytically active unit such as an organocatalytic unit at the open metal coordination sites of the framework by coordination.

2.5. Protocols for Characterization of MOF-Based Heterogeneous Catalysts and Their Catalytic Properties

Before reviewing MOF-based heterogeneous catalysts in detail, here we briefly summarize some standard protocols used for characterization of MOF-based catalysts and investigation of their catalytic properties. A characteristic feature of MOFs is their crystalline nature, which allows us to get their structural information in atomic scale by single-crystal X-ray diffraction studies. State of the art single-crystal X-ray diffraction facilities equipped

with high flux synchrotron radiations are commonly used these days to characterize the structures of MOFs and investigate their structural changes in a single-crystal-to-single-crystal manner.[134−139] In combination with single-crystal X-ray diffraction, powder X-ray diffraction (PXRD) measurements are used to confirm the structure and phase purity of bulk materials. PXRD is also utilized to check the maintenance of the structural integrity of MOFs after catalysis.

As mentioned above, the porosity of frameworks is important for their application in catalysis. Gas sorption experiments after removal of guest (solvent) molecules in the pores are commonly adopted for accessing the "permanent" porosity of MOFs. The analysis of gas sorption isotherms provides the pore size and surface area of the frameworks. Often, frameworks collapse upon guest (solvent) removal by evacuation (and heating), losing crystallinity as judged by PXRD. In many cases, however, the original framework structures are restored upon exposure to the solvent vapor or soaking in the solvent, indicating that the bond connectivity and topology of the framework remained intact in the desolvated state. To avoid the framework collapse or distortion upon guest removal, supercritical CO_2 treatment[140] and freeze-drying method[141] have been used. However, unlike other applications such as gas storage, catalysis usually does not require the "permanent" porosity of a framework as it usually works in the presence of solvents. For catalysis, the porosity and pore accessibility of MOFs in solution are more important, which is often assessed by dye inclusion experiments using visible or fluorescent dyes such as BBR-250[121] or Reichardt's dye.[142] Size selectivity of frameworks in guest inclusion is also demonstrated by sorption of dye molecules of different sizes.

In assessing the asymmetric heterogeneous catalytic activities of chiral MOFs, several experimental protocols have been commonly employed. A common method to demonstrate the heterogeneous nature of the reaction system is the "filtration test" where the filtered supernatant from the reaction medium is tested for its reactivity; for heterogeneous reaction systems, the supernatant should show no or little catalytic activity. The size selectivity of MOF catalysts is demonstrated by performing catalytic reactions with a series of substrates of different sizes.

1199

dx.doi.org/10.1021/cr2003147 |*Chem. Rev.* 2012, 112, 1196–1231

Table 1. Toolbox for Chiral MOFs for Asymmetric Catalysis
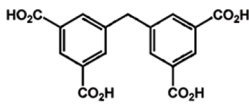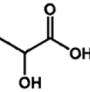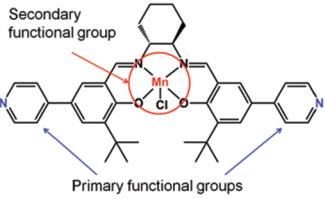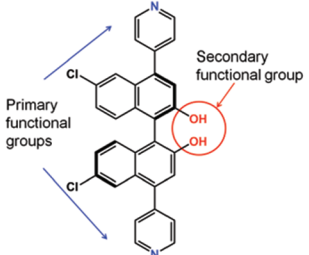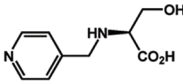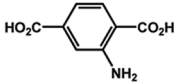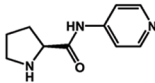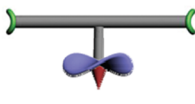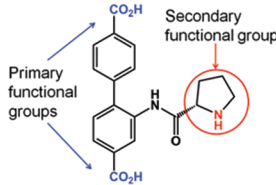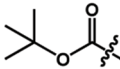
Building block	Note	Example	Strategy
	Metal ion for framework formation	Zn^{2+}, Cu^{2+}, Cd^{2+}	all
	Metal ion or cluster (SBU) at the node of framework	Zn^{2+}, Cd^{2+} or $[Zn(\mu_4\text{-}O)(O_2CR)_6]$	MNP, MPD MPP, OPP OPD
	(Catalytically active) metal ion or cluster (SBU) with open coordination site(s) at the node of framework	Ln^{3+}, $[Zn_2(sol)_2(O_2CR)_6]$	MNC, MNM, MNP, OPP-coordination
	Catalytically active metal ion introduced to privileged catalytic unit	Ti^{4+}, Mn^{2+} Zn^{2+}	MPD, MPP
	(Catalytically active) chiral metal node with open coordination site(s) built with achiral linkers	$[Ce(sol)(O_2CR)_6]$	MNA
	Achiral (organic) multitopic linker		MNM, OPP-coordination
	Achiral multitopic (multidentate) linker		MNA
	Chiral (organic) multitopic linker		MNC, MNM, MNP
	Chiral multitopic linker containing privileged metal catalyst unit		MPD
	Chiral multitopic linker containing privileged ligand unit		MPP

Table 1. Continued

Building block	Note	Example	Strategy
	Catalytically active simple chiral multitopic linker		MOF-based simple organic catalyst
	Functionalizable achiral multitopic linker		OPP-covalent
	Monotopic ligand containing privileged organocatalyst (secondary) unit		OPP-coordination, OPD-coordination
	Achiral multitopic linker containing covalently attached privileged organocatalyst unit		OPD-covalent
	Protection group of organocatalysts		OPD-coordination & covalent

In particular, no or slow conversion of large substrates that do not fit the pores of MOFs indicates that the catalysis mainly occurs inside the pores of MOFs not on the surface. Enantiomeric excess (ee) values usually measured by gas chromatography (GC) or high performance liquid chromatography (HPLC) equipped with chiral columns are used to indicate the degree of enantioselectivity of MOF-based asymmetric catalysts. In addition, people frequently reported recyclability of catalysts by performing catalytic reactions with recycled catalysts.

3. HETEROGENEOUS ASYMMETRIC CATALYSIS USING MOFS

About two dozen reports on MOF-based asymmetric catalysts have thus far appeared in the literature. As described in the previous section, we classify asymmetric MOF catalysts according to their working principle and synthetic strategies (Scheme 3). In this section, the synthetic strategies, crystal structures, and catalytic activities of the frameworks in each class are presented in detail.

3.1. Metal Catalysis

Metal ions properly situated in a chiral environment can act as an asymmetric catalyst. MOFs constructed from metal ions or clusters (SBU) and organic multitopic ligands inherently have metal ions at the nodes of the frameworks. Some metal ions at the nodes have coordinated solvent molecules, which can be easily removed or replaced by substrates without losing the structural integrity of the frameworks. Such metal nodes with open

coordination sites can be utilized as a catalyst in chemical transformations, especially as a Lewis acid catalyst. In this Review, we will use the term "metal node catalysts" for such chiral MOF catalysts and discuss their synthetic strategies in detail in section 3.1.1. Another more rational approach involves incorporation of well-established or privileged asymmetric organometallic catalyst units, such as BINAP, BINOL, and chiral salen-based metal catalysts, into the linkers (or struts) of frameworks to produce chiral MOFs, which can catalyze a wide range of chemical reactions with high enantioselectivity. In this Review, we will call them "MOF-based privileged metal catalysts" and discuss the synthetic strategies in detail in section 3.1.2.

3.1.1. Asymmetric Catalysis Promoted by Metal Ions at the Nodes of Frameworks — "Metal Node Catalysts". To build metal node catalysts, three different approaches have been taken. These approaches are classified as MNC, MNA, and MNM depending on whether chiral, achiral, or mixed (both chiral and achiral) primary ligands, respectively, are employed in the chiral framework formation. Here, we describe these approaches in detail below.

a. Metal Node Catalysts Built with Chiral Primary Ligands (MNC). One strategy to build chiral frameworks with open metal coordination sites at the nodes, which can serve as catalytic centers is shown in Scheme 4, utilizes homochiral primary ligands to create chiral pores in the frameworks (MNC). To encourage the generation of open metal coordination site at the nodes, several tactics have been used, including (a) use of large lanthanide ions, which in general favor high coordination numbers, (b) use

Scheme 3. Representative Strategies To Construct of MOF-Based Asymmetric Catalysts[a]
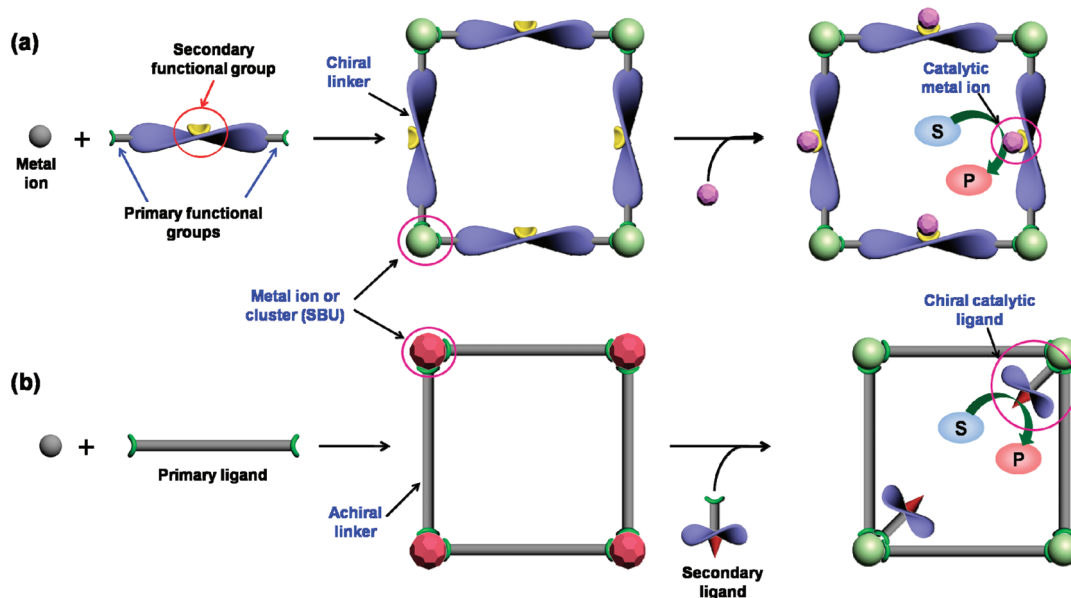
[a] (a) MPP: Construction of MOF using a dual functional ligand containing a privileged ligand unit followed by introduction of catalytically active metal ion via postsynthetic modification. (b) OPP: Construction of achiral MOF using primary ligands followed by introduction of catalytically active secondary ligands containing a privileged organocatalyst unit via postsynthetic modification.

of metal ions (especially Cu(II) or Zn(II)) and carboxylate ligands to form dinuclear metal paddle wheel structure at the nodes, and (c) use of 3-fold symmetry ligands to produce sodalite or HKUST-1 (**tbo**)[143] type frameworks.

Construction of catalytically active chiral MOFs having open metal coordination sites at the nodes of the frameworks was first reported by Lin and co-workers in 2001.[126] They prepared a series of homochiral MOFs with a general formula of $[Ln(L_1-H_2)(L_1-H_3)(H_2O)_4] \cdot xH_2O$ (L_1-H_4 = 2,2′-diethoxy-1, 1′-binaphth-alene-6,6′-bisphosphonic acid, Ln = La, Ce, Pr, Nd, Sm, Gd, Tb, $x = 9-14$, **1a−g**) (Figure 2) using L_1 and lanthanide metal ions as building blocks.

The resulting chiral MOFs have a 2D layered structure, which is further extended into a 3D framework with 1D channels via hydrogen bonding between the 2D layers. Each metal node is coordinated by four oxygen atoms of the phosphonate groups of four different binaphthylbisphosphonates and four H_2O molecules in a square antiprismatic geometry (Figure 3a). The high propensity of lanthanide ions to achieve a high coordination number encouraged the coordination of the labile water molecules to the metal ions at the nodes. The frameworks have large chiral channels with a largest dimension of 12 Å and ∼30% void volume (Figure 3b). The frameworks retained their structural integrity even after removal of solvent molecules. The existence of both large chiral channels and metal ions with easily removable solvent molecules at the node makes the framework a good candidate for Lewis acid catalysis.

The Lewis acid catalytic activity of the framework composed of Sm (**1e**) was examined in several reactions including ring-opening reaction of mesocarboxylic anhydride, cyanosilylation of aldehydes, and Diels−Alder reaction. Although the yield was moderate to good for the cyanosilylation of aldehydes (Table 3), the enantioselectivity was disappointingly low (<5%). Despite the existence of chirality in the struts of the framework, a near achiral environment around the catalytically active Sm centers

resulted in such a low enantioselectivity, illustrating a limitation of this approach.

The same approach was also taken by Tanaka et al. who reported the synthesis of a copper-BINOL-based chiral framework and its catalytic activity in the asymmetric ring-opening reaction of epoxides with amines.[144] They chose Cu(II) ion for construction of the chiral MOF having open metal coordination sites at nodes as the metal ion has high propensity to form dinuclear paddle wheel type SBUs with carboxylate ligands. A crystalline solid of $[Cu_2(5,5′-BDA)_2(H_2O)_2]$ (**2**) was obtained by slow diffusion of N,N-dimethylaniline into methanolic solution of BINOL derivative, (R)-5,5′-H$_2$BDA (2,2′-dihydroxy-1,1′-binaphthalene-5,5′-dicarboxylic acid, (R)-H$_2$−L_2), and copper nitrate. The chiral framework **2** had dinuclear Cu(II) paddle wheel motifs at the nodes, which were linked by L_2 to form a 2D square grid net (Figure 4a). The axial position of the copper paddle wheels was coordinated by MeOH, which can be easily removed upon evacuation. Removal of the solvent resulted in the loss of crystallinity, which was, however, restored upon resorption of solvent as judged by PXRD. The 2D layers are stacked in an A−B−A sequence (Figure 4b), which blocks the open channels of the square grids.

The chiral framework **2** with Lewis acidic Cu sites was successfully used as a catalyst in asymmetric ring-opening reaction of epoxides with aromatic amines (Table 4). While (S)-BINOL ligand was ineffective in the catalytic ring-opening reaction of epoxides, **2** catalyzed the reaction to afford the corresponding amino alcohols in a moderate yield and enantioselectivity. Although it was not reported whether the catalytic reaction took place in the pores or on the surface of the crystalline solid, the latter is more likely, considering the framework structure (A−B−A type stacking of the 2D grids).

Recently, Kaskel, Glorius, and co-workers also took this approach to synthesize homochiral MOFs with catalytically active metal nodes.[142] For the construction of a framework having large pores and coordinatively unsaturated metal sites at

Table 2. List of Chiral MOF-Based Asymmetric Catalysts

entry	catalytic MOF	catalytic reaction	conversion (%)	ee (%)	type MOF	reference
1	$[Sm(L_1-H_2)(L_1-H_3)(H_2O)_4]\cdot xH_2O$ (1e)	cyanosilylation of aldehydes	55−69	<5	MNC	126
2	$[Cu_2(L_2)_2(H_2O)_2]\cdot MeOH\cdot 2H_2O$ (2)	ring-opening reaction of epoxides	15−54	43−51		144
3	Zn_3(ChirBTB-1)$_2$ (3)	Mukaiyama aldol reaction	22−83	0−40		142
4	Zn_3(ChirBTB-2)$_2$ (4)		0−74	0−8		
5	$[Zn_2(bdc)(\text{L-lac})(DMF)]\cdot DMF$ (5)	oxidation of sulfides	60−100	0[a]	MNM	151
6	Ce-**MDIP**-1 and -2 (6, 7)	cyanosilylation of aldehydes	>95	91−98	MNA	131
7	$\{Zr[Ru(L_8)(DMF)_2Cl_2]\}\cdot 2MeOH$ (8)	hydrogeneation of β-keto esters	>99	67−95	MPD	159
8	$\{Zr[Ru(L_9)(DMF)_2Cl_2]\}\cdot 2MeOH$ (9)		>99	16−79		
9	$\{Zr[Ru(L_8)(DPEN)Cl_2]\}\cdot 4H_2O$ (10)	Hhydrogenation of aromatic ketones	>99	93−97		163
10	$\{Zr[Ru(L_9)(DPEN)Cl_2]\}\cdot 4H_2O$ (11)		>99	59−84		
11	$[Zn_2(bpdc)_2(L_{24})]\cdot 10DMF\cdot 8H_2O$ (24)	epoxidation	71	82		128
12	$[Zn_4(\mu_4\text{-O})(L_{25-27})_3]$ (25−27)		54−99	38−92		121
13	$\{Zn_4O[Ru(L_{29})(py)_2]Cl\}\cdot 7DBF\cdot 7DEF$ (29)	cyclopropanation	7.8−54	51−91		174
14	$[Zr(L_{12-14})]\cdot xH_2O$ (12−14)	diethylzinc additions to aldehydes	70−99	29−72	MPP	166
15	$[Cd_3Cl_6(L_{15})_3]\cdot 4DMF\cdot 6MeOH\cdot 3H_2O$ (15)		>99	80−93		127
16	$[Cd_3(L_{15})_4(NO_3)_6]\cdot 6MeOH\cdot 5H_2O$ (16)		>99	60−90		167
17	$[Cu_2(L_{18b-21b})(solvent)_2]$ (18b−21b)		99	70−94		130
18	$[Zn_2(L_{20b})(DMF)(H_2O)]\cdot 2EtOH\cdot 4.3DMF\cdot 4H_2O$ (22b)		99	12−30		168
19	$[Cu_2(L_{23})(H_2O)_2]\cdot 7.6DEF\cdot 9.6MeOH$ (23)	carbonyl-ene reaction[b]	89−92	23−50[c]		169
		hetero Diels−Alder reaction	52−80	33−55		
20	$[Zn_4(\mu_4\text{-O})(L_{28})_3]\cdot 40DBF\cdot 6EtOH\cdot H_2O$ (28)	sequential epoxidation and ring-opening of epoxide	57−60	50−81	MPP and MNC	172
21	$[Zn_3(\mu_3\text{-O})(L_{29}-H)_6]\cdot 2H_3O\cdot 12H_2O$ (31)	transesterification	77	∼8	MOF-based simple organic catalyst	80
22	$[Cu(asp)(bpe)_{0.5}]\cdot 0.5H_2O\cdot 0.5MeOH$ (33)	methanolysis of cis-2,3-epoxybutane	30−59	10−17	OPP	178
23	$[Cu_2(L_{34})_2Cl_2]\cdot H_2O$ (34)	1,2-addition of α,β-unsaturated ketones	88−98	55−99		179
24	$[Cr_3O(L_{35}\text{ or }L_{36})_x(H_2O)_{2-x}F(bdc)_3]\cdot 0.15(H_2bdc)\cdot H_2O$ (35, 36)	Aldol reaction	58−91	29−76		129
26	$[Cd_3(BTB)_2(\text{L-PYI})]$ (37)		42−97	58−61	OPD	131
27	$[Zn_4O(L_{39})_3]$ (39)			29	OPD	133

[a] Although no asymmetric induction was observed, the products enantioselectively absorbed inside the pores with ee ranging from 20% to 27% depending on substrates leaving equal amount of other enantiomer in the solution. [b] The reaction required more than the stoichiometric amount of the catalyst. [c] Diastereomeric excess with Mosher ester form.

Scheme 4. A Synthetic Strategy for MOF-Based Metal Node Catalysts Using Chiral Primary Ligand (MNC)
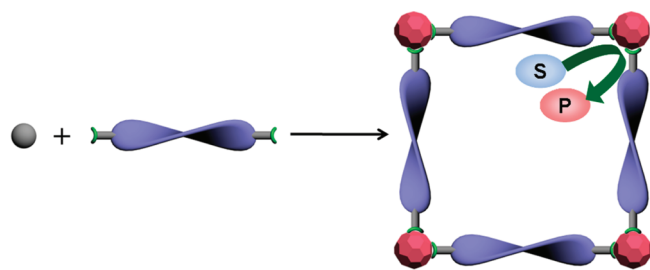
the nodes, they chose a triangular BTB (4,4′,4″-benzene-1,3,5-triyltribonzoate) as a parent ligand, which had been used to form MOFs with large pores such as HKUST-1[143] and MOF-14.[145] To introduce a chiral moiety in close vicinity to open accessible metal nodes, they introduced a well-known chiral auxiliary, oxazoline, to the ortho position of the benzoates (Figure 5). The resulting ligands ChirBTB-1 (L_3) and ChirBTB-2 (L_4) bearing 4-iso-propyloxazolidin-2-one or 4-benzyloxazolidin-2-one groups, respectively, at the ortho position of their benzoate groups reacted with Zn^{2+} to form chiral frameworks, Zn_3(ChirBTB-1)$_2$ (3) and Zn_3(ChirBTB-2)$_2$ (4) (Figure 5). Although 3 and 4 have the same molecular formula, the structures are quite different. Similar to HKUST-1, 3 has a twisted boracite (**tbo**) topology[146−148] with dinuclear Zn paddle wheel units at the nodes. Among three different types of pores present in 3, the largest pore ∼33 Å in diameter has accessible Zn sites pointing toward the center of the pore, which can serve as catalytic sites. On the other hand, in 4, trinuclear $M_3(RCO_2)_6$ units, another common SBU in MOFs, serve as 6-connecting nodes, which were then connected by the chiral linkers to form a chiral 3D net with "**cys**" topology.[147,148] Two different types of channels are presented in the framework
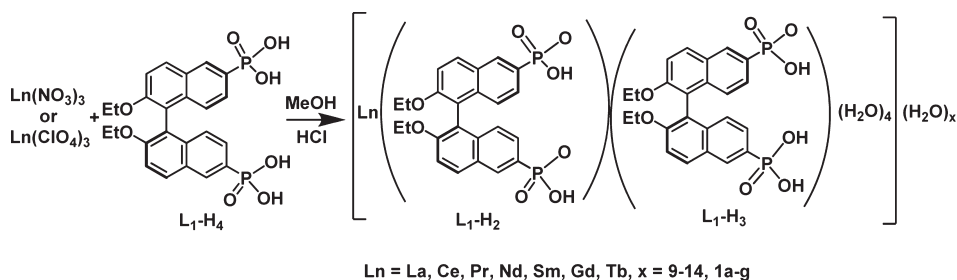
Figure 2. Synthesis of $[Ln(L_1-H_2)(L_1-H_3)(H_2O)_4]\cdot xH_2O$ (**1a**−**g**). Reprinted with permission from ref 88. Copyright 2009 Springer.
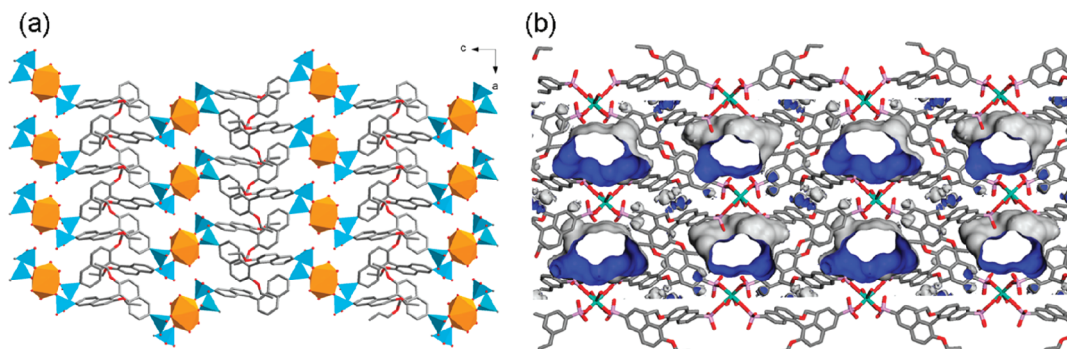

Figure 3. (a) A view of 2D framework of **1f** down the *b* axis (the coordination environments of P atoms and Gd atoms are represented with blue and orange polyhedra, respectively), and (b) Connolly surface of framework **1f** showing 1D channels between 2D layers. Reprinted with permission from ref 88. Copyright 2009 Springer.

Table 3. Asymmetric Cyanosilylation of Aldehydes Catalyzed by 1e
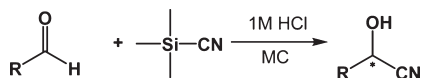
substrate	catalyst loading (mol %)	conversion (%)	ee (%)
Ar	10	69	<5
−CH₂−CH₃	10	55.3	<5
1-naphthyl	10	61	<5

running through all three directions with the largest channel size of 18×18 Å². Even though the authors failed to prove the permanent porosity of the frameworks by gas sorption, fluorescence dye inclusion experiments clearly demonstrated the porous nature of the frameworks in solution.

Because **3** and **4** both have large pores and accessible metal ions at the nodes, they can be used as a Lewis acid catalyst. Especially, the chiral auxiliaries are located right next to the metal nodes providing a unique opportunity for asymmetric Lewis acid catalysis. Both **3** and **4** were tested in the Mukaiyama aldol reactions of aldehydes with 1-methoxy-1-(trimethylsiloxy)-2-methyl-1-propene, which generally requires a strong Lewis acid catalyst (Table 5). The observed ee values of the reaction depend on the solvent used. While no enantioselectivity was observed for benzaldehyde in CH₂Cl₂ using **3** as a catalyst, 9% ee was observed in *n*-heptane. For the same catalytic reaction, **4** showed comparable ee values, 8% and 6% in CH₂Cl₂ and *n*-heptane, respectively. The highest ee values up to 40% and 16% were obtained using **3** as a catalyst for the conversion of

1-napthaldehyde in CH₂Cl₂ and *n*-heptane, respectively. Despite the relatively low enantioselectivity, this is an interesting approach for the asymmetric catalysis harnessing open metal sites at the nodes and chiral auxiliaries positioned near the metal nodes.

b. Metal Node Catalysts Built with Mixed (Chiral and Achiral) Primary Ligands (MNM). The second strategy to build chiral frameworks with open metal coordination sites at the nodes is shown in Scheme 5, which utilizes both achiral primary ligands and readily available homochiral primary ligands such as amino acids to form homochiral frameworks. In this strategy, metal ions and homochiral primary ligands form chiral 1D[149] chains or 2D[150] grids, which are further extended into 2D or 3D structures by rigid, achiral linkers in a one-pot synthesis. One advantage of the MNM strategy over the MNC is the use of cheap, naturally existing chiral molecules as a building block for homochiral frameworks, instead of synthetic chiral building blocks, which often require costly and laborious synthesis. In 2006, Kim, Fedin, and co-workers took this strategy to synthesize a homochiral MOF having catalytically active metal nodes.[151]

Reaction of zinc nitrate, L-lactic acid, and 1,4-benzenedicarboxylic acid (H₂bdc) in DMF produced a homochiral framework $[Zn_2(bdc)(L-lac)(DMF)]\cdot DMF$ (**5**·DMF), in which zinc ions and chiral primary ligand, L-lactic acid, formed 1D chiral chains (serving as SBUs) interconnected through the achiral bdc to afford a chiral 3D open-framework (Figure 6). One of two independent Zn ions has a labile solvent molecule coordinated to the metal ion, which can thus be utilized as a Lewis acid catalyst.

The homochiral framework with permanent porosity, **5**·DMF, was utilized in enantioselective sorption of pharmaceutically important sulfoxides (Scheme 6).[152] The DMF molecules in the pores can be removed by heating under vacuum. The partially evacuated material **5**·0.4DMF showed significant

1204

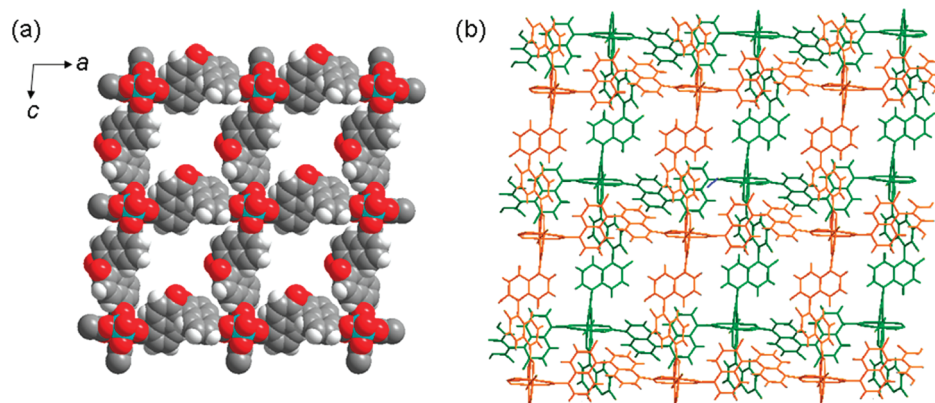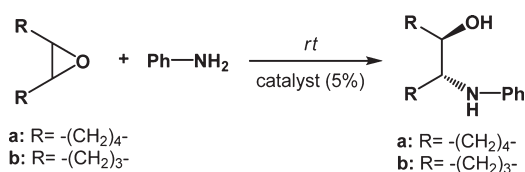dx.doi.org/10.1021/cr2003147 |*Chem. Rev.* 2012, 112, 1196−1231

Figure 4. (a) 2D square grid net structure of **2**, and (b) A—B—A stacking of 2D grids viewed along the *b* axis. Copyright 2008 Royal Society of Chemistry.

Table 4. Asymmetric Ring-Opening Reaction of Epoxides with Amine Catalyzed by 2

a: R= -(CH₂)₄-
b: R= -(CH₂)₃-

a: R= -(CH₂)₄-
b: R= -(CH₂)₃-

catalyst	epoxide	solvent	time (h)	yield (%)	ee (%)
2	**a**	toluene	48	54	45
2	**b**	toluene	48	15	43
2	**a**	no solvent	24	51	51
2	**b**	no solvent	24	30	50
L₂	**a**	no solvent	24	3	2
L₂	**b**	no solvent	24	1	0

enantioselective sorption ability for the aromatic sulfoxides with small substituents (ee values ∼20%) in favor of *S* isomer. Furthermore, **5** showed a remarkable catalytic activity in the oxidation of thioethers to sulfoxides by urea hydroperoxide (UHP) or H_2O_2. Although the selectivity and conversion (for sulfoxide over sulfone, >90%) were reasonable with UHP for the substrates with small substituents, the substrates with bulk substituents failed to show any measurable conversion, suggesting that the catalysis occurred inside the pores. Even higher conversion (up to 100%) and chemoselectivity was observed with H_2O_2 as the oxidant in a mixed solvent system. The catalytic activity of **5** for selective sulfoxidation remained similar even after 30 cycles. Unfortunately, no or little asymmetric induction was found in the catalytic sulfoxidation reactions. Apparently, the chiral ligand (L-lac) attached to the metal nodes was not effective for chiral induction in the sulfoxidation promoted by the metal. Nevertheless, enantioenriched sulfoxides were obtained by enantioselective sorption of the resulting racemic mixture by the chiral pores of **5** (stoichiometric or comparable amount of **5** was used), which occurred simultaneously with the catalytic process. Thus, after catalytic oxidation of sulfide, (*S*)-sulfoxide was preferentially absorbed by the pore of **5** leaving an equal amount of the excess *R* enantiomer in the solution phase (∼20% ee). The combination of the high catalytic activity and enantioselective sorption property of **5** provides a unique

opportunity to device a one-step process to produce enantioen-riched products. The Fedin group extended this work to produce several other homochiral MOFs with open metal coordination sites at the nodes.[153] Although their application in enantioselective sorption was studied, their (asymmetric) catalytic activity has not yet been reported.

This strategy allows easy synthesis of homochiral MOFs using readily available homochiral ligands. However, it is often difficult to predict the structures of the resulting frameworks and whether or not they have open metal coordination sites at the nodes.

c. Metal Node Catalysts Built with Achiral Primary Ligands and Chiral Templates (MNA). Chiral MOFs with topological chirality such as (10,3)-a net can be constructed from achiral linkers, and two enantiomeric forms can be resolved by using chiral templates such as enantiopure solvents of crystallization, counterions, or auxiliaries. For example, Rosseinsky et al. employed enantiopure coligand 1,2-propanediol as a template to induce the formation of homochiral MOFs with a doubly interpenetrated (10,3)-a net.[154] Enantioselective sorption was demonstrated with the homochiral frameworks, but no catalytic activity was reported even though the metal nodes have labile ligands.

Another way to construct chiral MOFs from achiral linkers is to utilize chirality generated by two or more noncoplanar chelate rings around metal nodes upon framework formation as schematically illustrated in Scheme 7 (MNA). A chiral template can induce a particular enantiomeric form of the chiral frame-work. For example, in 2010, Duan and co-workers reported a catalytically active homchiral MOF constructed from an achiral chelating ditopic primary ligand with an assistance of a chiral template.[131] Solvothermal reaction of $Ce(NO_3)_3$ and achiral ligand, methylenediisophthalic acid (H_4**MDIP**), in the presence of chiral template, L- or D-*N-tert*-butoxy-carbonyl-2-(imidazole)-1-pyrrolidone (L- or D-**BCIP**), produced MOFs, Ce-**MDIP**-1 (**6**) or Ce-**MDIP**-2 (**7**), respectively. Enantiomorphic **6** and **7** were crystallized in the chiral space group $P2_1$, but with opposite chirality to each other (Figure 7). They have a noninterpenetrat-ing 3D network containing chiral channels with a cross-section of 10.5×6.0 Å² along the *a* axis. Interestingly, the chiral inducer (L- or D-**BCIP**) was not included in the frameworks as confirmed by single-crystal X-ray crystallography and elemental analysis. Each cerium ion was coordinated by five monodentate carboxylate groups of **MDIP**, two oxygen atoms from one bidentate carboxy-late group of **MDIP**, and one water molecule. Most importantly,
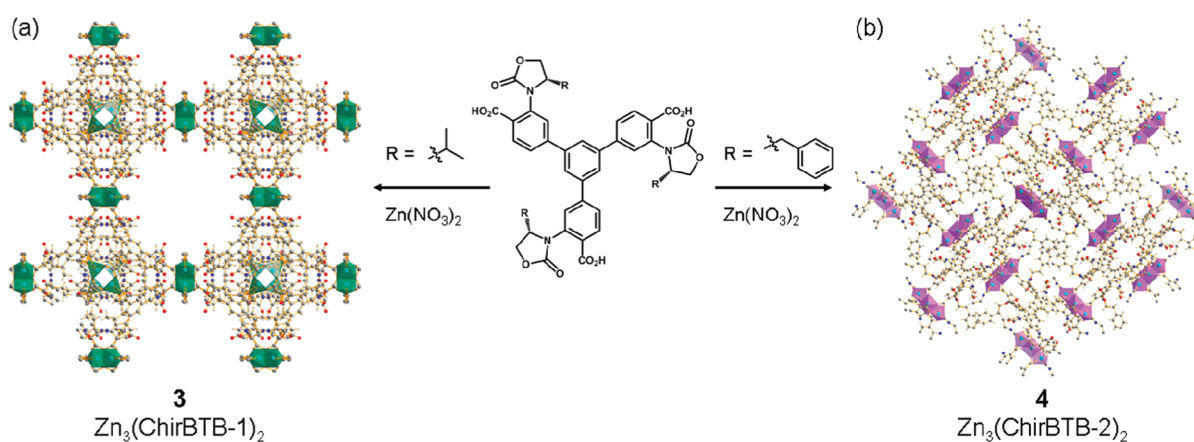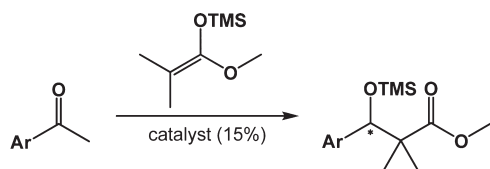
Figure 5. Structures of (a) $Zn_3(ChirBTB-1)_2$ and (b) $Zn_3(ChirBTB-2)_2$ viewed along the c axis. Reprinted with permission from ref 142. Copyright 2011 Wiley-VCH.

Table 5. Asymmetric Mukaiyama Aldol Reactions Catalyzed by 3 and 4

Ar	catalyst	yield (%)	ee (%)
	Solvent: Dichloromethane		
Ph	3	83	0
1-Naph	3	31	40
Ph	4	66	8
1-Naph	4	0	
	Solvent: *n*-Heptane		
Ph	3	77	9
1-Naph	3	77	16
Ph	4	43	6

the coordination geometry of the Ce metal node in **6** and **7** was chiral, and they are mirror images of each other (Figure 7).

Because the Ce metal nodes containing labile water molecules in the coordination sphere can serve as a Lewis acid catalyst, the catalytic activities of **6** and **7** in asymmetric cyanosilylation of aldehydes were examined (Table 6). Remarkably, although **6** and **7** are composed of only achiral building blocks, they showed excellent enantioselectivity (>91%) in the asymmetric cyanosilylation with high conversion (>95%). In contrast, despite a good conversion (>95%), the corresponding homogeneous catalyst $Ce(NO_3)_3 \cdot 6H_2O$, showed no enantioselectivity in the same reaction. Filtration tests confirmed the heterogeneous nature of the asymmetric catalysis of **6** and **7**, which can be recycled at least three times without a significant loss of catalytic activity and enantioselectivity. Although the authors did not provide any explanation for the origin of enantioselectivity of **6** and **7**, the strong Cotton effects of their CD spectra suggest that the local chiral environment generated by achiral building blocks around the metal centers provide strong chiral induction to the substrates during the catalysis.

In general, it is difficult to pin down the exact origin of the enantioselectivity of MOF metal node catalysts reported so far due to the lack of their homogeneous counterparts. Furthermore, despite their conceptual simplicity, it is difficult to rationally design chiral MOFs having open coordination sites at metal nodes with a proper chiral environment around the catalytic centers to achieve high enantioselectivity in chemical reactions. Especially, controlling the distance and relative orientation between the catalytic center and chiral induction unit in a framework to achieve high enantioselectivity remains challenging.

d. Metal Node Catalysts by Postsynthetic Modification (MNP). Metal node catalysts reported so far utilize metal ions at the nodes, which are incorporated into frameworks during the framework formation, as catalytic centers. However, some metal ions cannot be incorporated into the nodes of frameworks by direct synthesis using the strategies discussed above, even though they might have interesting catalytic activities. At least in principle, however, such metal ions of interest can be introduced at the nodes of a framework by metathesis—exchange with the existing metal ions at the nodes of the framework (Scheme 8). Several research groups have recently demonstrated the full[155,156] or partial exchange[157,158] of metal ions at the nodes of achiral frameworks without disrupting the framework structures. Although there is no such example yet, such postsynthetic modification process through metathesis of metal ions at the nodes should be useful in converting catalytically inactive chiral frameworks into a series of metal node catalysts with identical framework structures but different catalytic activities.

3.1.2. Asymmetric Catalysis Promoted by Privileged Metal Catalyst Units Directly Incorporated into the Frameworks—"MOF-Based Privileged Metal Catalysts" (MPD and MPP). Although metal ions at the nodes of MOFs can be exploited as a catalytic center as described above, a rational design of such metal node catalysts with high enantioselectivity is rather difficult due to the lack of their homogeneous counterparts. A more rational approach involves incorporation of well-established or privileged asymmetric organometallic catalyst units, such as BINAP, BINOL, and chiral salen-based metal catalysts, into the linkers (or struts) of a framework to produce chiral MOFs catalyzing a wide range of chemical reactions with high enantioselectivity, which we now call "MOF-based privileged metal catalysts" in this Review. To introduce privileged metal catalyst units at the struts of frameworks, two

Scheme 5. A Synthetic Strategy for MOF-Based Metal Node Catalysts Using Mixed Chiral and Achiral Primary Ligands (MNM)
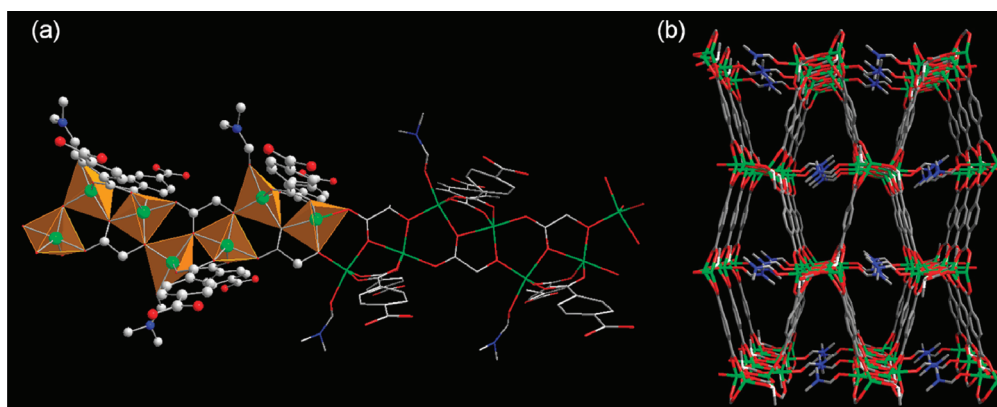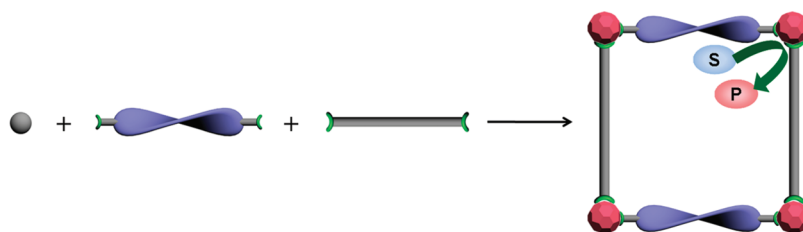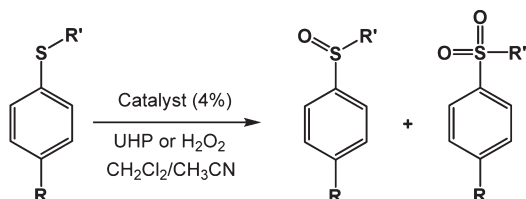

Figure 6. (a) 1D chiral SBU composed of Zn and L-lactate, and (b) chiral 3D open-framework composed of 1D SBU and BDC. Reprinted with permission from ref 151. Copyright 2011 Wiley-VCH.
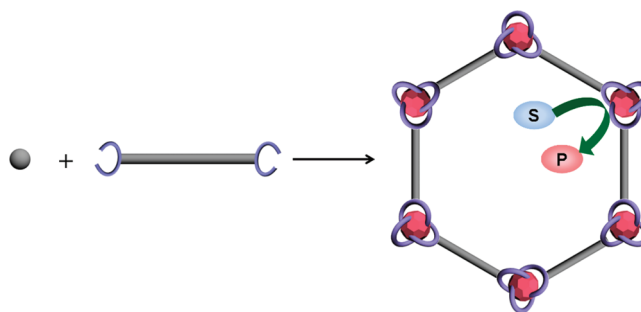
Scheme 6. Oxidation of Sulfoxides Catalyzed by 5

Scheme 7. A Synthetic Strategy for MOF-Based Metal Node Catalysts Using a Chelating Ditopic Achiral Primary Ligand (MPP)

complementary synthetic strategies have been developed. One strategy (MPD; metal catalysis—privileged catalyst—direct incorporation) involves direct incorporation of a precatalyst unit into the struts of a framework during the framework formation, utilizing a framework-forming metal ion and a chiral primary ligand containing the precatalyst unit (Scheme 9). The other strategy (MPP; metal catalysis—privileged catalyst—postsynthetic modification) involves chiral frameworks built with a dual functional primary ligand containing primary functional groups for framework formation and an orthogonal secondary functional group, to which a catalytically active metal ion is introduced via postsynthetic functionalization (Scheme 10). While MPD strategy provides a versatile way to synthesize a wide range of MOF-based privileged catalysts, it is not compatible with some labile Lewis acid catalysts or reactive transition metal catalysts, which can be overcome by the MPP approach. However, the latter tolerates only secondary functional groups chemically orthogonal to the primary functional groups, which limits its use in the construction of MOF-based privileged catalysts.

a. Noncrystalline MOF-Based Privileged Metal Catalysts Built with BINAP or BINOL. Lin and co-workers first adopted the MPD strategy (Scheme 9) for the construction of catalytically active organic—inorganic hybrid materials.[159] Chiral linkers equipped

with both primary functional groups for framework formation and a chiral secondary functional group for asymmetric catalytic sites were prepared by functionalization of BINAPs. The resulting chiral linkers, 2,2′-bis(diphenylphosphino)-1,1′-binaphthyl-6,6′-bis-(phosphonic acid) (L_8—H_4) and 2,2′-bis(diphenylphosphino)-1,1′-binaphthyl-4,4′-bis(phosphonic acid) (L_9—H_4), were further functionalized by introduction of catalytically active Ru ions to the chiral secondary functionality. Using linkers composed of the chiral metal complexes, porous zirconium phosphonate coordination polymers, $\{Zr[Ru(L_8)(dmf)_2Cl_2]\}\cdot2MeOH$ (Zr—Ru—L_8, **8**) and $\{Zr[Ru(L_9)(dmf)_2Cl_2]\}\cdot2MeOH$ (Zr—Ru—L_9, **9**), were prepared (Figure 8). Unfortunately, their structural information was not available because of the amorphous nature of the coordination polymers. Nitrogen adsorption experiment, however, indicated that **8** and **9** possess a high degree of porosity.
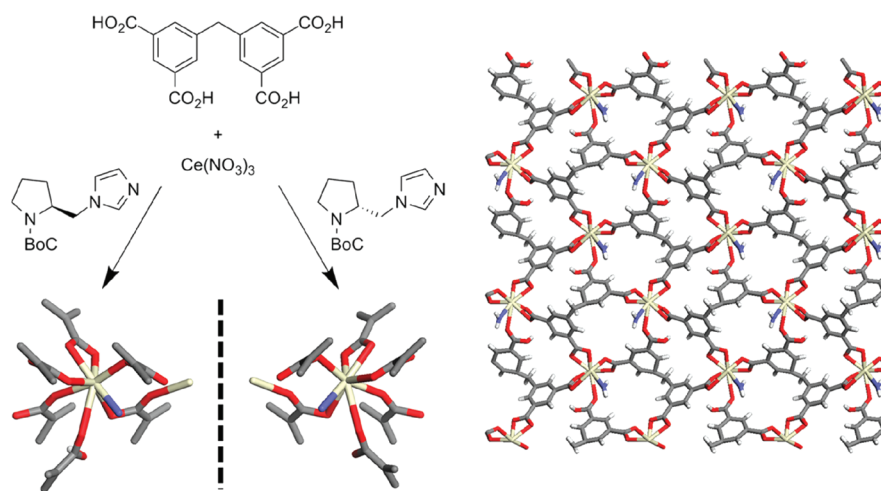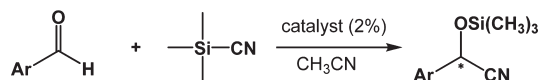
1207

dx.doi.org/10.1021/cr2003147 |*Chem. Rev.* 2012, 112, 1196–1231

Figure 7. Mirror image structures of Ce-**MDIP**-1(**6**) and Ce-**MDIP**-2 (**7**) and 3D network structure of Ce-**MDIP**-1 (**7**).

Table 6. Asymmetric Cyanosilylation of Aldehydes Catalyzed by 6 and 7

	6		7		$Ce(NO_3)_3 \cdot 6H_2O$	
Ar	yield (%)	ee (%)	yield (%)	ee (%)	yield (%)	ee (%)
Ph	>95	93	>95	94	95	
4-MeOPh	>95	91	>95	97	97	
1-Naph	>95	98	>95	>98	97	
2-Naph	>95	>98	>95	>98	98	

Despite the noncrystalline nature of the coordination polymers, the high degree of porosity with integrated catalytic active sites made them good heterogeneous catalysts. As summarized in Table 7, both **8** and **9** showed high catalytic activity for asymmetric hydrogenation of β-keto esters. The catalytic hydrogenation of various β-alkyl-substituted β-keto esters using **8** showed complete conversion with over 90% ee values, which are comparable to that of the homogeneous counterpart.[160−162] The heterogeneous catalyst **8** was easily recyclable up to five times without significant deterioration of enantioselectivity. Despite high conversion, however, the hydrogenation reaction using **9** gave much lower ee values presumably due to substituent effects on BINAP.

Although over 90% enantioselectivity was achieved by **8** for β-alkyl-substituted β-keto esters, the enantioselectivity for β-aryl substituted substrates was much lower. To improve the enantioselectivity for β-aryl-keto esters, the same group also synthesized analogous Zr-phosphonated coordination polymers having chelating DPEN (1,2-diphenylethylenediamine) ligand coordinated to the Ru center, $\{Zr[Ru(L_8)(DPEN)Cl_2]\}\cdot 4H_2O$ (**10**) and $\{Zr[Ru(L_9)(DPEN)Cl_2]\}\cdot 4H_2O$ (**11**).[163] Nitrogen adsorption measurements showed that both **10** and **11** are porous with a rather wide pore size distribution. The catalytic activities of **10** and **11** for the asymmetric hydrogenation of aromatic ketones were examined (Table 8). At only 0.1 mol % catalyst loading, **10** gave complete conversion with remarkably high ee values (>93%), which are significantly higher than that (∼80%) of the corresponding homogeneous catalyst Ru(BINAP)(DPEN),[164,165] whereas **11**

yielded only modest ee values. The catalyst **10** was successfully recycled up to six times without loss of the catalytic activity and enantioselectivity.

Lin and co-workers also utilized the MPP strategy involving the introduction of catalytically active metal ions to the struts of preassembled chiral frameworks (Scheme 10). In 2004, using BINOL-derived bisphosphonic linkers L_{12}, L_{13}, and L_{14}, they synthesized Zr-phosphonate coordination polymers, $[Zr(L_{12})] \cdot xH_2O$ (**12**), $[Zr(L_{13})] \cdot xH_2O$ (**13**), and $[Zr(L_{14})] \cdot xH_2O$ (**14**), respectively (Figure 9).[166] Similar to coordination polymers **8** and **9** discussed above, **12**−**14** were also amorphous. Nitrogen adsorption measurements confirmed the porous nature of the polymers, and their surface areas varied depending on the size of the BINOL-based linkers. The chiral nature of the solids was confirmed by solid-state CD spectroscopy.

Most importantly, they have free secondary functional groups (chiral dihydroxy groups) ready to take up catalytically active metal ions to generate asymmetric catalytic sites. Treating the amorphous porous chiral zirconium phosphonates **12**−**14** with excess of $Ti(O^iPr)_4$ generated active catalysts for the asymmetric addition of diethylzinc to aldehydes to yield chiral secondary alcohols with good conversion and moderate to good ee values (Table 9). The heterogeneous nature of the catalytic system was proved by the fact that the supernatant solution was unable to activate $Ti(O^iPr)_4$ for the catalytic reaction. In a control experiment, the porous zirconium phosphonate derived from 2,2′-diethoxy-1,1′-binaphthyl-6,6′-bis(styrylphosphonic acid) (**14-OEt₂**), in which the chiral dihydroxy group was protected, produced only a racemic mixture.

b. Crystalline MOF-Based Privileged Metal Catalysts Built with BINOL or Its Analogues. Although the Lin group successfully synthesized chiral porous coordination polymers for asymmetric catalysis using both MPD and MPP strategies, they were amorphous, which made the detailed structural characterization of the active sites impossible. In 2005, the same group finally succeeded in synthesizing a crystalline homochiral MOF using a pyridyl functionalized BINOL linker.[38] A rigid BINOL derivative having pyridyl groups on 4 and 4′ positions, (R)-6,6′-dichloro-2,2′-dihydroxy-1,1′-binaphthyl-4,4′-bipyridine (L_{15}), reacted with CdCl₂ to afford a chiral MOF with a molecular formula $[Cd_3Cl_6(L_{15})_3] \cdot 4DMF \cdot 6MeOH \cdot 3H_2O$ (**15**), which crystallized in the chiral P1 space group. In **15**, octahedrally coordinated Cd(II)

Scheme 8. A Synthetic Strategy for MOF-Based Metal Node Catalysts via Postsynthetic Modification (MNP)
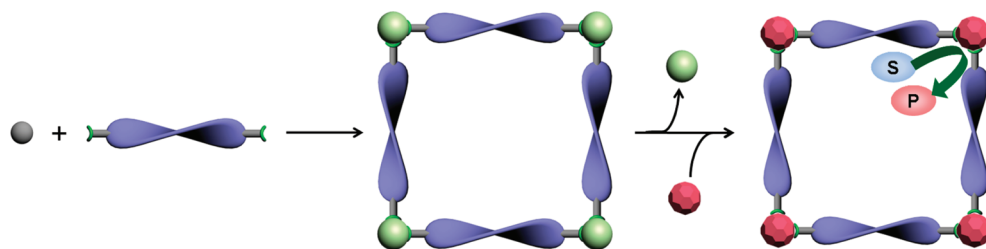
Scheme 9. A Synthetic Strategy for MOF-Based Privileged Metal Catalysts by Direct Incorporation of Precatalyst via Postsynthetic Modification (MPD)
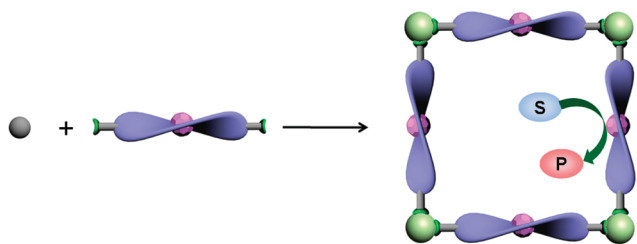
ions were doubly bridged by chloride ions to form 1D zigzag chains $[Cd(\mu\text{-}Cl)_2]_n$ serving as SBUs, which were further extended into a noninterpenetrating 3D porous network by coordination of the metal ions to the pyridyl groups of L_{15}. The resulting framework has large 1D channels of $1.6 \times 1.8 \text{ nm}^2$ cross-section and contains 54.4% void space (Figure 10a). Powder XRD and CO_2 adsorption experiments demonstrated the permanent porosity of the framework even after guest removal.

Even though the chiral dihydroxy groups of two-thirds of the linkers were not accessible because of shielding by neighboring naphthyl rings, those of the remaining linkers were exposed to the open channels rendering the formation of catalytically active metal centers, $Ti(BINOL)(O^iPr)_2$, upon treatment with $Ti(O^iPr)_4$ (Figure 10b). The Ti coordinated framework (**15-Ti**) was an active heterogeneous asymmetric catalyst for diethylzinc addition to aldehydes showing complete conversion and high ee ranging from 80% to 93% (Table 9), which is comparable to that of the homogeneous counterpart $BINOL\text{-}Ti(O^iPr)_4$. The size selectivity of the catalysts was examined using dendritic aldehydes of varying sizes. The homogeneous catalyst, $BINOL\text{-}Ti(O^iPr)_4$, showed similar catalytic activity for all dendritic aldehydes regardless of the size of aldehydes, whereas the yield and ee of the reaction catalyzed by **15-Ti** decreased as the size of dendritic aldehydes increased, which suggested the catalysis mainly occurred inside the channels of **15-Ti**.

In 2007, Lin and co-workers synthesized two more homochiral MOFs using the same pyridyl functionalized BINOL ligand (L_{15}) and Cd^{2+} ion, but with different counteranions.[167] Ligand, L_{15}, reacted with cadmium salts, $Cd(NO_3)_2\cdot4H_2O$ and $Cd(ClO_4)_2\cdot6H_2O$, produced $[Cd_3(L_{15})_4(NO_3)_6]\cdot6MeOH\cdot5H_2O$ (**16**) and $[Cd_3(L_{15})_2(H_2O)_2]\cdot[ClO_4]_2\cdot2DMF\cdot4MeOH\cdot3H_2O$ (**17**), respectively. Although **16** and **17** were synthesized under similar reaction conditions, they adopted completely different structures depending on the counteranions of metal sources. Compound **16** crystallized in the tetragonal $P4_122$ space group with two types of Cd(II) centers in the asymmetric unit. The first

type of Cd(II) centers was octahedrally coordinated by four ligands and two nitrate ions to form a 2D square grid with dimensions of $20.3 \times 20.3 \text{ Å}^2$, while the second type of Cd(II) centers was coordinated by two nitrate ions and two ligands to form 1D polymeric chains. The zigzag 1D chains and 2D grids were joined to each other by bridging nitrate ions to form a 2-fold interpenetrated 3D framework with large interconnected channels whose dimensions were $4.9 \times 13.1 \text{ Å}^2$ parallel to the a and b axes and $13.5 \times 13.5 \text{ Å}^2$ parallel to the c axis (Figure 11). On the other hand, **17** crystallized in a $P4_32_12$ space group with each Cd(II) center coordinated by four ligands and two water molecules to form an interlocked 2D rhombic grids (Figure 11b). It has 1D channels with dimensions of $1.2 \times 1.5 \text{ nm}^2$. The stability and the permanent porosity of these frameworks were confirmed by PXRD and CO_2 adsorption experiments, respectively.

Treatment of **16** with excess $Ti(O^iPr)_4$ generated active catalyst **16-Ti**, which catalyzed the addition of diethylzinc to aromatic aldehydes with almost complete conversion and high ee values up to 90% (Table 9). By contrast, a mixture of **17** and $Ti(O^iPr)_4$ under the same conditions showed no catalytic activity for asymmetric diethylzinc addition. A careful inspection of the structure of **17** revealed that the chiral dihydroxy groups required for generation of an active catalyst were hindered by the metal hinges $[Cd(py)_2(H_2O)_2]$ formed by the strong $\pi\cdots\pi$ interactions from the interpenetrating 2D rhombic grids. The structural congestion around the chiral dihydroxy groups apparently prevented the fromation of complexes with $Ti(O^iPr)_4$. The drastic difference in the catalytic activities of **16** and **17** is remarkable, given that they were constructed from exactly the same ligand and metal ions but only with different counteranions, which highlights the importance of framework structures in determining catalytic activities.

Extending this strategy, Lin et al. recently reported a series of isoreticular chiral MOFs using BINOL-based linkers (L_{18a}–L_{21a}), (L_{18b}–L_{21b}) carrying carboxylate terminated functional groups with different lengths at 4, 4′, 6, and 6′ positions of BINOL (Figure 12a).[130] Reaction of these linkers with $Cu(NO_3)_2\cdot2.5H_2O$ in DEF/H_2O afforded a series of isostructural chiral MOFs $[Cu_2(L)(solvent)_2]$ with a 3D-net consisting of copper paddle-wheel SBUs and the tetracarboxylate linkers. The resulting frameworks have tunable channel sizes ranging from 1.3×1.1 to $3.2 \times 2.4 \text{ nm}^2$ depending on the length of the linkers (Table 10). Although the frameworks did not retain their structural integrity upon guest removal, they regained the pristine structures upon exposure to solvents. Dye uptake assay using Brilliant Blue R-250 (BBR-250) ($1.8 \times 2.2 \text{ nm}^2$) confirmed the porosity, size selectivity, and accessibility of the frameworks to substrates (Table 10).

Once again, the chiral dihydroxy groups pointing toward the open channels of the frameworks were used for introduction

1209

dx.doi.org/10.1021/cr2003147 |*Chem. Rev.* 2012, 112, 1196–1231

Scheme 10. A Synthetic Strategy for MOF-Based Privileged Metal Catalysts by Incorporation of Catalytic Metal Ions via Postsynthetic Modification (MPP)
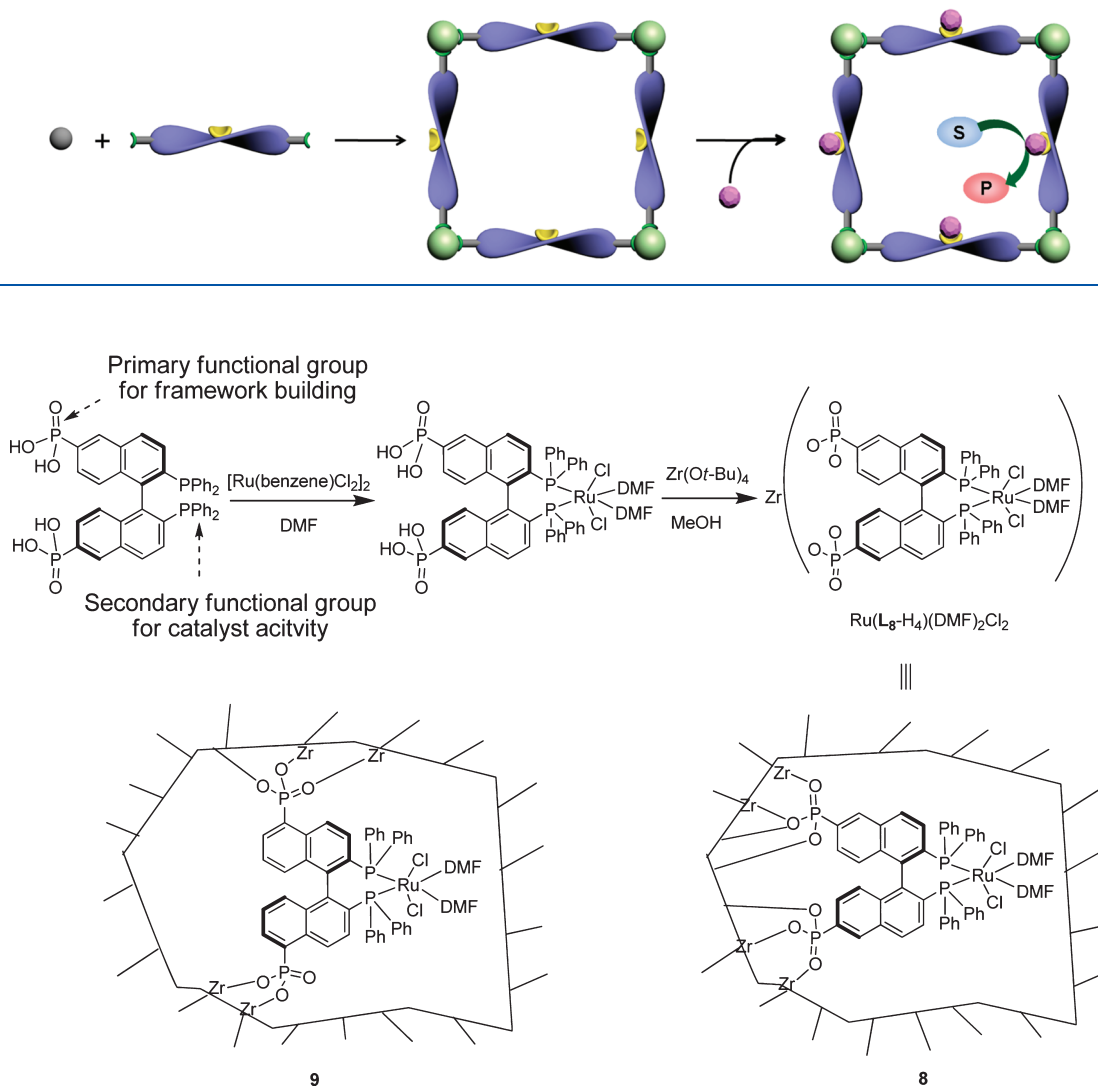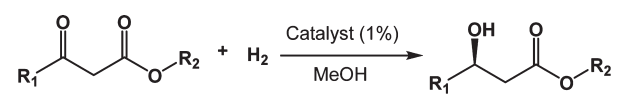

Figure 8. Synthesis of Zr−Ru−L_8 (**8**) and Zr−Ru−L_9 (**9**). Reprinted with permission from ref 88. Copyright 2009 Springer.
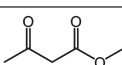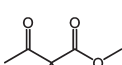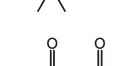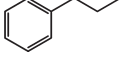
of catalytically active metal ions to afford chiral catalysts. For example, treatment of excess amount of Ti(O^{i}Pr)$_4$ to **20b** led to an active catalyst (**20b-Ti**) for asymmetric diethylzinc addition to aromatic aldehydes with high selectivity for secondary chiral alcohols (up to 92%), complete conversion (>99%), and high enantiomeric excess (up to 91%) (Table 9, entries 5−8). The catalytic activity of **20b-Ti** including enantioselectivity and conversion was similar to that of the homogeneous counterpart (**L$_{20b}$−Me$_4$**) (Table 9, entries 5−8). A control experiment performed with **20a** constructed from BINOL having diethoxy instead of dihydroxy in combination with Ti(O^{i}Pr)$_4$ showed excellent conversion but no enantioselectivity (Table 9, entry 10). The heterogeneous nature of the catalytic system was demonstrated by the fact that the catalytic reaction using supernatant of the **20b-Ti** system gave only a racemic mixture. The catalyst was recyclable at least five times without losing catalytic activity and structural integrity.

Other frameworks **18b**, **19b**, and **21b** were also employed in the same reaction to examine the dependence of the enantioselectivity on the size of the open channel. Although the conversion is equally
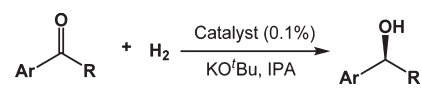
high, **18b-Ti**, the catalyst with smallest channels, showed almost no enantioselectivity, which suggested that the reaction did not take place inside the channels; instead, it was catalyzed by the excess Ti(O^{i}Pr)$_4$ in solution. The larger channels in **19b-Ti** allow the reaction to occur at the chiral Ti centers inside the framework resulting in decent enantioselectivity (70% ee). The higher ee values (>80% ee) for the reaction catalyzed by **20b-Ti** and **21b-Ti** with even larger channels suggested that facile diffusion of substrates into the framework is important for suppressing the background reaction and thereby increasing enantioselectivity.

The isoreticular frameworks (**18b−21b**) were also active catalysts for addition of alkynylzinc to aromatic aldehydes (Table 11, entries 1−4). Once again, the performances of the chiral MOF catalysts were highly dependent on the sizes of the open channels of the frameworks. For example, the reaction catalyzed by **18b-Ti** or **19b-Ti** showed no enantioselectivity in the final product, whereas that catalyzed by **21b-Ti** having larger open channels exhibited high enantioselectivity (77%).

Table 7. Asymmetric Hydrogenation of β-Keto Esters Catalyzed by 8 and 9

substrate	T	H$_2$ pressure [psi]	8[a] ee (yield) [%]	9[a] ee (yield) [%]
	60 °C	700	94.0 (100)	
	RT	1400	95.0 (100)	73.1 (90)
	RT	1400	93.3 (100)	78.8 (70)
	RT	1400	92.0 (100)	65.0 (90)
	RT	1400	69.6 (100)	15.7 (50)

[a] All reactions were carried out for 20 h.

Table 8. Asymmetric Hydrogenation of Aromatic Ketones Using 10 and 11

substrate	10[a] ee (%)	11[a] ee (%)
Ar = Ph, R = Me	96.4 (97.1)[b]	79.0 (81.3)[b]
Ar = 4'-MeO–Ph, R = Me	96.0	79.9
Ar = 4'-Cl–Ph, R = Me	94.9	59.3

[a] All of the reactions were carried out for 20 h. [b] Homogeneous reactions.

Using the same tetracarboxylate ligands L_{20a} and L_{20b}, Lin and co-workers also synthesized another set of chiral MOFs $[Zn_2(L_{20a})(DMF)(H_2O)]\cdot2EtOH\cdot4.3DMF\cdot H_2O$ (22a) and $[Zn_2(L_{20b})(DMF)(H_2O)]\cdot2EtOH\cdot4.3\text{-}DMF\cdot4H_2O$ (22b).[168] The isostructural frameworks consisted of two different Zn ions triply bridged by carboxylate groups of three different linkers to form $\{Zn_2(\mu_2\text{-}CO_2)_3(\mu_1\text{-}CO_2)\}$ SBU (Figure 13a). Each linker as well as each Zn_2 unit acts as a 4-connecting node to form a 2-fold interpenetrated 3D net with **unc** topology. Despite the interpenetration, 22b possesses large open channels with dimensions of 1.5 × 2.0 nm^2 along the a axis. Frameworks 22a and 22b have permanent porosity as confirmed by gas sorption (BET surface area 1335 m^2 g^{-1}, 22a and 1657 m^2 g^{-1}, 22b) and dye inclusion experiments.

Treatment of 22b with Ti(O^{i}Pr)$_4$ generated 22b-Ti, an active catalyst for diethylzinc addition to aldehydes. However, the enantioselectivity of the catalytic reaction was low (<30%) as compared to that of the chiral MOFs built with the same

tetracarboxylate linkers and copper ions described above.[130] Single-crystal X-ray structure analysis of 22b-Ti provided a clue for the low enantioselectivity. Two interpenetrating networks in 22b were in close proximity, allowing Ti(O^{i}Pr)$_4$ to react with two BINOL moieties from two interpenetrating networks to form an intermolecular [Ti(BINOLate)$_2$(O^{i}Pr)$_2$] complex rather than an intramolecular [Ti(BINOLate)(O^{i}Pr)$_2$] complex (Figure 14), which explained the much weaker chiral induction. This work demonstrated the importance of framework structure information for the development of better asymmetric heterogeneous catalysts.

Recently, Jeong and co-workers also utilized a similar dual functional enantiopure linker, (S)-2,2'-dihydroxy-6,6'-dimethyl-(1,1'-biphenyl)-4,4'-dicarboxylic acid (L_{23}), in which the two phenyl rings are orthogonal to each other to avoid the steric repulsion between the hydroxy and methyl groups, to synthesize a homochiral MOF containing chiral dihydroxy groups on the linkers of the framework.[169] Reaction of L_{23} with copper nitrate produced $[Cu_2(L_{23})(H_2O)_2]\cdot7.6DEF\cdot9.6MeOH$ (23) having a NbO net topology,[170] which consists of four connecting copper paddle wheel SBUs and the dicarboxylate linkers (Figure 15). The framework has 2 × 2 × 2 nm^3 sized cubic pores and hexagonal channels with a free aperture diameter of 1.4 nm along the crystallographic [111] direction. Although the framework lost the structural integrity upon removal of solvent molecules filling the channels, it regained the original structure after soaking in the same solvent.

Catalytic sites can be introduced to the chiral dihydroxy groups pointing toward the channels by postsynthetic modification. For example, treating 23 with ZnMe$_2$ generated active Lewis acid catalyst 23-Zn, which promoted the carbonyl-ene reaction shown in Scheme 11. However, excess (3 equiv) 23-Zn was needed to achieve high conversion (~90%) and modest enantioselectivity (50%) due to product inhibition. Although the reaction rate was comparable to that of the homogeneous counterpart, the higher affinity of the product than the substrate to the Zn ion center prevented catalytic turnover, which make 23-Zn unsuitable for practical applications.

Treatment of 23 with Ti(O^{i}Pr)$_4$ produced another active Lewis acid catalyst (23-Ti) for a Diels−Alder reaction between Danishefsky's diene and aldehyde. With a catalytic amount of 23-Ti coupled with 0.9 equiv of Ti(O^{i}Pr)$_4$, good conversion (up to 80%) and modest enantiomeric excess (up to 55% ee) were achieved (Table 12, entry 4−7). Control experiments confirmed that the catalytic site of the reaction is the Ti attached chiral dihydroxy units of the framework. Interestingly, the heterogeneous catalyst afforded higher ee and conversion than the homogeneous counterpart. This improvement in the chemical yield as well as enantiomeric excess can be explained by the contribution of an exaggerated chiral environment of the framework. The catalyst can be recycled at least three times without losing the catalytic activity.

c. Crystalline MOF-Based Privileged Metal Catalysts Built with Chiral Metal(salen) Complexes. In 2006, Hupp and Nguyen et al. reported an MOF-based heterogeneous Jacobsen's catalyst by incorporating chiral Mn-salen complex (R,R)-(−)-1,2-cyclohexane-diamino-N,N'-bis(3-*tert*-butyl-5-(4-pyridyl)salicylidene)Mn^{III}Cl (L_{24}) into a metal−organic framework as a strut via an MPD (Scheme 9) approach.[128] Reaction of Zn(NO$_3$)$_2\cdot6H_2O$ with L_{24} and H$_2$BPDC produced $[Zn_2(bpdc)_2(L_{24})]\cdot10DMF\cdot8H_2O$ (24), having a pillared square grid net structure (Figure 16).

Figure 9. Synthesis of BINOL derived Ti-based catalysts **12**−**14**. Reprinted with permission from ref 88. Copyright 2009 Springer.
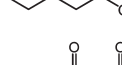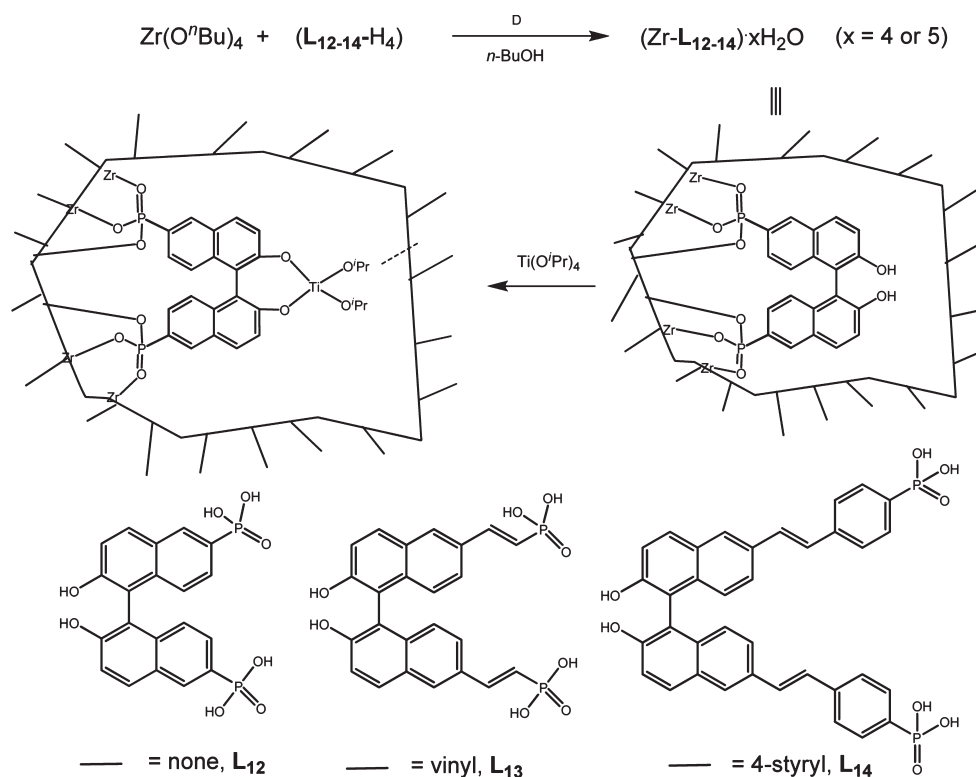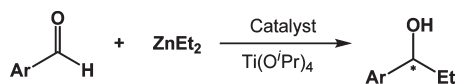
Table 9. Asymmetric Alkyl Addition to Aromatic Ketones Using BINOL-Based MOFs

			catalyst		
entry	Ar	catalyst	loading (mol %)	conversion	ee
1	Ph	**14**	20	95	59
2	Ph	**15**	13	>99	94
3	Ph	**L$_{15}$**	20	>99	83
4	Ph	**16**	12	>99	82
5	Ph	**18b**	13	98	<3
6	Ph	**19b**	13	98	70
7	Ph	**20b**	13	>99	82
8	Ph	**21b**	13	>99	84
9	Ph	**L$_{19}$−Me$_4$**	13	>99	86
10	Ph	**20a**	13	>99	0
11	1-naphthyl	**12**	20	95	59
12	1-naphthyl	**13**	20	70	61
13	1-naphthyl	**14**	20	95	72
14	1-naphthyl	**14−(OEt)$_2$**	20	68	0
15	1-naphthyl	**15**	13	>99	88
16	1-naphthyl	**16**	12	>99	90
17	1-naphthyl	**20b**	13	>99	91
18	4-Cl−Ph	**14**	20	95	43
19	4-Cl−Ph	**15**	13	>99	86
20	4-Cl−Ph	**16**	12	>99	60
21	4-Cl−Ph	**20b**	13	>99	80

Despite a 2-fold interpenetration, which caused one-half of the catalytic Mn sites to be blocked by the adjacent interpenetrated framework, the resulting framework has 57% void space with distorted-rectangular (6.2 × 15.7 Å^2) and rhombic (6.2 × 6.2 Å^2) channels along the c and a axis, respectively.

The catalytic activity of **24** in epoxidation of olefins was studied using 2,2-dimethyl-2H chromene as a substrate and 2-($tert$-butylsulfonyl) iodosylbenzene as an oxidant. The corresponding epoxide was obtained in good yield (70%) and enantioselectivity (82% ee). The enantioselectivity of **24** was slightly lower than its homogeneous counterpart, which may be due to the loss of flexibility in the salen ligand upon framework immobilization or to the electronic effect arising from coordination of the pyridyl groups to Zn metal nodes. The framework-immobilized catalyst **24** exhibited almost constant reactivity during the reaction time examined (3.4 h), whereas the homogeneous counterpart **L$_{24}$** started to lose much of its activity after first few minutes, presumably due to oxidation of the salen ligand. Spatial separation of the catalytic centers in **24** prevented the oxidation of the salen ligand, resulting in remarkable stability of the catalyst, which highlighted one of the advantages of MOF catalysts over homogeneous catalysts. The catalyst **24** was recycled up to three times without a significant change of conversion, enantioselectivity, and TON (Table 13). The competitive size selectivity experiments clearly demonstrated that the catalytic reaction occurs mainly inside the channels.

Expanding this strategy, Lin and co-workers recently constructed a series of isoreticular chiral metal−organic frameworks (CMOFs) incorporating chiral Mn-salen complexes.[121] A series of chiral Mn-salen incorporating linear ditopic carboxylate chiral ligands of varying sizes (**L$_{25}$−H$_2$**, **L$_{26}$−H$_2$**, and **L$_{27}$−H$_2$**) were synthesized. Reaction of these ligands with zinc nitrate produced
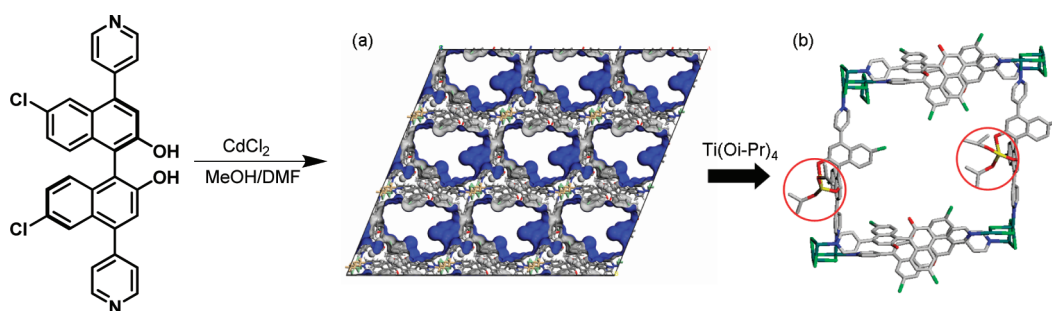
Figure 10. (a) Connolly surface of **15** clearly showing the large 1D chiral channels, and (b) schematic representation of the active (BINOL)Ti(O^{i}Pr)$_2$ catalytic sites (marked by a red circle) in the open channels of **15**. Reprinted with permission from ref 88. Copyright 2009 Springer.
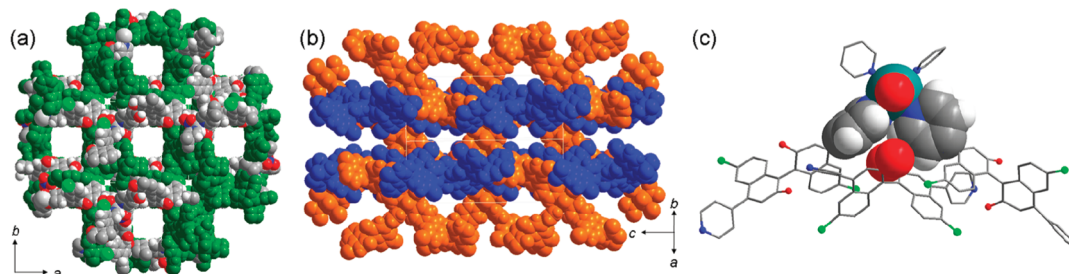

Figure 11. (a) 2-fold interpenetrated 3D framework, **16**, with large interconnected channels, (b) interlocked 2D rhombic grids **17**, and (c) the steric congestion around the chiral dihydroxy groups of L$_{15}$ ligands arising from the interpenetration of 2D rhombic grids through $\pi \cdots \pi$ stacking interactions. Reprinted with permission from ref 167. Copyright 2007 Wiley-VCH.

isoreticular frameworks having a general formula of $[Zn_4(\mu_4\text{-}O)(L)_3]$ with the **pcu** (primitive cubic) topology, analogous to MOF-5.[171] Framework interpenetration was controlled by using different-sized solvents in the synthesis. For example, reaction of L$_{25}$−H$_2$ and L$_{26}$−H$_2$ with Zn(NO$_3$)$_2$·6H$_2$O in DMF/EtOH afforded a 2-fold interpenetrated $[Zn_4(\mu_4\text{-}O)(L_{25})_3]$·20DMF· 2H$_2$O (*int*-**25**) and $[Zn_4(\mu_4\text{-}O)(L_{26})_3]$·42DMF (*int*-**26**), respectively, whereas that in DEF/EtOH produced noninterpenetrated $[Zn_4(\mu_4\text{-}O)(L_{25})_3]$·22DEF·4H$_2$O (**25**) and $[Zn_4(\mu_4\text{-}O)\text{-} (L_{26})_3]$·23DEF·23EtOH·4H$_2$O (**26**), respectively (Figure 17). The longest linker, L$_{27}$−H$_2$, gave only 3-fold interpenetrated $[Zn_4(\mu_4\text{-}O)(L_{27})_3]$·38DMF·11EtOH·4H$_2$O (**27**) regardless of the solvents used. The open channel and pore sizes of the isoreticular salen frameworks were systematically tunable by changing the length of the dicarboxylate struts and by controlling the interpenetration (Table 14). Although a negligible surface area was observed for the evacuated frameworks by N$_2$ adsorption experiments, the porosity of the frameworks was confirmed by dye inclusion experiments.

The catalytic activities of the chiral MOFs were evaluated for asymmetric epoxidation with unfunctionalized olefins in the presence of an oxidant, 2-(*tert*-butyl-sulfonyl)iodosylbenzene. As shown in entries 1−3 of Table 15, interpenetrated frameworks, *int*-**25**, *int*-**26**, and **27**, gave modest to good conversion (54−80%) with modest ee (47−64%) for the epoxidation of 1*H*-indene. Similarly, **26** and **27** were highly effective in asymmetric epoxidation of a variety of unfucntionalized alkenes to afford chiral epoxides with good to excellent yields and moderate to good ee values (Table 15, entries 5−13). In terms of conversion and enantioselectivity, the catalytic activities of the chiral MOFs were comparable to that of their homogeneous counterpart, L$_{27}$−Me$_2$.

The correlation between the rate of epoxidation and the size of open channels was investigated. The reaction rate increased as

the size of open channels of the frameworks increased in the order of *int*-**25** < **27** < *int*-**26** < **26** < **25** (Figure 18). This trend suggested that the diffusion of the substrates and oxidant played an important role in determining the reaction rate in the asymmetric epoxidation catalyzed by the chiral MOFs. However, the catalytic activities of **25** and **26** were comparable to that of a homogeneous counterpart, which suggested the catalytic activity of the chiral MOFs with large open channels is limited by the intrinsic reactivity of the catalytic molecular building blocks. The catalysts were recyclable at least three times without significant loss of catalytic activity and structural integrity.

Recently, Lin and co-workers utilized another Mn(salen) dicarboxylate ligand L$_{28}$ to synthesize chiral MOFs $[Zn_4(\mu_4\text{-}O) (L_{28})_3]$·40DBF·6EtOH·H$_2$O (**28**).[172] Although the resulting framework was built upon the same SBU, $[Zn_4(\mu_4\text{-}O)\text{-} (carboxylate)_6]$, as that of their previous work,[121] the 3D network structure was different. In their previous work, the well-established 6-connected octahedral nodes were connected to form a **pcu** $(4^{12}6^3)$ net topology, whereas in **28**, highly distorted octahedral nodes were connected to form an unusual **lcy** $(3^5 5^9 6^3)$ topology.[173] The **lcy** topology can be represented by closed packing of 7-node cages constructed from one triangular face and three pentagonal faces (Figure 19a and b). Despite a 2-fold interpenetration, the resulting framework has 88% void space with triangular shaped open channels with an edge length of 2.9 nm running along [001] and [1-1-1] directions in the crystal structure (Figure 19c). Dye uptake assay using BBR-250 demonstrated the porosity and pore accessibility of the open channels to large molecules.

As expected, **28** showed high catalytic activity in asymmetric epoxidation of unfunctionalized alkenes with moderate to good conversion (60−99%) and modest to good ee (22−84%), which are comparable to those of the homogeneous Mn(salen)
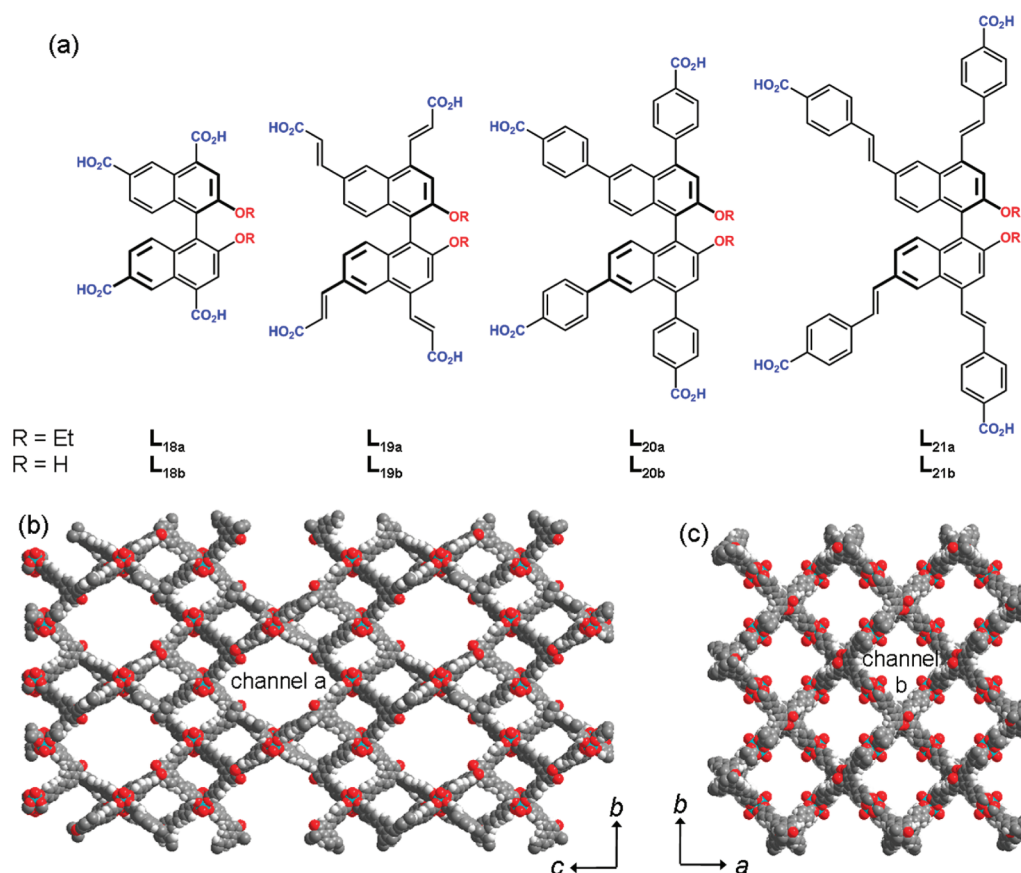
1213

dx.doi.org/10.1021/cr2003147 |*Chem. Rev.* 2012, 112, 1196−1231

(a)

R = Et L_{18a} L_{19a} L_{20a} L_{21a}
R = H L_{18b} L_{19b} L_{20b} L_{21b}

(b)

channel a

(c)

channel b

Figure 12. (a) Ligands of the frameworks, (b) 3D network structure of **18b**−**21b** viewed along the *a* axis showing channel a, and (c) 3D network structure of **18b**−**21b** viewed along the *c* axis showing channel b. Reprinted with permission from ref 130. Copyright 2010 Nature Publishing Group.

Table 10. Key Structural Features of 18b−21b

	18b	19b	20b	21b
formula	$Cu_2(L_{18b})(DEF)_2$	$Cu_2(L_{19b})(H_2O)_2$	$Cu_2(L_{20b})(H_2O)_2$	$Cu_2(L_{21b})(H_2O)_2$
void space (%)	73.3	84.8	87.1	92.9
channel size (nm^2)	1.3×1.1	2.2×1.5	3.0×2.0	3.2×2.4
	0.8×0.8	1.3×1.3	1.6×1.6	2.1×2.1
dye uptake (wt %)	1.9	64.5	117	124

Table 11. Alkynylzinc Additions to Aldehydes Catalyzed by a Series of BINOL-Based Chiral MOFs

entry	catalyst	Ar	conversion (%)	ee (%)
1	**20b**	4-Me−Ph	>99	71
2	**20b**	4-Cl−Ph	>99	59
3	**20b**	1-Naph	>99	31
4	**20b**	Ph	>99	76
5	**18b**	Ph	>99	0
6	**19b**	Ph	>99	0
7	**21b**	Ph	>99	77
8	**20a**	Ph	>99	0

catalytic struts.[121] The catalyst was successfully recycled four times with slight deterioration in conversion and ee after each use. Most notably, **28** catalyzed sequential asymmetric epoxidation of alkenes and ring-opening reaction of the generated epoxides with $TMSN_3$, which were apparently promoted by Mn(salen) and $[Zn_4(\mu_4\text{-}O)(\text{carboxylate})_6]$ units, respectively, with satisfactory conversion and enantioselectivity (Table 16). It was noted that the ee values of the ring-opening products and the epoxides generated from the epoxidation step are essentially identical. In control experiments, the ring-opening reaction in the presence of 1 mol % of a homogeneous Mn(salen) complex afforded <5% yield, whereas the same reaction in the presence of 1 mol % of MOF-5 as a catalyst produced the product in 30% yield. On the basis of these results, they concluded that the ring-opening reaction was primarily catalyzed by the $[Zn_4(\mu_4\text{-}O)(\text{carboxylate})_6]$ SBUs in **28**. Although the detailed mechanism of the sequential chemical transformations, especially the ring-opening of generated

1214

dx.doi.org/10.1021/cr2003147 |*Chem. Rev.* 2012, 112, 1196−1231
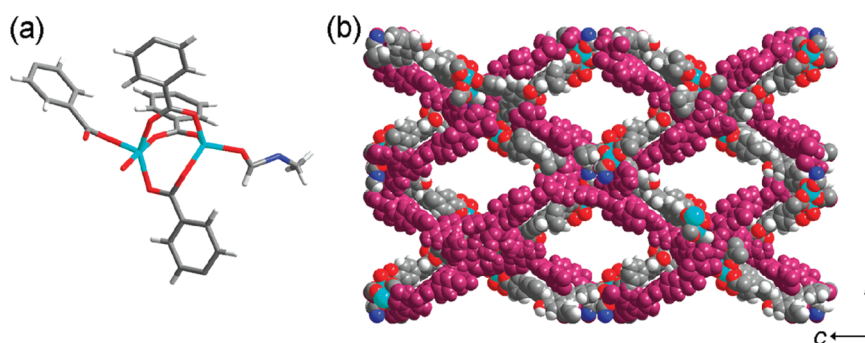
Figure 13. (a) Structure of $[Zn_2(\mu_2\text{-}CO_2)_3(\mu_1\text{-}CO_2)]$ SBU, and (b) interpenetrated 3D net with **unc** topology of **22b**. Reprinted with permission from ref 168. Copyright 2010 Wiley-VCH.
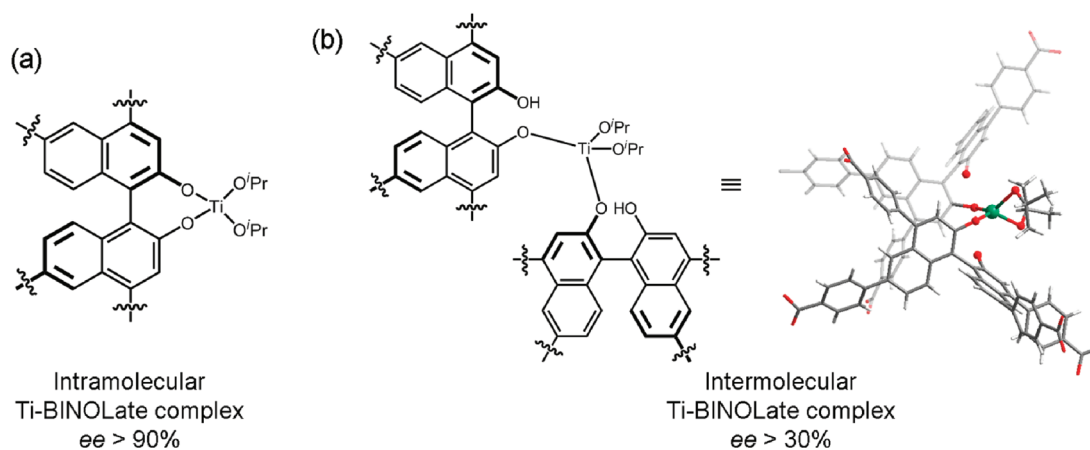
Figure 14. (a) Intramolecular Ti–BINOLate complex and (b) intermolecular Ti–BINOLate complex and its X-ray crystal structure. Reprinted with permission from ref 168. Copyright 2010 Wiley-VCH.
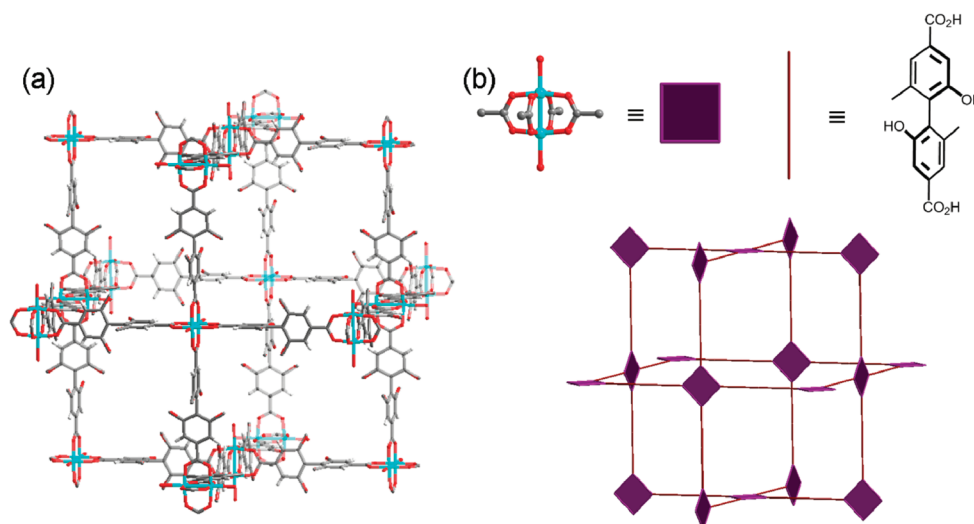
Figure 15. (a) 3D open channel structure of **23** and (b) NbO net. Reprinted with permission from ref 169. Copyright 2011 Royal Society of Chemistry.

epoxides catalyzed by the apparently innocent $[Zn_4(\mu_4\text{-}O)\text{-}(carboxylate)_6]$ SBUs, needs to be elucidated, this work illustrated one of the future directions of MOF-based asymmetric catalysts.

Another recent development in this area involves the synthesis of metallosalen-based MOFs containing catalytically active metal ions other than manganese. The Lin group and Hupp and Nguyen group independently prepared homochiral MOFs constructed from other metallosalen complexes using MPD, or MPD followed by MPP strategy, respectively. Lin and co-workers prepared enantiopure Ru^{III}(salen) dicarboxylic acid ligand,

$[Ru(L_{29}-H_2)(py)_2]Cl$, to synthesize chiral MOFs $\{Zn_4(\mu_4-O)[Ru(L_{29})(py)_2]Cl\}\cdot 7DBF\cdot 7DEF$ (*int*-29) and $\{Zn_4(\mu_4-O)[Ru(L_{29})(py)_2]Cl\}\cdot 18DEF\cdot 5DMF\cdot 6H_2O$ (29).[174] The resulting frameworks, *int*-29 and 29, were isostructural to *int*-25 and 25, respectively (Figure 20). While the open channels of *int*-29 (0.4×0.3 nm^2) were too small to accommodate guest molecules, those of 29 (1.4×1.0 nm^2) were large enough to take organic substrates for catalysis. Dye uptake assay with BBR-250 showed 30 wt % dye uptake for 29, demonstrating the porosity and pore accessibility of the open channels. Treatment of *int*-29 and 29 with a reducing agent such as LiBEt$_3$H or NaB(OMe)$_3$H caused a color change of the crystals from dark green to dark red (Figure 20), suggesting the reduction of Ru^{III} to Ru^{II} in the frameworks. The oxidation state of the Ru centers of the reduced frameworks, *int*-29R and 29R, was characterized by UV/vis/NIR spectra. Upon reduc-

tion of *int*-29 and 29, the characteristic LMCT bands of Ru^{III}-salen at 771 nm disappeared with concomitant appearance of a new MLCT band of Ru^{II}-salen at 520 nm. Air oxidation of the reduced frameworks, *int*-29R and 29R, restored initial *int*-29 and 29, respectively. The reversible reduction/oxidation of *int*-29 and 29 occurred in a single-crystal-to-single-crystal fashion.

Scheme 11. Carbonyl-ene Reaction Promoted by 23-Zn
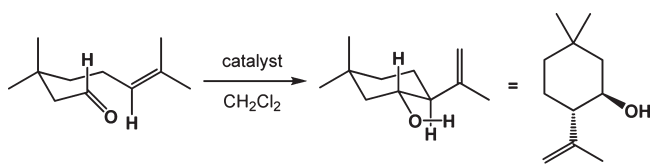
Table 13. Asymmetric Epoxidation of 2,2-Dimethyl-2H-chromene Catalyzed by 24
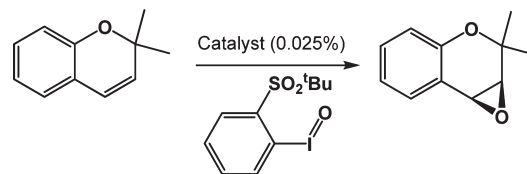
cycle	TON	yield (%)	ee (%)
first	1430	71	82
second	1420	71	82
third	1320	66	82

Table 12. Hetero Diels—Alder Reactions Catalyzed by 23-Ti

entry	catalyst	diol:Ti(O^{i}Pr)$_4$ (mol %)	t (days)	yield^a (%)	ee^a (%)
1		0:20	3	10	
2		0:20	3	7	
3	23	30:0	3	not reacted	
4	23-Ti	30:45	5	52	33
5	23-Ti	30:60	5	77	48
6	23-Ti	30:90	5	79	55
7	23-Ti	30:90	5	80	55
8	L$_{23}$-Ti	30:90	5	58	18

^{a}Yield and ee values were determined after the acid workup.
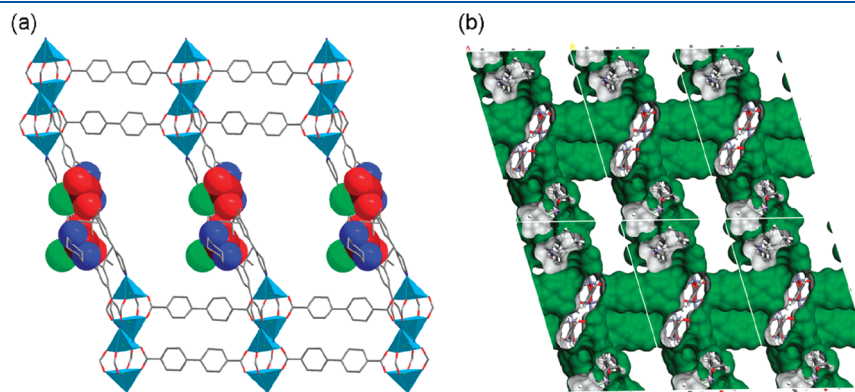
Figure 16. (a) Crystal structure of 24 showing interpenetrated networks and pore openings, and (b) the Connolly surface of the framework. Reprinted with permission from ref 88. Copyright 2009 Springer.
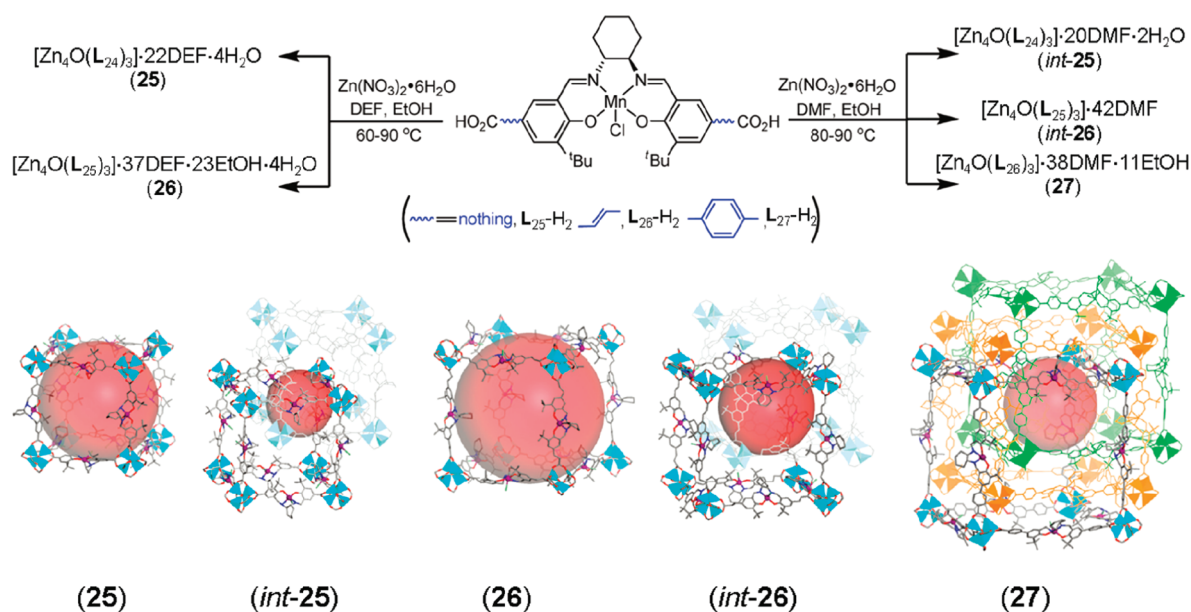
Figure 17. Synthesis of chiral MOFs **25**–**27**, *int*-**25**, and *int*-**26** and different cavity sizes shown as red balls in **25** (2.6 nm), *int*-**25** (1.4 nm), **26** (3.2 nm), *int*-**26** (2.0 nm), and **27** (1.8 nm). Reprinted with permission from ref 121. Copyright 2010 American Chemical Society.

Table 14. Key Parameters of Chiral MOFs 25–27

	int-**25**	**25**	*int*-**26**	**26**	**27**
cell dimensions (Å)	29.7 × 29.7 × 72.7	29.6 × 29.6 × 72.5	35.9 × 35.9 × 87.8	35.9 × 35.9 × 87.9	41.9 × 41.9 × 100.3
interpenetration	2-fold	no interpenetration	2-fold	no interpenetration	3-fold
void space %	61.1	80.2	76.8	88.4	75.9
largest channel size (nm^2)	0.8 × 0.6	2.0 × 1.6	1.5 × 0.7	2.5 × 2.3	1.1 × 0.8
largest cavity (nm)	1.4	2.6	2.0	3.2	1.8

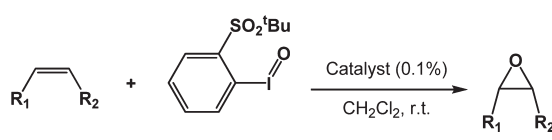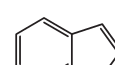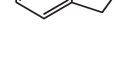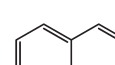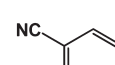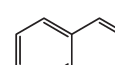Because $[Ru^{II}(salen)(py)_2]$ complex was already known to catalyze cyclopropanation reactions transferring the carbene fragment from ethyldiazoacetate to various olefins with excellent enantio- and diastereoselectivities under homogeneous conditions,[175] Lin et al. tested the catalytic activities of the Ru^{II}-salen-derived frameworks, *int*-**29R** and **29R**, for a cyclopropanation reaction. Although the reduced framework **29R** generated by treating **29** with LiBEt$_3$H catalyzed the cyclopropanation of styrene, the yield of the reaction was disappointingly low (7.8%) with modest enantio- and diastereoselectivity (Table 17, entry 1), which was probably due to the oxidation of Ru^{II} to Ru^{III} during the catalysis. No catalytic activity of **29** (Ru^{III}) in cyclopropanation was confirmed by a control experiment (Table 17, entry 3). To prevent the oxidation of the catalyst during the catalysis, the cyclopropanation reaction was carried out in the presence of both catalyst (**29R**) and reducing agent (NaBH(OMe)$_3$), which results in improved yield (54%) and enantio- and diastereoselectivity (Table 17, entry 2). Control experiments using homogeneous counterpart, $[Ru(\mathbf{L_{29}}-Me_2)(py)_2]$, gave 28% and 53% yield in the absence and in the presence of the reducing agent, respectively (Table 17, entries 4 and 5). The heterogeneity of the reaction was demonstrated by a filtration test. Despite the reduced yield and stereoselectivity, **29R** was recyclable with negligible leaching (>0.01%). As expected, *int*-**29R** showed no catalytic activity for cyclopropanation because of the small open channel size. Although the catalytic activity of the Ru^{II}-salen frameworks was lower than that of homogeneous Ru-salen catalysts,[175] this work

demonstrated reversible switching of the catalytic activity of MOFs by reduction/oxidation.

Recently, Nguyen and Hupp et al. reported the selective surface and near-surface modification of MOF crystals to study the surface effect of crystals in catalysis.[176] Extending this strategy, they demonstrated the introduction of various metal ions including Co^{II}, Zn^{II}, Cr^{II}, Cu^{II}, Ni^{II}, and Mn^{II} to the salen strut of a salen-derived MOF by postsynthetic modification (Figure 21a).[177] They first synthesized noncatenated MOF, Mn^{III}SO-MOF (Mn^{III}-**30**), using a tetracarboxylic acid and a dipyridyl Mn-salen complex.[176] Treating Mn^{III}-**30** soaked in methanol with H_2O_2 resulted in the formation of Mn depleted framework (90% depletion), dSO-MOF (d-**30**). After complete drying of d-**30**, the crystals were soaked in solutions containing metal salts (M = Cr^{II}, Co^{II}, Mn^{II}, Ni^{II}, Cu^{II}, and Zn^{II}) to produce various remetalated frameworks, MSO-MOF (M-**30**). The crystals showed an immediate change in color (Figure 21b) to the ones reported for the homogeneous metallo-salen analogues. ICP-OES analysis of the remetalated frameworks confirmed almost 100% remetalation of the salen sites. Interestingly, Cu-**30** displayed a much higher Cu content than that expected for remetalation of only the salen sites, as a result of the partial exchange of the framework constituting Zn^{II} ions with Cu^{II} as observed by others.[155–158] MALDI-TOF-MS, TGA, and PXRD analyses confirmed the maintenance of the structural integrity of the remetalated frameworks (Figure 21c). The catalytic activities of d-**30** and Mn^{II}-**30** were assessed. As expected, d-**30** showed no catalytic activity for epoxidation, whereas Mn^{II}-**30** restored the catalytic activity with a

1217

dx.doi.org/10.1021/cr2003147 | *Chem. Rev.* 2012, 112, 1196–1231

Table 15. Asymmetric Epoxidations of Alkenes Catalyzed by a Series of Chiral MOFs

$$R_1 \diagdown R_2 + \text{(ArI=O, } SO_2{}^tBu) \xrightarrow[\text{CH}_2\text{Cl}_2, \text{ r.t.}]{\text{Catalyst (0.1\%)}} R_1 \diagdown R_2 \text{ (epoxide)}$$

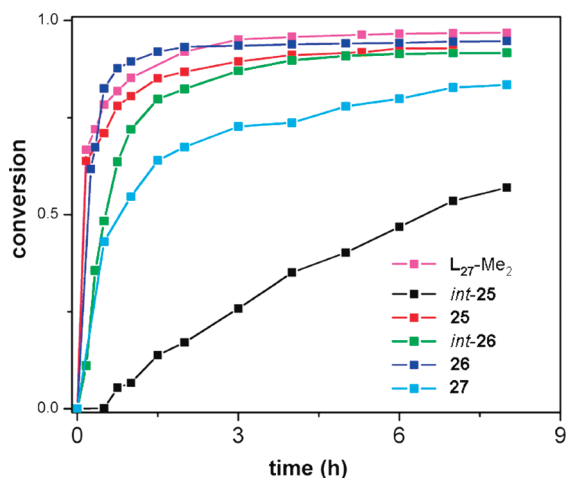| entry	catalyst	alkene	conversion (%)	ee (%)
1	int-**25**		63	47
2	int-**26**	indene	80	64
3	**27**		54	61
4	**L27**-Me₂		60	64
5	**27**		82	92
6	**26**	2,2-dimethyl-2H-chromene	87	85
7	**L27**-Me₂		90	92
8	**27**		60	79
9	**26**	NC-chromene	79	83
10	**L27**-Me₂		82	88
11	**27**		>99	42
12	**26**	dihydronaphthalene	>99	38
13	**L27**-Me₂		>99	45

Figure 18. Plots of percent conversions versus time for epoxidation of 2,2-dimethyl-2H-chromene catalyzed by chiral MOFs int-**25** (black), **25** (red), int-**26** (green), **26** (blue), **27** (cyan), and **L27**—Me₂ (purple). Reprinted with permission from ref 121. Copyright 2010 American Chemical Society.

somewhat lower enantioselectivity (37% ee) than that of Mn^{III}-**30** (80% ee).[176] This synthetic strategy, MPD followed by MPP, may provide a unique opportunity to synthesize various metallosalen-based MOFs, which are difficult to prepare because of competitive self-association.
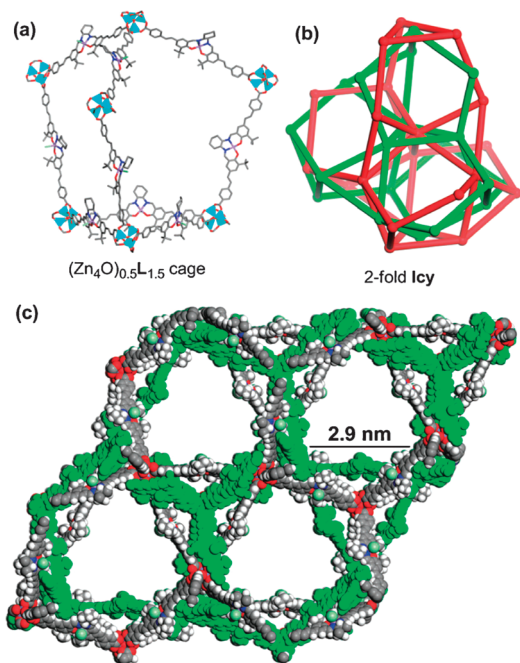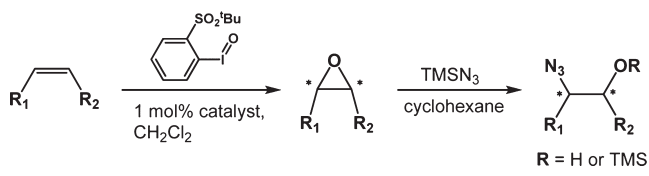

Figure 19. (a) Structure of 7-node polyhedron constituting **28**, (b) schematic representation of 2-fold interpenetrating network of **28**, and (c) space-filling model of **28** viewed perpendicular to the (001) plane. Reprinted with permission from ref 172. Copyright 2011 Royal Society of Chemistry.
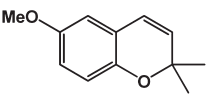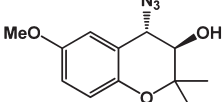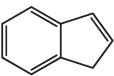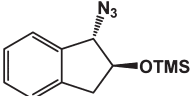
Both MPD and MPP strategies exploiting well-established privileged catalyst or ligand units incorporated into frameworks represent the most successful synthetic strategies for MOF-based asymmetric catalysts with high catalytic activity and enantioselectivity, which is reflected in the fact that more than one-half of MOF-based catalysts reported to date have been synthesized by either the MPD or the MPP strategy. However, these complementary strategies also have some limitations. As stated above, the MPD strategy is not compatible with some labile Lewis acid catalysts or reactive transition metal catalysts, which may be overcome at least in part by the MPP approach. The MPP strategy, in turn, is not compatible with some privileged ligands as they would react with framework-forming metal ions during the framework formation, which may be overcome in part by the MPD approach. The MPP strategy also does not tolerate some highly reactive metal precursors for the catalytic site generation during the postsynthetic modification as they destroy the framework.

3.2. Organic Catalysis

As described in the Introduction, asymmetric catalysis using small chiral organic molecules or organocatalysts has drawn much attention in homogeneous catalysis for the past decade because of its advantages over metal asymmetric catalysts including the absence of trace metal contaminations, high tolerance to water and air, and high availability at a low cost. During the early years of developing MOF-based heterogeneous asymmetric catalysts, many efforts were made to utilize chiral linkers derived from readily available small chiral organic molecules (or nature's "chiral pool") such as tartaric acid and various amino acids for the construction of chiral MOFs. Some of the resulting chiral MOFs exhibited asymmetric catalytic activities due to the presence of catalytically active organic moieties exposed to the pores, as described in section 3.2.1, but their

Table 16. Sequential Asymmetric Epoxidation/Ring-Opening Reactions of Alkenes Catalyzed by 28

entry	starting material	product	yield (%)	ee (%)
1			57	81 (82)[a]
2			60	50 (48)[a]

[a]The ee of corresponding epoxides.

enantioselectivities were usually disappointingly low. To overcome this problem, more rational strategies have since been developed such as incorporation of privileged organocatalytic units into the framework formation either by direct incorporation or postsynthetic modification, which will be described in detail in section 3.2.2.

3.2.1. Asymmetric Catalysis Promoted by Simple Organic Catalytic Units Incorporated into Chiral Frameworks. In 2000, Kim et al. reported the first homochiral MOF that can catalyze a chemical reaction in an enantioselective manner.[80] It was also the first MOF demonstrating that an organic unit embedded in a chiral pore can catalyze an asymmetric transformation. Reaction of an enantiopure tartaric acid derivative L_{31} with zinc nitrate afforded the homochiral framework, $[Zn_3(\mu_3\text{-}O)(L_{31}\text{−H})_6] \cdot 2H_3O \cdot 12H_2O$ (31), known as POST-1. The carboxylate group of L_{31} bound to zinc ions to form a planar oxo-bridged trinuclear cluster, $[Zn_3((\mu_3\text{-}O)(\text{carboxylate})_6]$, serving as an SBU in the framework formation (Figure 22). The SBUs are further interconnected via the pyridyl groups of L_{31} to form a 2D extended layer with a "chicken-wire" structure ((6,3)-net).[115] Through noncovalent interactions, the 2D layers are stacked perpendicular to the *c* axis generating large triangular-shaped chiral 1D channels (13.4 Å), which are filled with solvent molecules (void volume ∼47%). Interestingly, one-half of the six pyridyl groups present in each trinuclear unit $([Zn_3(\mu_3\text{-}O)(L_{31}\text{−H})_6]^{2−})$ are coordinated to the zinc ions of three neighboring trinuclear units, and the remaining one-half extrude into the channel without any interactions with the framework, two of which are protonated to balance the framework charge. N-Alkylation of these pyridyl groups demonstrated their accessibility and reactivity. Furthermore, Kim et al. successfully demonstrated the modulation of the pore size and framework charge by the N-alkylation, which may be considered as the first example of postsynthetic modification. The accessible free pyridyl units in chiral channels enabled POST-1 to perform heterogeneous, asymmetric catalysis.

The catalytic activity of POST-1 was investigated in a transesterification reaction. Reaction of 2,4-dinitrophenyl acetate and

ethanol in the presence of POST-1 yielded ethyl acetate in 77% yield. In the absence of POST-1, or in the presence of POST-1 with N-methylated free pyridyl units, however, very little conversion was observed, demonstrating the catalytic activity of the pyridyl units of POST-1. Transesterification of 2,4-dinitrophenyl acetate with bulkier alcohols such as 2-butanol, neopentanol, and 3,3,3-triphenyl-1-propanol occurred with a much slower or negligible rate, suggesting that the catalysis mainly occurred in the channels. Most importantly, the reaction of 2,4-dinitrophenyl acetate with a large excess of *rac*-1-phenyl-2-propanol in the presence of D-POST-1 or the enantiomorphic L-POST-1 produced corresponding esters with ∼8% enantiomeric excess in favor of *S* or *R* enantiomer, respectively (Scheme 12). The low enantioselectivity was presumably due to the fact that the catalytically active units (dangling pyridyl groups) are a bit too far from the chiral wall of the pores. Despite the modest ee value, this was the first example of catalytic asymmetric induction mediated by well-defined modular porous materials, and, furthermore, the first example of MOF-based heterogeneous organic catalysis. From a catalyst design perspective, it is interesting to note that the chiral linker L_{31} plays a dual role by forming a chiral framework (primary ligand) and at the same time serving as a catalytic unit (secondary ligand) in POST-1.

In 2008, Rosseinsky and co-workers reported an aspartic-acid-based chiral MOF showing Brønsted acid catalytic activity.[178] Reaction of copper nitrate, 1,2-bis(4-pyridyl)ethylene (bpe), and L-aspartic acid (L-asp) resulted in the formation of $[Cu(L\text{-asp})(bpe)_{0.5}] \cdot 0.5H_2O \cdot 0.5MeOH$ (32). The framework exhibits a 3D pillared layer structure, where each 2D chiral Cu(L-asp) layer is bridged by *trans*-configured bpe ligands. The framework is robust and porous as revealed by the reversible adsorption of methanol at room temperature and also by PXRD data. The interlayer separation of the *trans*-configured bpe pillared framework generates pore windows of 4.1 × 4.3 Å² and elongated channels of 8.6 × 3.2 Å². Upon treatment of anhydrous HCl (1 equiv) in diethylether, Brønsted acid sites on the framework were generated, resulting in the protonated framework, $[Cu(L\text{-asp})(bpe)_{0.5}] \cdot HCl \cdot H_2O$ (L-33). The similarity in the PXRD patterns of 32 and L-33 suggested no major structural changes in the framework upon protonation.
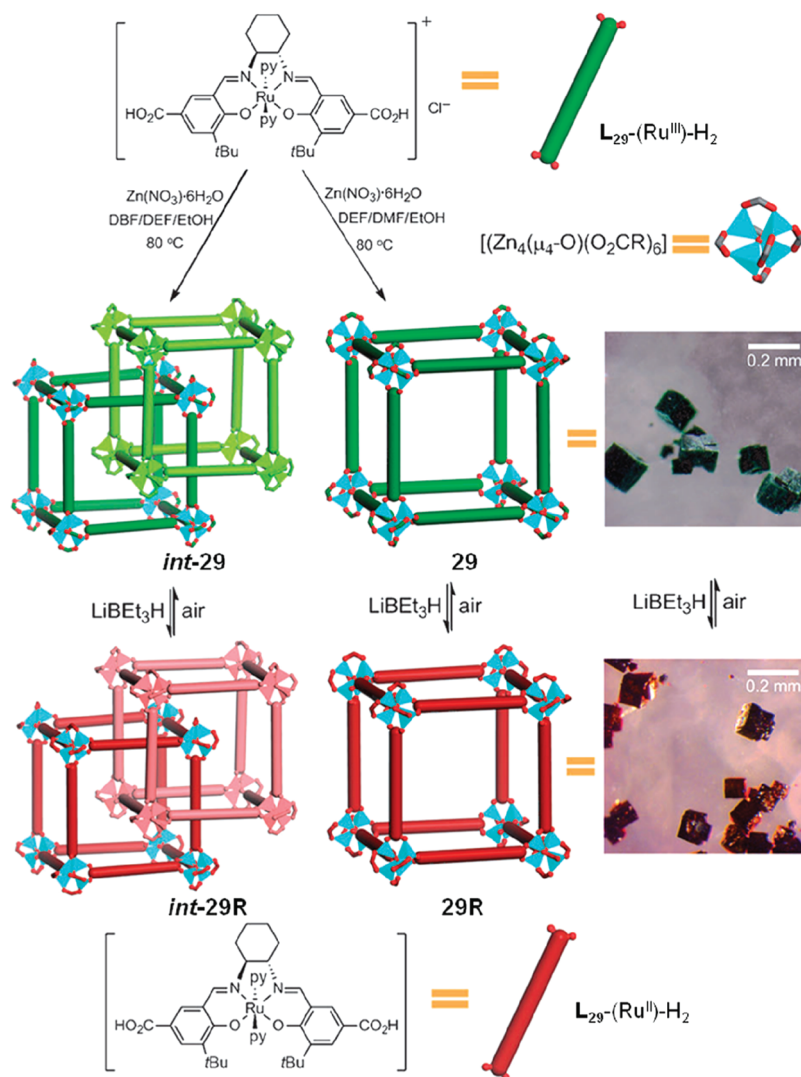
Figure 20. Synthesis and single-crystal-to-single-crystal reduction/oxidation of *int*-**29** and **29**. The photographs illustrate the typical colors and morphologies of **29** (green) and **29R** (red). Reprinted with permission from ref 174. Copyright 2011 Wiley-VCH.

Table 17. Asymmetric Cyclopropanation of Substituted Olefins Using 29
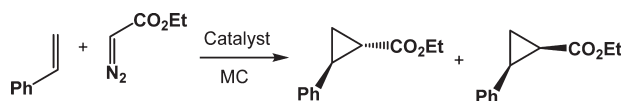
entry	catalyst	mol % cat.	yield (%)	dr	ee (%) (trans)	ee (%) (cis)
1	**29R**	3	7.8	4.2	65	51
2	**29R**[a]	3	54	7	91	84
3	**29**	3	1			
4	*int*-**29R**	3	1	1.2	33	47
5	$[Ru(\mathbf{L_{29}}-Me_2)(py)_2]$	1	28	9.6	92	85
6	$[Ru(\mathbf{L_{29}}-Me_2)(py)_2]$[a]	1	53	10.9	98	92

[a] With $NaBH(OMe)_3$ in solution.

Furthermore, IR spectroscopy confirmed the formation of COOH moiety in the framework (Figure 23), which is located close to the chiral centers of the aspartate ligand.

Methanolysis of *cis*-2,3-epoxybutane was examined using the chiral framework L-**33**. The reaction yields are in the range of 30—65% with 10% ee. The reduced diffusivity of the reagents
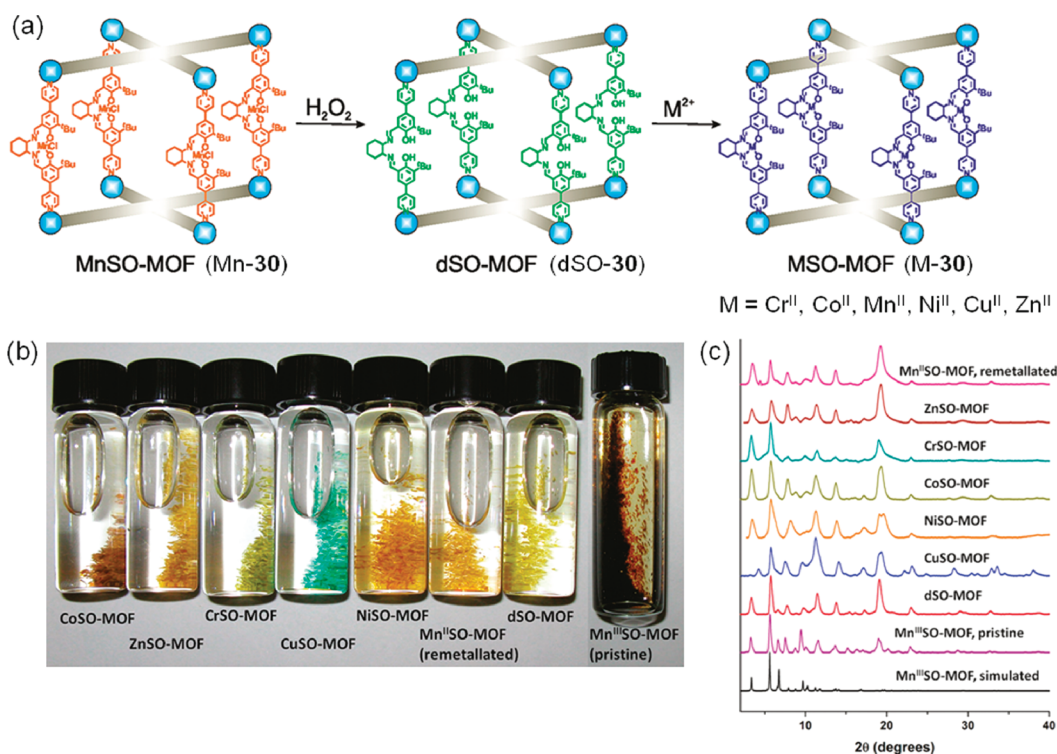
Figure 21. (a) Demetalation of Mn-**30** and its subsequent remetalation, (b) photos of Mn-**30** and remetalated products (M-**30**) crystals, and (c) PXRD profiles of the MOFs. Reprinted with permission from ref 177. Copyright 2011 American Chemical Society.
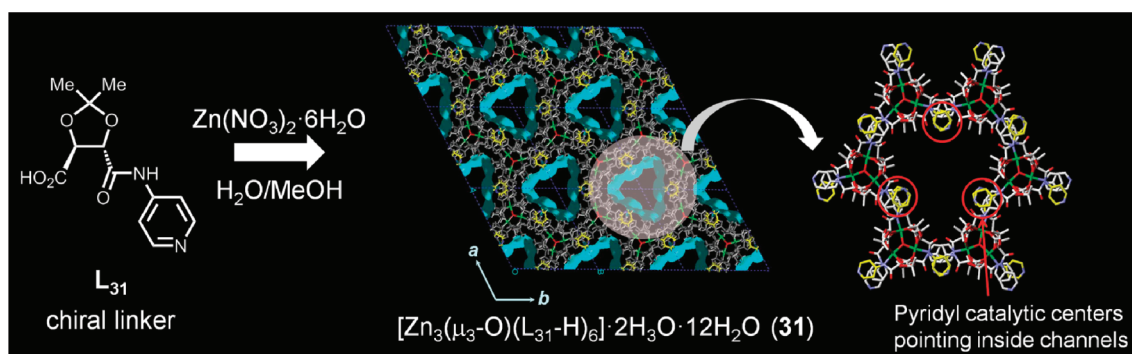
Figure 22. Structure of POST-1 (**31**) showing large chiral channels along the *c* axis and catalytic site at chiral pocket in POST-1 (**31**). Reprinted with permission from ref 80. Copyright 2000 Nature Publishing Group.

into the small pores resulted in lower yields than the reference homogeneous catalyst H_2SO_4 (Table 18). When the reaction was performed at 0 °C, the ee values increased to 17% (D-**33** 6% ee at 25 °C and 13% ee at 0 °C). The filtered supernatant from the reaction medium was inactive in the catalysis, confirming the heterogeneous nature of the catalytic system. The absence of catalytic conversion for bulky substrates such as (2,3-epoxypropyl)-benzene demonstrated that the reaction mainly occurred inside the channels.

In 2009, Wang and co-workers reported a serine-based chiral MOF that can catalyze 1,2-addition of α,β-unsaturated ketones in an enantioselective manner.[179] They first prepared a multi-topic chiral ligand, (S)-3-hydroxy-2-(pyridin-4-ylmethylamino)-propanoic acid (L₃₄), by attaching a pyridyl moiety to the amine group of serine, which served as both a primary (framework forming) and a secondary (catalytic) ligand. Reaction of copper

chloride and L₃₄ afforded a 2D homochiral MOF, $[Cu_2(L_{34})_2-Cl_2]\cdot H_2O$ (**34**). Two crystallographically independent copper metal nodes are present in the framework. Each metal node is coordinated by a carboxylate, amine, and hydroxy groups of one L₃₄ and a pyridyl group from the other L₃₄. In addition, one copper ion is additionally coordinated by one chloride ion resulting in a distorted square pyramidal geometry, whereas two chloride ions coordinate to the other copper metal ion affording an octahedral geometry. As a result, a framework consisting of 1D chains is constructed (Figure 24a). The 1D chains are interconnected by chloride ions to form a thick double layered 2D lamellar framework, which is further extended into a 3D porous framework via noncovalent interactions (Figure 24b and c) with chiral 1D channels (5.1 Å × 2.9 Å). An important feature of the coordination geometry of the framework is that the nitrogen atom of the amine group contains additional chiral information,

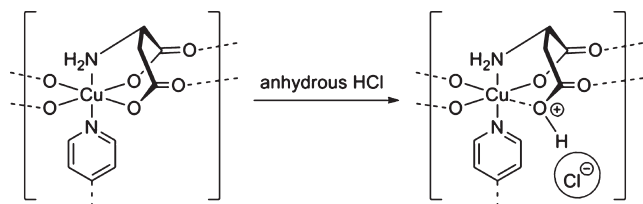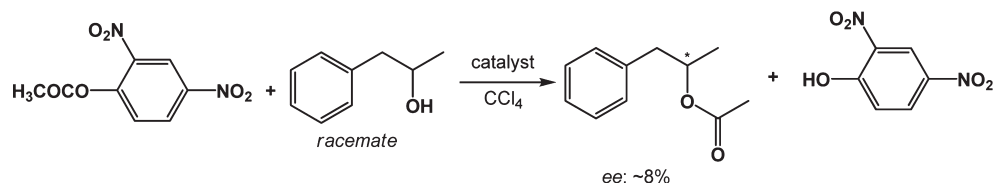**Scheme 12. Transesterifications Catalyzed by POST-1 (31)**

ee: ~8%

Figure 23. Protonation of a carboxylate group of **32** located next to an active metal center resulting in MOF (L-**33**). Reprinted with permission from ref 90. Copyright 2011 Wiley-VCH.

which is induced by the neighboring chiral carbon atom and stabilized through the interaction with the copper atom.

Framework **34** catalyzed 1,2-addition of Grignard reagent to α,β-unsaturated ketones in excellent conversion (88−98%) and good to moderate enantioselectivity (51−99%). Control experiments showed that free **L_34** produced 1,2-addition product in 84% conversion and 51% ee (entry 2 in Table 19), whereas copper chloride did not show any catalytic activity, suggesting that the reaction was promoted by the organic functionality in the framework of **34**. Furthermore, the framework showed much higher enantioselectivity (88%) (entry 3 in Table 19) than the homogeneous counterpart, **L_34** (51%) (entry 2 in Table 18). The authors proposed that the additional chirality around the metal nodes generated by the coordinated amine group in the framework may be responsible for the higher enantioselectivity. The catalytic reaction using the supernatant solution of **34** failed to promote the transformation, confirming the heterogeneous nature of the catalytic system. However, the structural study suggested the catalytic reaction occurred mainly on the surface of the crystals because the size of the 1D channels is too small to accommodate substrates.

The use of catalytically active simple chiral linkers derived from nature's "chiral pool" offers a simple, facile route to construct MOF-based asymmetric catalysts (Scheme 13), but this strategy has several drawbacks: (1) rational design of frameworks with specific structures and functionalities is difficult due to the complex binding modes of such catalytically active linkers, (2) such catalytically active (organic) linkers often lose their catalytic activity by coordination to metal ions during the framework formation, (3) resulting chiral frameworks in general show unsatisfactory enantioselectivity, and (4) the exact nature and location of the catalytic center are often obscure. Incorporation of well-established privileged organocatalysts into the framework provides an alternative way to overcome the problems.

3.2.2. Asymmetric Catalysis Promoted by Privileged Organocatalytic Units Incorporated into Frameworks (OPP and OPD). The surge of interest in (homogeneous) organocatalysts in the past decade also prompted the development of MOF-based heterogeneous organocatalysts by incorporation of well-studied privileged organocatalysts such as proline into metal−organic frameworks. Similar to the MOF-based privileged metal catalysts, two strategies

Table 18. Methanolysis of *cis*-2,3-Epoxybutane Catalyzed by 33
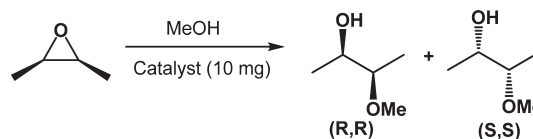
catalyst	temperature (°C)	yield (%)	ee (%)	TOF
L-**33**	25	59	+10	4.8
L-**33**	0	30	+17	2.6
H₂SO₄	25	100	+2	

have been used to introduce privileged organocatalysts, direct incorporation (OPD: organocatalysis−privileged catalysis−direct incorporation) and postsynthetic modification (OPP: organocatalysis−privileged catalysis−postsynthetic modification). As described in detail in the following sections, direct incorporation of privileged organocatalysts (OPD) often requires protection of their catalytic sites to prevent their coordination to metal ions during the framework formation, and deprotection after the framework formation to generate active catalysts. On the other hand, the complementary postsynthetic modification strategy (OPP) provides an even more versatile way to synthesis MOF-based organocatalysts by permitting incorporation of privileged (chiral) organocatalysts into a framework via covalent or coordination bond modification (Scheme 14), often without protecting the catalytic center.

a. Asymmetric Catalysis Promoted by Privileged Organocatalytic Units Incorporated into Frameworks via Postsynthetic Modification (OPP). In 2009, Kim and co-workers reported a simple but efficient strategy to synthesize MOF-based organocatalysts by introducing privileged organoctalysts to open coordination site of metal nodes of a preassembled achiral framework via postsynthetic modification (OPP-coordination).[129] They first chose MIL-101 as a parent achiral MOF, which is ideally suited for postsynthetic modification for the following reasons. First, it has a thermally and chemically robust framework with large pores (2.9−3.4 nm) and windows (1.2−1.4 nm).[180] In MIL-101, four $[Cr_3(\mu_3\text{-}O)]$ SBUs are linked by terephthalate (or bdc) linkers to form supertetrahedra (ST), which are further interconnected by terephthalate to generate a hierarchically ordered framework (Figure 25a) containing two different types of spherical mesopores. Second, it has open metal coordination sites, which can be easily generated by heating. Whzile one chromium ion in the $[Cr_3(\mu_3\text{-}O)]$ unit is coordinated by either a fluoride or a hydroxy ion, the remaining two chromium ions are coordinated by water molecules to complete an octahedral coordination geometry. The coordinated water molecules can be readily removed by
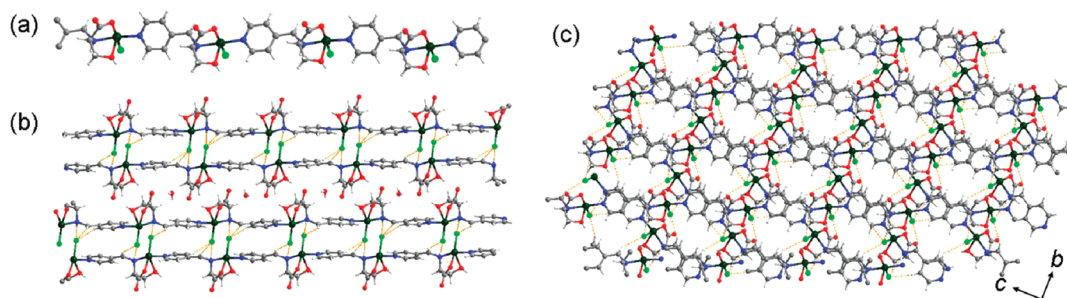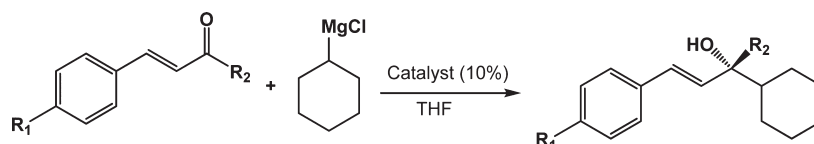
Figure 24. (a) Structure of 1D chains, (b) interconnected 1D chains to form a lamellar framework, and (c) packing diagram (viewed down the *a* axis) of **34**. Reprinted with permission from ref 179. Copyright 2009 Royal Society of Chemistry.
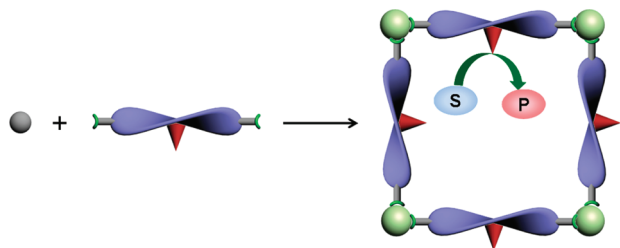
Table 19. 1,2-Addition of α,β-Unsaturated Ketones Catalyzed by 34

entry	R_1	R_2	catalyst	conversion (%)	ee (%)
1	H	Me	**34**	97	65
2	H	Me	**L₃₄**	84	51
3	H	Me	**34**	48	88[a]
4	Cl	Me	**34**	94	97

[a] The reaction temperature is −80 °C.

Scheme 13. A Synthetic Strategy for MOF-Based Simple Organic Catalysts

heating under dynamic vacuum, generating open metal coordination sites for introduction of organocatalytic units by postsynthetic modification. Two secondary (catalytic) ligands derived from L-proline, **L₃₅** ((*S*)-*N*-(pyridine-4-yl)-pyrrolidine-2-carboxamide) and **L₃₆** ((*S*)-*N*-(pyridine-3-yl)-pyrrolidine-2-carboxamide), were then synthesized, in which a 4- or 3-pyridyl unit was designed to be coordinated to the open metal coordination sites of the framework. Reaction of chiral linkers **L₃₅** or **L₃₆** with activated MIL-101 under refluxing condition in a noncoordinating solvent resulted in two new chiral MOFs $[\text{Cr}_3\text{O}(\textbf{L}_{35})_{1.8}(\text{H}_2\text{O})_{0.2}\text{F}(\text{bdc})_3] \cdot 0.15(\text{H}_2\text{bdc}) \cdot \text{H}_2\text{O}$, CMIL-1 (**35**) and $[\text{Cr}_3\text{O}(\textbf{L}_{36})_{1.75}(\text{H}_2\text{O})_{0.25}\text{F}(\text{bdc})_3] \cdot 0.15(\text{H}_2\text{bdc}) \cdot \text{H}_2\text{O}$, CMIL-2 (**36**), respectively. The coordination of the pyridyl terminal group to the metal center was confirmed by elemental analysis, TGA, and in situ IR spectra.

The catalytic activity of **35** and **36** in an asymmetric aldol reaction was examined using various aldehydes and ketones. Both catalysts promoted the aldol reaction with good conversion

(60−90%) and fair to good ee values (55−80%). Interestingly, as compared to the corresponding homogeneous catalyst, **L₃₅** (entry 2, Table 20), CMIL-1 (entry 1, Table 20) showed much higher enantioselectivity with comparable yields. The higher enantioselectivity of CMILs was ascribed to the restricted movement of the substrates in the pores of CMILs in combination with multiple chiral inductions. Furthermore, the difference in ee between **35** and **36** may be due to the bent shape of ligand **L₃₆**, which may impose additional steric hindrance to approaching aldehyde during the catalytic reaction, resulting in higher enantioselectivity. A large aldehyde that does not fit the pores of CMIL-1 showed no conversion, suggesting that the reaction mainly occurred inside the channels. CMIL-1 was recyclable up to three times without significant loss of catalytic activity, but started to lose its catalytic activity afterward by leaching of catalytic unit, **L₃₅**.

Although this strategy provides a simple, efficient, and versatile route to synthesize numerous catalytically active chiral MOFs from a robust achiral MOF for a variety of asymmetric transformations, slow leaching of the catalytic units coordinated to the metal nodes of frameworks especially in coordinating solvents such water and DMF limits the applications of the resulting MOFs. The introduction of organocatalytic units on the organic struts of preassembled frameworks by covalent modification (Scheme 15; OPP-covalent) would solve this problem, but no such example in asymmetric transformations has been reported yet.

b. Asymmetric Catalysis Promoted by Privileged Organocatalytic Units via Being Directly Incorporated into Frameworks (OPD). Recently, Duan and co-workers reported a direct incorporation of chiral organocatalyst units at metal nodes of an achiral framework

Figure 25. (a) Hierarchical structure of MIL-101 and schematic representation of (b) the large cage of MIL-101 delimited by the vertex sharing of the supertetrahedron (ST) (the vertices represent the center of each ST), (c) the ST cage drawn in polyhedron mode, (d) the μ_3-O bridged trimeric SBU chelated by six carboxylate, and (e,f) postmodification of the dehydrated chromium(III) centers with L-proline-derived auxiliary ligands. Reprinted with permission from ref 129. Copyright 2009 American Chemical Society.

in a one-pot synthesis, using a strategy shown in Scheme 16.[131] The reaction of Cd^{2+} ions, BTB (benzene-1,3,5-tribenzoate), which served as a primary (framework forming) ligand, and a protected monotopic chiral catalytic pendant ligand (secondary ligand), L-BCIP (BCIP = N-tert-butoxy-carbonyl-2-(imidazole)-1-pyrrolidine), afforded a catalytically active framework $[Cd_3(BTB)_2(L\text{-}PYI)]$ (**37**) (Figure 26a and b). Each cadmium ion is coordinated by three bidentate chelating carboxylate groups from three different BTB linkers to produce a 2D honeycomb network. However, a 2-fold interpenetration of the network resulted in an almost nonporous structure (Figure 26c). Interestingly, the Boc protecting group on the pyrrolidine moiety was spontaneously removed during the framework formation, leaving the catalytically active N—H groups of pyrrolidine exposed into the small interlayer spaces.

Table 20. Aldol Reaction Catalyzed by 35 and 36

Ar	catalyst	yield (%)	ee (%)
4-NO$_2$Ph	**35**	66	69
4-NO$_2$Ph	**L$_{35}$**	58	29
4-NO$_2$Ph	**36**	59	63
4-NO$_2$Ph	**L$_{36}$**	64	21
4-py	**35**	91	76
4-ClPh	**35**	74	70
2-Naph	**35**	80	63

1224

dx.doi.org/10.1021/cr2003147 |*Chem. Rev.* 2012, 112, 1196–1231

Scheme 15. A Synthetic Strategy for MOF-Based Organocatalysts via Postsynthetic Modification Using Covalent Modification (OPP-Covalent)
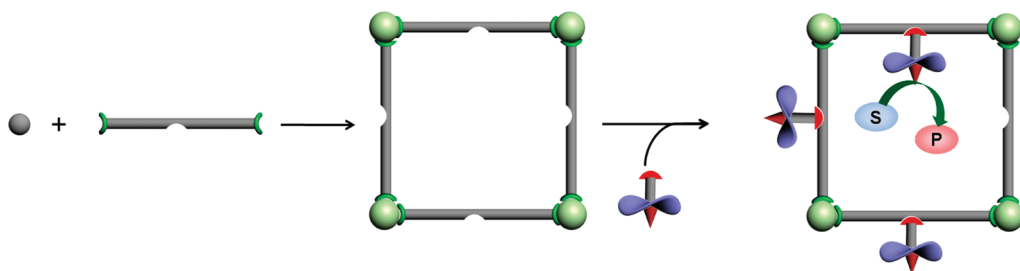
Scheme 16. A Synthetic Strategy for MOF-Based Organocatalysts via Direct Incorporation of Privileged Organocatalyst Unit Using Metal Coordination (OPD-Coordination)
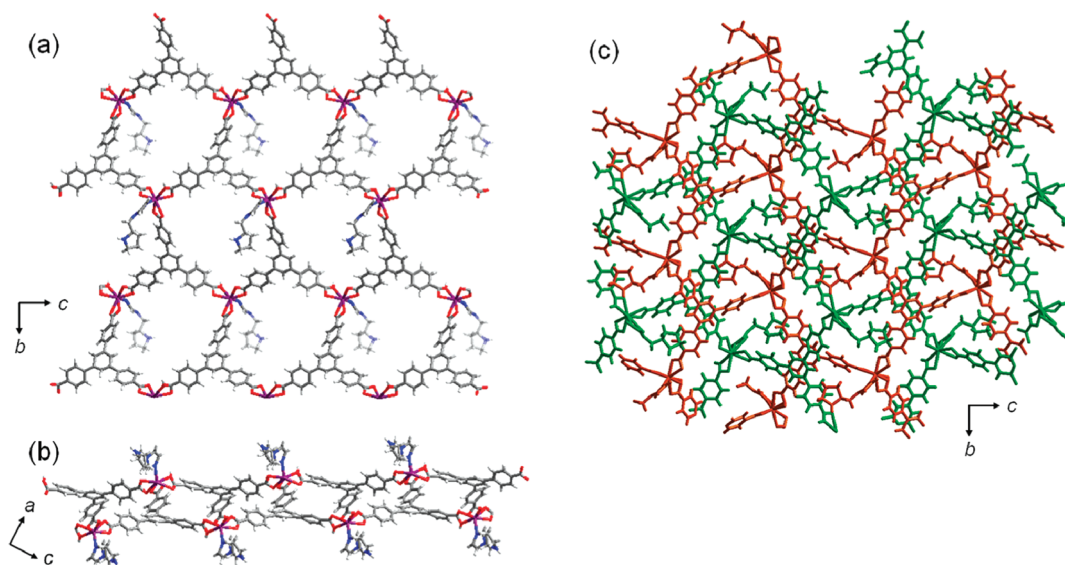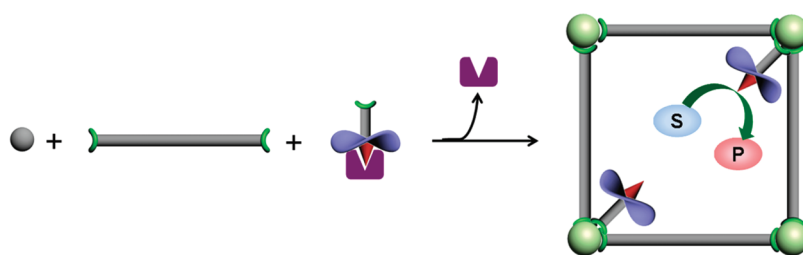
Figure 26. (a) 2D honeycomb network of **37**, (b) perspective view of 2D network along the *b*-axis, and (c) 2-fold interpenetration of the network. Copyright 2010 American Chemical Society.

The catalytic activity of **37** in asymmetric aldol reactions was tested using various aromatic aldehydes and cyclohexanone. Modest to high conversion (42−97%) and moderate enantioselectivity (58−61%) (Table 21) were observed. A set of control experiments confirmed that the pyrrolidine sites in the framework are responsible for the catalytic aldol reaction. Similar to CMILs, heterogeneous catalyst **37** showed higher ee but lower conversion than its homogeneous counterpart. However, because the pore size of the framework is too small to accommodate substrates of aldol reaction, as revealed by the X-ray analysis, the reaction appeared to take place on the surface of the crystals.

Recently, Telfer and co-workers reported another strategy (Scheme 17) to synthesize MOF-based organocatalysts, utilizing a ligand having primary functional groups used for framework formation and a protected organocatalytic unit.[133] A chiral ligand containing a protected organocatalyst, (*S*)-2-(1-(*tert*-butoxycarbonyl)pyrrolidine-2-carboxamido)biphenyl-4,4′-dicarboxylic acid (**L$_{38}$**), was synthesized in which a catalytically active pyrrolidine moiety was protected with a Boc group to avoid the amine group protonation or coordination to metal ions. Reaction of **L$_{38}$** with $Zn(NO_3)_2 \cdot 6H_2O$ afforded a new chiral framework, [Zn_4-(μ_4-O)(**L$_{38}$**)$_3$] (**38**), having a homologue structure to MOF-5.[42]

Because of the steric effect of the bulky Boc protecting groups, the resulting framework adopted a noninterpenetrated structure. The divergent carboxylate groups link the Zn_4O nodes to generate a framework with cubic topology (Figure 27). Thermal treatment of **38** removed the Boc group from the proline group on the organic struts producing catalytically active $[Zn_4(\mu_4\text{-}O)(L_{39})_3]$ (**39**). All attempts to prepare **39** directly using Boc-deprotected ligand, (*S*)-2-(pyrrolidine-2-carboxamido)biphenyl-4,4′-dicarboxylic acid (L_{39}), failed. The diameter of the pore windows ranges from 5 to 10.5 Å. The porosity and pore accessibility of the framework were confirmed by dye uptake experiments, but the framework collapsed upon guest removal as confirmed by N_2 gas sorption experiments.

Asymmetric aldol reactions were employed to examine the catalytic activity of **39** (Table 22). In an aldol reaction of acetone and nirtobenzaldehyde, the framework gave a low ee (29%) as compared to its homogeneous counterpart (52%) (Table 22). The reaction of cyclopentanone and 4-nitrobenzaldehyde in **39** resulted in a 3:1 diastereomeric ratio (dr) with an ee of 14% for the anti isomer and 3% for the syn isomer. A filtration test confirmed the heterogeneous nature of the catalytic system. Framework **38** with Boc-protected pyrrolidine units showed no catalytic conversion, indicating that the unprotected pyrrolidine groups are responsible for the catalytic activity. The framework was recyclable up to three times, but the activity of the catalyst diminishes after every cycle due to the partial collapse of the framework. The enantioselectivity of **39** was low as compared to its homogeneous counterpart, which was ascribed to a lack of organization in the transition state of the reaction as a consequence of several factors, including the absence of accessible hydrogen-bond donors for chiral induction on the catalytic unit.

The introduction of well-established privileged organocatalysts to a framework opened a new avenue to MOF-based heterogeneous asymmetric catalysts with high catalytic activity and enantioselectivity. However, each of the strategies presented here still suffers some limitations including (1) slow leaching of catalytic units

attached to metal nodes via coordination (OPP-coordination and OPD-coordination), (2) difficulty in predicting resulting framework structures (OPD-coordination), and (c) difficulty in deprotecting catalytic units without disrupting structural integrity and sacrificing enantioselectivity (OPD-covalent). Some of the limitations may be easily overcome by unexplored (for example, OPP-covalent) or yet-to-be-discovered strategies. Despite the current limitations, the future of MOF-based privileged organocatalysts is bright because of their advantages over corresponding metal catalysts including lower cost, high tolerance to water and air, and lack of toxic metal ion contamination.

4. CRITICAL ISSUES IN MOF-BASED ASYMMETRIC CATALYSTS

The past decade has witnessed a tremendous progress in asymmetric catalysis using chiral MOFs, which offer many advantages over other heterogeneous catalysts, including their highly crystalline nature, high catalyst loading, uniform catalytic centers, and wide structural and functional variations of the frameworks. The recent progress in MOF-based asymmetric catalysts including

Table 21. Asymmetric Aldol Reactions Catalyzed by 37
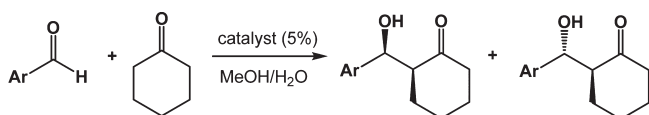
		37		L-PYI	
entry	Ar	yield (%)	ee (%)	yield (%)	ee (%)
1	2-nitrophenyl	42	60	92	25
2	3-nitrophenyl	77	61	93	25
3	4-nitrophenyl	97	58	98	21
4	1-napthyl	8	n.d.	6	n.d.

Figure 27. Synthesis of **38** from L_{38} containing Boc-protected proline and thermolytic expulsion of the Boc moiety of **38** to **39**. Reprinted with permission from ref 133. Copyright 2011 American Chemical Society.

Scheme 17. A Synthetic Strategy for MOF-Based Organocatalysts via Direct Incorporation of Privileged Organocatalyst Unit Using Covalent Attachment (OPD-Covalent)
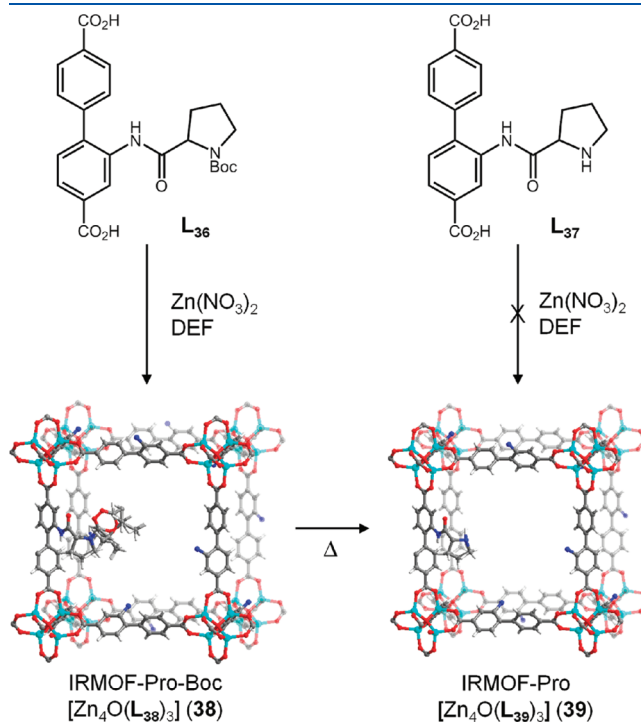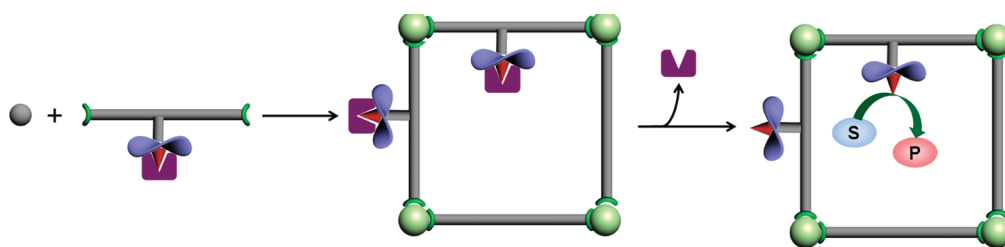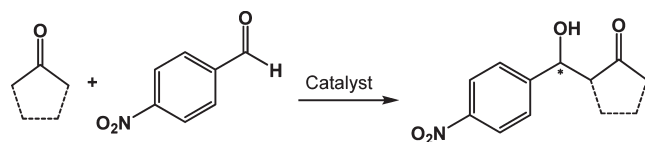
Table 22. Aldol Reactions Catalyzed by 39

ketone/ catalyst	time (h)	catalyst loading (mol %)	dr (syn:anti)	ee
		Acetone		
38	60	≥ 50		no reaction
39	40	100		29%
H$_2$–L$_{39}$	96	20		52%
		Cyclopentanone		
38	30	≥ 50		no reaction
39	30	100	1:3	3% (syn), 14% (anti)
H$_2$–L$_{39}$	96	20	2:3	86% (syn), 78% (anti)

rational design of frameworks incorporating privileged metal catalyst or organocatalyst units has convincingly proved that these emerging catalysts provide a new exciting opportunity for the synthesis of enantiopure compounds including chiral drugs. However, several issues need to be addressed before their practical applications.

First, we need to better understand the asymmetric catalysis taking place in nanometer-sized pores and channels of MOFs. As described in section 3.1.2, Lin et al. recently carried out systematic studies to delineate the relationship between open channel sizes and catalytic activities including conversion rates and enantioselectivity of MOF-based privileged metal catalysts, using a series of isoreticular MOFs with systematically varied pore/channel sizes.[121,130] As the channel size increases above a threshold value, the catalytic activity including conversion rate of MOF-based privileged metal catalysts converges to that of its homogeneous counterpart, which demonstrates the importance of facile diffusion of substrates into the frameworks to achieve a high conversion rate and, in some cases, high enantioselectivity as well by suppressing background reaction. Such systematic studies are needed to understand the structure–catalytic activity relationship of other MOF-based asymmetric catalysts.

Another important issue is to understand the effect of spatial confinement on asymmetric catalysis and the catalytic mechanism in a confined space such as in the pores/channels of MOFs.[181] Although large pore sizes allow facile diffusion of substrates, the size- and shape-selectivity of the catalysts in general decrease with increasing pore size. Moreover, recent experimental and/or molecular dynamics simulation studies of asymmetric catalysts confined in pores of mesoporous silica demonstrated that their ee values are boosted by spatial restriction.[182] Similarly, several MOF-based asymmetric catalysts reported much higher enantioselectivity than their homogeneous counterparts.[129,169] Once again, systematic studies combining experimental and theoretical (computational) approaches are needed to address this issue. In particular, computational studies such as molecular dynamics simulations are likely to be highly useful in understanding the asymmetric catalysis taking place in the pores of MOF-based privileged catalysts. For example, a recent computational study by Snurr, Broadbelt, and co-workers elucidated the steric effects on asymmetric epoxidation catalyzed by MOF-based Jacobsen catalysts. Computational studies will also help us elucidate the mechanism of asymmetric catalysis in the pores of MOFs, which

may or may not be the same as that of their homogeneous counterparts.[184] However, only a few computational studies have been reported to date.[132,183,184] In addition to theoretical studies, in situ X-ray crystallography[185] and time-resolved X-ray diffraction studies[186] using high flux synchrotron radiations should be useful in characterizing key intermediates of the catalytic reactions promoted by MOF-based asymmetric catalysts. Ultimately, such computational and experimental studies may guide us to rationally design high-performance MOF-based asymmetric catalysts for practical applications.

Hydrolytic stability of frameworks is critically important for practical applications of MOF-based heterogeneous catalysts. Two recent efforts to improve the hydrolytic stability of frameworks are worth noting. Lillerud and co-workers synthesized isoreticular frameworks UiO-66 and UiO-67 built upon hydrolytically stable SBU, [Zr(O)$_3$(OH)$_3$(O$_2$CR)$_{12}$], which showed remarkable hydrolytic and mechanical stability compared with other MOFs.[187] Cohen and co-workers reported the improved hydrolytic stability of IRMOF-3 by attaching hydrophobic functional groups to the amine groups on the linkers.[188] However, further studies are needed to enhance the hydrolytic stability of MOF-based catalysts, which will expand their scope of applications.

A recent review article by Lin also covered critical issues for asymmetric catalysis with chiral MOFs.[189] In addition, other general issues of MOF-based catalysts such as diffusion of substrates and products, framework interpenetration, and suppression of surface catalysis are covered by Hupp and Nguyen in their review article concerning MOF catalysts.[74,190]

5. CONCLUSIONS AND PERSPECTIVES

Although MOFs and some of their applications such as gas storage have been studied for more than 20 years, their application in asymmetric catalysis is only beginning to blossom. Recent developments in MOF-based asymmetric catalysts have propelled new interest into heterogeneous asymmetric catalysis. In this Review, we surveyed several synthetic strategies for MOF-based asymmetric catalysts, and their pros and cons. In particular, the synthetic strategies involving incorporation of privileged metal catalysts or organocalysts into the frameworks have paved a way to a rational design of MOF-based asymmetric catalysts with high catalytic activity and enantioselectivity. Several privileged metal catalysts such as Mn(salen) and BINOL-Ti have been successfully introduced into frameworks via either direct incorproation or postsynthetic modification, respectively. Similarly, privileged organocatalysts such as proline can be incorporated into frameworks via either direct incorporation or postsynthetic modification method using covalent or coordinative bond attachment. Isoreticular frameworks with tunable pore sizes have been used as a platform to synthesize a series of MOF-based privileged metal catalysts, and to understand the relationship between open channels sizes and catalytic activities including conversion rates and enantioselectivity.

Despite the remarkable progresses made in MOF-based asymmetric catalysts, many challenges as well as opportunities still remain. Besides the design flexibility and framework tunability, the presence of two independent sites, metal nodes and organic linkers, to introduce catalytic units makes MOFs a versatile platform for a new type catalysts including tandem catalysts and cooperative catalysts. For example, incorporation of two independent catalytic units at the metal nodes and/or organic linkers, which work in a sequential or co-operative manner, will produce tandem or cooperative asymmetric catalysts. Also, analogues to the elegant work of

1227

dx.doi.org/10.1021/cr2003147 |*Chem. Rev.* 2012, 112, 1196–1231

MacMillan[191,192,193] in homogeneous phase, the combination of a privileged organocatalyst and a well-known photoredox unit such as Ru(bpy)$_3$ incorporated into a single framework may potentially be used to realize a light-driven MOF-based organocatalyst. MOF-based privileged metal or ograno-catalysts may provide a unique opportunity to study the mechanism of asymmetric catalysis by allowing the structural characterization of key intermediates involved in the catalytic cycle using in situ crystallography or time-resolved X-ray diffraction techniques. With this great potential, MOF-based asymmetric catalysts will likely become, in the next decade, one of the important class of materials in chirotechnology involved in large-scale production of optically pure organic molecules including chiral drugs.

AUTHOR INFORMATION

Corresponding Author

*E-mail: kkim@postech.ac.kr.

BIOGRAPHIES
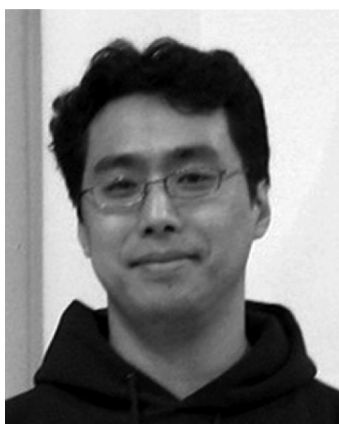
Minyoung Yoon was born in Seoul, Korea, in 1981. He received his B.S. and Ph.D. degrees in Chemistry under Professor Kimoon Kim from Pohang University of Science and Technology (POSTECH) in 2005 and 2011, respectively. He is currently a postdoctoral research fellow at the Division of Advanced Materials Science at POSTECH. His current research focuses on applications of novel porous materials for catalysis, gas storage/separation, and ion conduction.

R. Srirambalaji was born in India. He received his B.Sc. and M.Sc. degrees in Chemistry from University of Madras, Chennai, and his Ph.D. from the Indian Institute of Technology, Kanpur, India, under the guidance of Prof. G. Anantharaman. Since 2010, he has been working in the group of Prof. Kimoon Kim and Prof. Danil N. Dybtsev as a postdoctoral researcher in the Division of Advanced Materials Science at POSTECH. His current research interests include the area of metal—organic frameworks and metal biomolecule frameworks and their applications in catalysis and gas storage/separation.

Kimoon Kim studied chemistry at Seoul National University (B.S., 1976), KAIST (M.S., 1978), and Stanford University (Ph.D., 1986). After postdoctoral work at Northwestern University, he joined Pohang University of Science and Technology where he is now a Distinguished University Professor. He is also director of the Center for Smart Supramolecules (CSS), and head of the Division of Advanced Materials Science (AMS) supported by WCU program. His current research focuses on developing novel functional materials and systems based on supramolecular chemistry.

ACKNOWLEDGMENT

LIST OF ABBREVIATIONS

L-asp	L-aspartic acid
btb	4,4′,4″-benzene-1,3,5-triyltribenzoate
bdc	1,4-benzenedicarboxylic acid (terephthalic acid)
bpe	1,2-bis(4-pyridyl)ethylene
BINOL	1,1′-bi-2-naphthol
BET	Brunauer—Emmett—Teller
BINAP	2,2′-bis(diphenylphosphino)-1,1′-binaphthyl
BBR-250	Brilliant Blue R-250
H$_2$BPDC	2,2′-bipyridyl-3,3′-dicarboxylic acid
Mnsalen	(R,R)-(−)-1,2-cyclohexanediamnio-N,N′-bis(3-tert-butyl-5-(4-pyridyl)salicylidene)-MnCl
CD	circular dichroism
CMOPM	chrial metal organic porous material
CMIL	chiral Matériauxs de l'Institut Lavoisier
ChirBTB	chiral 4,4′,4″-benzene-1,3,5-triyltribonzoate
1D, 2D, and 3D	one-, two-, and three-dimensional
dr	diastereomeric ratio
DMF	N,N′-dimethylformamide

1228

dx.doi.org/10.1021/cr2003147 |Chem. Rev. 2012, 112, 1196–1231

DEF	*N,N′*-diethylformamide
DPEN	1,2-diphenylethylenediamine
EtOH	ethanol
ee	enantiomeric excess
GC	gas chromatography
HPLC	high-performance liquid chromatography
HKUST	Hong Kong University of Science and Technology
IRMOF	isoreticular metal organic framework
IR	infrared
int	interpenetrated
L-Lac	L-lactic acid
MIL	Matériauxs de l'Institut Lavoisier
MOF	metal organic framework
MOPM	metal organic porous material
MOM	metal organic material
MeOH	methanol
MNC	metal node catalysts built with chiral primary ligands
MDP	metal catalysis—privileged catalyst—direct incorporation
MPP	metal catalysis—privileged catalyst—postsynthetic modification
MNM	metal node catalysts — built with mixed (chiral and achiral) primary ligands
MNA	metal node catalysts — built with achiral primary ligands and chiral templates
MNP	metal node catalysts — postsynthetic modification
OPD	organocatalysis—privileged catalyst—direct incorporation
OPP	organocatalysis—privileged catalyst—postsynthetic modification
PXRD	powder X-ray diffraction
PCP	porous coordination polymer
POST	Pohang University of Science and Technology
py	pyridine
SBU	secondary building unit
Boc	*N-tert*-butoxy-carbonyl
tert	tertiary
$Ti(O^iPr)_4$	titanium tetraisopropoxide
TOF	turnover frequency
TON	turnover number
TADDOL	*α,α,α′,α′*-tetraaryl-1,3-dioxolan-4,5-dimethanol
BCIP	*N-tert*-butoxy-carbonyl-2-(imidazole)-1-pyrrolidone
UHP	urea hydroperoxide
PCN	porous coordination network
TGA	thermogravimetric analysis
MALDI-TOF-MS	matrix-assisted laser desorption ionization-time-of-flight-mass spectroscopy

REFERENCES

(1) Gardner, M. *The New Ambidextrous Universe*, 3rd ed.; W. H. Freeman & Co.: New York, 1990.

(2) Heilbronner, E.; Dunitz, J. D. *Reflections on Symmetry*; VHCA: Basel, 1993.

(3) Hoffmann, R. *The Same and Not the Same*; Columbia University Press: New York, 1995.

(4) Brunner, H. *Rechts oder links in der Natur und anderswo*; Wiley-VCH: Weinheim, 1999.

(5) Blaschke, G.; Kraft, H. P.; Fickentscher, K.; Köhler, F. *Arzneim. Forsch.* **1979**, *29*, 1640.

(6) Ward, T. J. *Anal. Chem.* **2006**, *78*, 3947.

(7) Morrison, J. D., Ed. *Asymmetric Synthesis*; Academic Press: New York, 1985.

(8) Nobel Prize homepage. http://nobelprize.org/nobel_prizes/chemistry/laureates/2001/.

(9) Noyori, R. *Angew. Chem., Int. Ed.* **2002**, *41*, 2008.

(10) Sharpless, B. K. *Angew. Chem., Int. Ed.* **2002**, *41*, 2024.

(11) Knowles, W. S. *Angew. Chem., Int. Ed.* **2002**, *41*, 1998.

(12) Yoon, T. P.; Jacobsen, E. N. *Science* **2003**, *299*, 1691.

(13) Kitamura, M.; Tokunaga, M.; Ohkuma, T.; Noyori, R. *Org. Synth.* **1998**, *9*, 589.

(14) Kang, Y. K.; Kim, D. Y. *Bull. Korean Chem. Soc.* **2008**, *29*, 2093.

(15) Berkessel, A.; Vogl, N. *Eur. J. Org. Chem.* **2006**, 5029.

(16) Ohrai, K.; Kondo, K.; Sodeoka, M.; Shibasaki, M. *J. Am. Chem. Soc.* **1994**, *116*, 11737.

(17) Bandini, M.; Cozzi, P. G.; Ronchi, A. U. *Chem. Commun.* **2002**, 919.

(18) Zhang, W.; Loebach, J. L.; Wilson, S. R.; Jacobsen, E. N. *J. Am. Chem. Soc.* **1990**, *112*, 2801.

(19) MacMillan, D. W. C. *Nature* **2008**, *455*, 304.

(20) Doyle, A. G.; Jacobsen, E. N. *Chem. Rev.* **2007**, *107*, 5713.

(21) List, B. *Angew. Chem., Int. Ed.* **2010**, *49*, 1730.

(22) Dalko, P. I.; Moisan, L. *Angew. Chem., Int. Ed.* **2001**, *40*, 3726.

(23) List, B. *Chem. Rev.* **2007**, *107*, 5413.

(24) Dalko, P. I.; Moisan, L. *Angew. Chem., Int. Ed.* **2004**, *43*, 5138.

(25) Bertelsen, S.; Jørgensen, K. A. *Chem. Soc. Rev.* **2009**, *38*, 2178.

(26) Carreira, E. M.; Fettes, A.; Martl, C. *Org. React.* **2006**, *67*, 1.

(27) List, B. *Chem. Commun.* **2006**, *8*, 819.

(28) List, B.; Pojarliev, P.; Martin, H. J. *Org. Lett.* **2001**, *3*, 2423.

(29) Pansare, S. V.; Pandya, K. *J. Am. Chem. Soc.* **2006**, *128*, 9624.

(30) List, B.; Pojarliev, P.; Biller, W. T.; Martin, H. *J. Am. Chem. Soc.* **2002**, *124*, 827.

(31) Yang, J. W.; Chandler, C.; Stadler, M.; Kampen, D.; List, B. *Nature* **2008**, *452*, 453.

(32) Nugent, W. A.; RajanBabu, T. V.; Burk, M. J. *Science* **1999**, *259*, 479.

(33) Jones, C. W.; McKittrick, M. W.; Nguyen, J. V.; Yu, K. *Top. Catal.* **2005**, *34*, 67.

(34) Mizuno, N.; Misono, M. *Chem. Rev.* **1998**, *98*, 199.

(35) Hattori, H. *Chem. Rev.* **1995**, *95*, 537.

(36) Trindade, A. F.; Gois, P. M. P.; Afonso, C. A. M. F. *Chem. Rev.* **2009**, *109*, 418.

(37) Fraile, J. M.; Garcia, J. L.; Mayoral, J. A. *Chem. Rev.* **2009**, *109*, 360.

(38) Hu, A.; Yee, G. T.; Lin, W. *J. Am. Chem. Soc.* **2005**, *127*, 12486.

(39) Kim, H. Y.; Kim, S.; Oh, K. *Angew. Chem., Int. Ed.* **2010**, *49*, 4476.

(40) Belser, T.; Jacobsen, E. N. *Adv. Synth. Catal.* **2008**, *350*, 967.

(41) Li, H.; Eddaoudi, M.; O'Keeffe, M.; Yaghi, O. M. *Nature* **1999**, *402*, 276.

(42) Eddaoudi, M.; Kim, J.; Rosi, N.; Vodak, D.; Wachter, J.; O'Keeffe, M.; Yaghi, O. M. *Science* **2002**, *295*, 469.

(43) Dybtsev, D. N.; Chun, H.; Kim, K. *Angew. Chem., Int. Ed.* **2004**, *43*, 5033.

(44) Matsuda, R.; Kitaura, R.; Kitagawa, S.; Kubota, Y.; Belosludov, R. V.; Kobayashi, T. C.; Sakamoto, H.; Chiba, T.; Takata, M.; Kawazoe, Y.; Mita, Y. *Nature* **2005**, *436*, 238.

(45) Kubota, Y.; Takata, M.; Matsuda, R.; Kitaura, R.; Kitagawa, S.; Kato, K.; Sakata, M.; Kobayashi, T. C. *Angew. Chem., Int. Ed.* **2005**, *44*, 913.

(46) Ma, S.; Zhou, H.-C. *J. Am. Chem. Soc.* **2006**, *128*, 11734.

(47) Murray, L. J.; Dinca, M.; Long, J. R. *Chem. Soc. Rev.* **2009**, *38*, 1294.

(48) Furukawa, H.; Ko, N.; Go, Y. B.; Aratani, N.; Choi, S. B.; Choi, E.; Yazaydin, A.; Snurr, R. Q.; O'Keeffe, M.; Kim, J.; Yaghi, O. M. *Science* **2010**, *329*, 424.

(49) Pan, L.; Adams, K. M.; Hernandez, H. E.; Wang, X.; Zheng, C.; Hattori, Y.; Kaneko, K. *J. Am. Chem. Soc.* **2003**, *125*, 3062.

(50) Dybtsev, D. N.; Chun, H.; Yoon, S. H.; Kim, D.; Kim, K. *J. Am. Chem. Soc.* **2004**, *126*, 32.

(51) Hayashi, H.; Cote, A. P.; Furukawa, H.; O'Keeffe, M.; Yaghi, O. M. *Nat. Mater.* **2007**, *6*, 501.

(52) Samsonenko, D. G.; Kim, H.; Sun, y.; Kim, G.-H.; Lee, H.-S.; Kim, K. *Chem. Asian. J.* **2007**, *2*, 484.

(53) Kim, H.; Samsonenko, D. G.; Yoon, M.; Yoon, J. W.; Hwang, Y. K.; Chang, J.-S.; Kim, K. *Chem. Commun.* **2008**, 4697.

(54) Li, J.-R.; Kuppler, R. J.; Zhou, H.-C. *Chem. Soc. Rev.* **2009**, *38*, 1477.

(55) Chen, B.; Xiang, S.; Qian, G. *Acc. Chem. Res.* **2010**, 1115.

(56) Jiang, H.-L.; Xu, Q. *Chem Commun.* **2011**, *47*, 3351.

(57) Li, J.-R.; Sculley, J.; Zhou, H.-C. *Chem. Rev.*, DOI: 10.1021/cr200190s.

(58) Qiu, Y. C.; Deng, H.; Mou, J. X.; Zeller, M.; Batten, S. R.; Wu, H. H.; Li, J. *Chem. Commun.* **2009**, 5415.

(59) Allendorf, M. D.; Bauer, C. A.; Bhakta, R. K.; Houk, R. J. T. *Chem. Soc. Rev.* **2009**, *38*, 1330.

(60) Achmann, S.; Hagen, G.; Kita, J.; Malkowsky, I. M.; Kiener, C.; Moos, R. *Sensor* **2009**, *9*, 1574.

(61) Jiang, H.-L.; Tatsu, Y.; Lu, Z.-L.; Xu, Q *J. Am. Chem. Soc.* **2010**, *132*, 5586.

(62) Cui, Y.; Yue, Y.; Qian, G.; Chen, B. *Chem. Rev.*, DOI: 10.1021/cr200101d.

(63) Kahn, O. *Molecular Magnetism*; VCH: Weinheim, 1993.

(64) Halder, G. J.; Kepert, C. J.; Moubaraki, B.; Murray, K. S.; Cashion, J. D. *Science* **2002**, *298*, 1762.

(65) Kepert, C. J. *Chem. Commun.* **2006**, 695.

(66) Rao, C. N. R.; Cheetham, A. K.; Thirumurugan, A. *J. Phys.: Condens. Matter* **2008**, *20*, 083202.

(67) Kurmoo, M. *Chem. Soc. Rev.* **2009**, *38*, 1353.

(68) Kim, H.; Sun, Y.; Kim, Y.; Kajiwara, T.; Yamashita, M.; Kim, K. *CrystEngComm* **2011**, *13*, 2197.

(69) Zhang, W.; Xiong, R.-G. *Chem. Rev.*, DOI:10.1021/cr200174w.

(70) Fujita, M.; Kwon, Y. J.; Washizu, S.; Ogura, K. *J. Am. Chem. Soc.* **1994**, *116*, 1151.

(71) Hasegawa, S.; Horike, S.; Matsuda, R.; Furukawa, S.; Mochizuki, K.; Kinoshita, Y.; Kitagawa, S. *J. Am. Chem. Soc.* **2007**, *129*, 2607.

(72) Alkordi, M. H.; Liu, Y. L.; Larsen, R. W.; Eubank, J. F.; Eddaoudi, M. *J. Am. Chem. Soc.* **2008**, *130*, 12639.

(73) Horike, S.; Dinca, M.; Tamaki, K.; Long, J. R. *J. Am. Chem. Soc.* **2008**, *130*, 5854.

(74) Lee, J.-Y.; Farha, O. M.; Roberts, J.; Scheidt, K. A.; Nguyen, S. T.; Hupp, J. T. *Chem. Soc. Rev.* **2009**, *38*, 1450.

(75) Farrusseng, D.; Aguado, S.; Pinel, C. *Angew. Chem., Int. Ed.* **2009**, *48*, 7502.

(76) Corma, A.; Garcia, H.; Llabres, F. X.; Xamena, I. *Chem. Rev.* **2010**, *110*, 4606.

(77) Jiang, H.-L.; Akita, T.; Ishida, T.; Haruta, M.; Xu, Q. *J. Am. Chem. Soc.* **2011**, *133*, 1304.

(78) Heitbaum, M.; Glorius, F.; Escher, I. *Angew. Chem., Int. Ed.* **2006**, *45*, 4732.

(79) Ding, K.; Uozumi, Y. *Handbook of Asymmetric Heterogeneous Catalysis*; Wiley-VCH: Weinheim, 2008.

(80) Seo, J. S.; Whang, D.; Lee, H.; Jun, S. I.; Oh, J.; Jeon, Y.; Kim, K. *Nature* **2000**, *404*, 982.

(81) Kesanli, B.; Lin, W. *Coord. Chem. Rev.* **2003**, *246*, 305.

(82) Lin, W. *J. Solid State Chem.* **2005**, *178*, 2486.

(83) Ngo, H. L.; Lin, W. *Top. Catal.* **2005**, *34*, 85.

(84) Lin, W. *MRS Bull.* **2007**, *32*, 544.

(85) Ma, L.; Abney, C.; Lin, W. *Chem. Soc. Rev.* **2009**, *38*, 1248.

(86) Liu, Y.; Xuan, W.; Cui, Y. *Adv. Mater.* **2010**, *22*, 4112.

(87) Lin, W. *Top. Catal.* **2010**, *53*, 869.

(88) Kim, K.; Banerjee, M.; Yoon, M.; Das, S. *Top. Curr. Chem.* **2010**, *293*, 115.

(89) Ma, L.; Lin, W. *Top. Curr. Chem.* **2010**, *293*, 175.

(90) Nickerl, G.; Henschel, A.; Grünker, R.; Gedrich, K.; Kaskel, S. *Chem. Ing. Tech.* **2011**, *83*, 90.

(91) Zaworotko, M. J. *Chem. Soc. Rev.* **1994**, *23*, 283.

(92) Batten, S. R.; Robson, R. *Angew. Chem., Int. Ed.* **1998**, *37*, 1460.

(93) Blake, A. J.; Champness, N. R.; Hubberstey, P.; Li, W.-S.; Withersby, M. A.; Schröder, M. *Coord. Chem. Rev.* **1999**, *183*, 117.

(94) Hagrman, P. J.; Hagrman, D.; Zubieta, J. *Angew. Chem., Int. Ed.* **1999**, *38*, 2638.

(95) Barton, T. J.; Bull, L. M.; Klemperer, W. G.; Loy, D. A.; McEnaney, B.; Misono, M.; Monson, P. A.; Pez, G.; Scherer, G. W.; Vartuli, J. C.; Yaghi, O. M. *Chem. Mater.* **1999**, *11*, 2633.

(96) Moulton, B.; Zaworotko, M. J. *Chem. Rev.* **2001**, *101*, 1629.

(97) Zaworotko, M. J. *Chem. Commun.* **2001**, 16.

(98) Khlobystov, A. N.; Blake, A. J.; Champness, N. R.; Lemenovskii, D. A.; Majouga, A. G.; Zyk, N. V.; Schröder, M. *Coord. Chem. Rev.* **2001**, *222*, 155.

(99) Kitagawa, S.; Kawata, S. *Coord. Chem. Rev.* **2002**, *224*, 11.

(100) Janiak, C. *J. Chem. Soc., Dalton Trans.* **2003**, 2781.

(101) James, S. L. *Chem. Soc. Rev.* **2003**, *32*, 276.

(102) Yaghi, O. M.; O'Keeffe, M.; Ockwig, N. W.; Chae, H. K.; Eddaoudi, M.; Kim, J. *Nature* **2003**, *423*, 705.

(103) Kitagawa, S.; Kitaura, R.; Noro, S.-I. *Angew. Chem., Int. Ed.* **2004**, *43*, 2334.

(104) Hill, R. J.; Long, D. L.; Champness, N. R.; Hubberstey, P.; Schröder, M. *Acc. Chem. Res.* **2005**, *38*, 337.

(105) Robson, R. *Dalton Trans.* **2008**, 5113.

(106) Kuppler, R. J.; Timmons, D. J.; Fang, Q. R.; Li, J. R.; Makal, T. A.; Young, M. D.; Yuan, D.; Zhao, D.; Zhuang, W.; Zhou, H. C. *Coord. Chem. Rev.* **2009**, *253*, 3042.

(107) Férey, G. *Chem. Soc. Rev.* **2008**, *37*, 191.

(108) Tranchemontagne, D. J.; Mendoza-Cortés, J. L.; O'Keeffe, M.; Yaghi, O. M. *Chem. Soc. Rev.* **2009**, *38*, 1257.

(109) Perry, J. J., IV; Perman, J. A.; Zaworotko, M. J. *Chem. Soc. Rev.* **2009**, *38*, 1400.

(110) O'Keeffe, M.; Yaghi O. M. *Chem. Rev.*, DOI: 10.1021/cr200205j.

(111) Gable, R. W.; Hoskins, B. F.; Robson, R. *J. Chem. Soc., Chem. Commun.* **1990**, 762.

(112) Abrahams, B. F.; Hoskins, B. F.; Robson, R. *J. Chem. Soc., Chem. Commun.* **1990**, 60.

(113) Abrahams, B. F.; Hoskins, B. F.; Liu, J.; Robson, R. *J. Am. Chem. Soc.* **1991**, *113*, 3045.

(114) Batten, S. R.; Hoskins, B. F.; Robson, R. *J. Chem. Soc., Chem. Commun.* **1991**, 445.

(115) Abrahams, B. F.; Hardie, M. J.; Hoskins, B. F.; Robson, R.; Williams, G. A. *J. Am. Chem. Soc.* **1992**, *114*, 10641.

(116) Abrahams, B. F.; Hoskins, B. F.; Michail, D. M.; Robson, R. *Nature* **1994**, *369*, 727.

(117) Chun, H.; Dybtsev, D. N.; Kim, H.; Kim, K. *Chem.-Eur. J.* **2005**, *11*, 3521.

(118) Liu, X.; Park, M.; Hong, S.; Oh, M.; Yoon, J. W.; Chang, J.-S.; Lah, M. S. *Inorg. Chem.* **2009**, *48*, 11507.

(119) Kim, H.; Das, S.; Kim, M. G.; Dybtsev, D. N.; Kim, Y.; Kim, K. *Inorg. Chem.* **2011**, *50*, 3691.

(120) Frahm, D.; Fischer, M.; Hoffmann, F.; Fröba, M. *Inorg. Chem.* **2011**, *50*, 11055.

(121) Song, F.; Wang, C.; Falkowski, J. M.; Ma, L.; Lin, W. *J. Am. Chem. Soc.* **2010**, *132*, 15390.

(122) He, H.; Yuan, D.; Ma, H.; Sun, D.; Zhang, G.; Zhou, H.-C. *Inorg. Chem.* **2010**, *49*, 7605.

(123) Tanabe, K. K.; Cohen, S. M. *Chem. Soc. Rev.* **2011**, *40*, 498.

(124) Cohen, S. *Chem. Rev.*, DOI: 10.1021/cr200179u.

(125) Sawaki, T.; Dewa, T.; Aoyama, Y. *J. Am. Chem. Soc.* **1998**, *120*, 8539.

(126) Evans, O. R.; Ngo, H. L.; Lin, W. *J. Am. Chem. Soc.* **2001**, *123*, 10395.

(127) Wu, C.-D.; Hu, A.; Zhang, L.; Lin, W. *J. Am. Chem. Soc.* **2005**, *127*, 8940.

(128) Cho, S.-H.; Ma, B.; Nguyen, S. T.; Hupp, J. T.; Albrecht-Schmitt, T. E. *Chem. Commun.* **2006**, 2563.

(129) Banerjee, M.; Das, S.; Yoon, M.; Choi, H. J.; Hyun, M. H.; Park, S. M.; Seo, G.; Kim, K. *J. Am. Chem. Soc.* **2009**, *131*, 7524.

(130) Ma, L.; Falkowski, J. M.; Abney, C.; Lin, W. Nat. Chem. 2010, 2, 838.

(131) Dang, D.; Wu, P.; He, C.; Xie, Z.; Duan, C. J. Am. Chem. Soc. 2010, 132, 14321.

(132) Oxford, G. A. E.; Snurr, R. Q.; Broadbelt, L. J. Ind. Eng. Chem. Res. 2010, 49, 10965.

(133) Lun, D. J.; Waterhouse, G. I. N.; Telfer, S. G. J. Am. Chem. Soc. 2011, 133, 5806.

(134) Suh, M. P.; Ko, J. W.; Choi, H. J. J. Am. Chem. Soc. 2002, 124, 10976.

(135) Das, M. C.; Bharadwaj, P. K. B. J. Am. Chem. Soc. 2009, 131, 10942.

(136) Maji, T. K.; Mostafa, G.; Matsuda, R.; Kitagawa, S. J. Am. Chem. Soc. 2005, 127, 17152.

(137) Min, K. S.; Suh, M. P. Chem.-Eur. J. 2001, 7, 303.

(138) Vittal, J. J. Coord. Chem. Rev. 2007, 251, 1781.

(139) Barbour, L. J. Aust. J. Chem. 2006, 59, 595.

(140) Nelson, A. P.; Farha, O. K.; Mulfort, K. L.; Hupp, J. T. J. Am. Chem. Soc. 2009, 131, 458.

(141) Ma, L.; Jin, A.; Xie, Z.; Lin, W. Angew. Chem., Int. Ed. 2009, 48, 9905.

(142) Gedrich, K.; Heitbaum, M.; Notzon, A.; Senkovska, I.; Frçhlich, R.; Getzschmann, J.; Mueller, U.; Glorius, F.; Kaskel, S. Chem.-Eur. J. 2011, 17, 2099.

(143) Chui, S. S.-Y.; Lo, S. M.-F.; Charmant, J. P. H.; Orpen, A. G.; Williams, I. D. Science 1999, 283, 5405.

(144) Tanaka, K.; Oda, S.; Shiro, M. Chem. Commun. 2008, 820.

(145) Chen, B.; Eddaoudi, M.; Hyde, S. T.; O'Keeffe, M.; Yaghi, O. M. Science 2001, 291, 1021.

(146) Friedrichs, O.-D.; O'Keeffe, M.; Yaghi, O. M. Acta Crystallogr. 2006, A62, 350.

(147) Blatov, V. A.; Proserpio, D. M. Acta Crystallogr. 2009, A62, 202.

(148) Center for Reticular Chemistry homepage. http://rcsr.anu.edu.au/.

(149) Dybtsev, D. N.; Yutkin, M. P.; Samsonenko, D. G.; Fedin, V. P.; Nuzhdin, A. L.; Bezrukov, A. A.; Bryliakov, K. P.; Talsi, E. P.; Belosludov, R. V.; Mizuseki, H.; Kawazoe, Y.; Subbotin, O. S.; Belosludov, V. R. Chem.-Eur. J. 2010, 34, 10348.

(150) Vaidhyanathan, R.; Bradshaw, D.; Rebilly, J. N.; Barrio, J. P.; Gould, J. A.; Berry, N. G.; Rosseinsky, M. J. Angew. Chem., Int. Ed. 2006, 45, 39.

(151) Dybtsev, D. N.; Nuzhdin, A. L.; Chun, H.; Bryliakov, K. P.; Talsi, E. P.; Fedin, V. P.; Kim, K. Angew. Chem., Int. Ed. 2006, 45, 916.

(152) Fernandez, I.; Khiar, N. Chem. Rev. 2003, 103, 3651.

(153) Dybtsev, D. N.; Yutkin, M. P.; Peresypkina, E. V.; Virovets, A. V.; Serre, C. S.; Férey, G.; Fedin, V. P. Inorg. Chem. 2007, 46, 6843.

(154) Kepert, C. J.; Prior, T. J.; Rosseinsky, M. J. J. Am. Chem. Soc. 2000, 122, 5158.

(155) Das, S.; Kim, H.; Kim, K. J. Am. Chem. Soc. 2009, 131, 3814.

(156) Prasad, T. K.; Hong, D.-H.; Suh, M. P. Chem.-Eur. J. 2010, 16, 14043.

(157) Dincă, M.; Long, J. R. J. Am. Chem. Soc. 2007, 129, 11172.

(158) Mi, L.; Hou, H.; Song, Z.; Han, H.; Xu, H.; Fan, Y.; Ng, S.-W. Cryst. Growth Des. 2007, 7, 2553.

(159) Hu, A.; Ngo, H. L.; Lin, W. Angew. Chem., Int. Ed. 2003, 42, 6000.

(160) Knowles, W. S. Adv. Synth. Catal. 2003, 345, 3.

(161) Zhang, Z.; Qian, H.; Longmire, J.; Zhang, X. J. Org. Chem. 2000, 65, 6223.

(162) Zhou, Y.-G.; Tang, W.; Wang, W.-B.; Li, W.; Zhang, X. J. Am. Chem. Soc. 2002, 124, 4952.

(163) Hu, A.; Ngo, H. L.; Lin, W. J. Am. Chem. Soc. 2003, 125, 11490.

(164) Ohkuma, T.; Ooka, H.; Ikariya, T.; Noyori, R. J. Am. Chem. Soc. 1995, 117, 10417.

(165) Doucet, H.; Ohkuma, T.; Murata, K.; Yokozawa, T.; Kozawa, M.; Katayama, E.; England, A. F.; Ikariya, T.; Noyori, R. Angew. Chem., Int. Ed. 1998, 37, 1703.

(166) Ngo, H. L.; Hu, A.; Lin, W. J. Mol. Catal. A: Chem. 2004, 215, 177.

(167) Wu, C. D.; Lin, W. Angew Chem., Int. Ed. 2007, 46, 1075.

(168) Ma, L.; Wu, C.-D.; Wanderley, M. M.; Lin, W. Angew. Chem., Int. Ed. 2010, 49, 8244.

(169) Jeong, K. S.; Go, Y. B.; Shin, S. M.; Lee, S. J.; Kim, J.; Yaghi, O. M.; Jeong, N. Chem. Sci. 2011, 2, 877.

(170) Furukawa, H.; Kim, J.; Ockwig, N. W.; O'Keeffe, M.; Yaghi, O. M. J. Am. Chem. Soc. 2008, 130, 11650.

(171) Rosi, N. L.; Eckert, J.; Eddaoudi, M.; Vodak, D. T.; Kim, J.; O'Keeffe, M.; Yaghi, O. M. Science 2003, 300, 1127.

(172) Song, F.; Wang, C.; Lin, W. Chem. Commun. 2011, 47, 8256.

(173) Qin, Y. Y.; Zhang, J.; Li, Z. J.; Zhang, L.; Cao, X. Y.; Yao, Y. G. Chem. Commun. 2008, 2532.

(174) Falkowski, J. M.; Wang, C.; Liu, S.; Lin, W. Angew. Chem., Int. Ed. 2011, 50, 8674.

(175) Miller, J. A.; Jin, W.; Nguyen, S. T. Angew. Chem., Int. Ed. 2002, 41, 2953.

(176) Shultz, A. M.; Farha, O. K.; Adhikari, D.; Sarjeant, A. A.; Hupp, J. T.; Nguyen, S. T. Inorg. Chem. 2011, 50, 3174.

(177) Shultz, A.; Sarjeant, A. A.; Farha, O. K.; Hupp, J. T.; Nguyen, S. T. J. Am. Chem. Soc. 2011, 133, 13252.

(178) Ingleson, M. J.; Barrio, J. P.; Bacsa, J.; Dickinson, C.; Park, H.; Rosseinsky, M. J. Chem. Commun. 2008, 1287.

(179) Wang, M.; Xie, M.-H.; Wu, C.-D.; Wang, Y.-G. Chem. Commun. 2009, 2396.

(180) Ferey, G.; Draznieks, C. M.; Serre, C.; Millange, F.; Dutour, J.; Surble, S.; Margiolaki, I. Science 2005, 309, 2040.

(181) Farha, O. K.; Malliakas, C. D.; Kanatzidis, M. G.; Hupp, J. T. J. Am. Chem. Soc. 2010, 132, 950.

(182) Thomas, J. M.; Raja, R. Acc. Chem. Res. 2008, 41, 708.

(183) Düren, T.; Bae, Y.-S.; Snurr, R. Q. Chem. Soc. Rev. 2009, 38, 1237.

(184) Oxford, G. A. E.; Dubbeldam, D.; Broadbelt, L. J.; Snurr, R. Q. J. Mol. Catal. A: Chem. 2011, 334, 89.

(185) Kawamichi, T.; Haneda, T.; Kawano, M.; Fujita, M. Nature 2009, 461, 633.

(186) Rischel, C.; Rousse, A.; Uschmann, I.; Albouy, P.-A.; Geindre, J.-P.; Audebert, P.; Gauthier, J.-C.; Fröster, E.; Martin, J.-L.; Antonetti, A. Nature 1997, 390, 490.

(187) Cavka, J. H.; Jakobsen, S.; Olsbye, U.; Guillou, N.; Lamberti, C.; Bordiga, C.; Lillerud, K. P. J. Am. Chem. Soc. 2008, 130, 13850.

(188) Nguyen, J. G.; Cohen, S. M. J. Am. Chem. Soc. 2010, 132, 4560.

(189) Wang, C.; Zheng, M.; Lin, W. J. Phys. Chem. Lett. 2011, 2, 1701.

(190) Weston, M. H.; Farha, O. K.; Hupp, J. T.; Nguyen, S. T. Chem. Rev., MOF theme issue.

(191) Nicewicz, D.; MacMillan, D. W. C. Science 2008, 322, 77.

(192) Nagib, D. A.; Scott, M. E.; MacMillan, D. W. C. J. Am. Chem. Soc. 2009, 131, 10875.

(193) Pham, P. V.; Nagib, D. A.; MacMillan, D. W. C. Angew. Chem., Int. Ed. 2011, 50, 6119.

1231

dx.doi.org/10.1021/cr2003147 |Chem. Rev. 2012, 112, 1196–1231